

Sheffield Hallam University

Thermal and Visual Imaging and Accelerometry Developments to Assist with Arthritis Diagnosis

NWAIZU, Harriet Uchenna

Available from the Sheffield Hallam University Research Archive (SHURA) at:

<http://shura.shu.ac.uk/25602/>

A Sheffield Hallam University thesis

This thesis is protected by copyright which belongs to the author.

The content must not be changed in any way or sold commercially in any format or medium without the formal permission of the author.

When referring to this work, full bibliographic details including the author, title, awarding institution and date of the thesis must be given.

Please visit <http://shura.shu.ac.uk/25602/> and <http://shura.shu.ac.uk/information.html> for further details about copyright and re-use permissions.

Thermal and Visual Imaging and Accelerometry Developments to Assist with Arthritis Diagnosis

Harriet Uchenna Nwaizu

A thesis submitted in partial fulfilment of the requirements of
Sheffield Hallam University
for the degree of Doctor of Philosophy

**Sheffield
Hallam
University** | Materials and
Engineering
Research Institute

June, 2019

Declaration

I declare that this thesis is my own work apart from where indicated by specific reference to other sources, that the work has been conducted in accordance with the Research regulations of Sheffield Hallam University, and that neither the thesis nor the original work contained therein has been submitted to this or any other institution for any other academic award.

Harriet Uchenna Nwaizu 04/06/2019

Abstract

Juvenile Idiopathic Arthritis (JIA) is a disease that causes pain and inflammation in the joints of children. Its early diagnosis is important to avoid damage to the joints. Joint warmth, redness and movement restriction may be indicators of active arthritis hence accurate objective means to measure temperature, colour and range of movement (ROM) at the joint may assist diagnosis.

In this study, three techniques with a potential to assist clinicians in diagnosing JIA were developed. These were based on high-resolution thermal imaging (HRTI), visual imaging and accelerometry. A detailed correlation analysis was performed between the developed methods and the consultant's clinical assessment of JIA diagnosis.

Twenty-two patients (age: mean=10.6 years, SD = 2 years) with JIA diagnosis were recruited. 18 participated in the thermal/visual imaging study only, 2 in the accelerometry study only and 2 in both thermal/visual imaging and accelerometry studies. Thermal and visual images of the front and back of the knees and ankles of 20 patients were studied. All ethical approvals from Sheffield Hallam University and the National Health Service (NHS) were duly obtained before commencing the study.

The thermal/visual imaging study involved developing image processing techniques to accurately identify and segment the regions of interest (ROIs). A tracking algorithm to accurately locate the ROIs was also implemented. An accelerometry system that is capable of recording movements from 4 channels was developed and its signals were processed by frequency spectrum analysis, short-time Fourier transform and wavelet packet analysis.

The thermal imaging results showed a combined 71% correlation (for the front of knees and ankles) with clinical assessment. It may be possible that patients whom their arthritic joint was cooler than their healthy joints may have relied on their healthy leg more extensively for mobility (due to the pain on the arthritic leg) thus increasing its joints temperature. It was also found that JIA may affect the skin colour with a combined 42% correlation between the knees and ankles. The accelerometry results showed a 75% correlation with clinical assessment.

The study for the first time brought together the three techniques of thermal imaging, visual imaging and accelerometry to assist with JIA diagnosis. The study demonstrated that the developed techniques have potential in assisting clinicians with JIA diagnosis. Improvements in timely diagnosis allow more effective treatment and can reduce the likelihood of joint damage in rheumatoid arthritis.

Acknowledgments

All thanks to God for giving me the guidance and strength to conclude this doctoral research.

I would like to express my deep thanks to my director of studies, Professor Reza Saatchi for his support, expertise, guidance, encouragement, valuable comments and suggestions on various aspects of this PhD work. I could not have imagined having a better advisor and mentor for my PhD considering his enthusiasm and great efforts in explaining things clearly and simply. Thank you for reviewing this thesis and for giving me every possible advice that has significantly improved its quality.

My special appreciation goes to Oliver Ward, Dr Daniel Hawley, Professor Derek Burke, and Dr Ben Heller for all their valuable contributions, comments, and feedback in this doctoral research.

I also want to say a big 'THANK YOU' to the children and young people of the Sheffield children hospital who participated in this study, and to their parents/guardian for giving their time to the study.

Thank you to the MERI administrators for their support through this doctoral research.

My appreciation also goes to my friends for all their encouragement and support.

Finally, a special thanks to my family for their selfless care and support. Words cannot express how grateful I am to my lovely parents for all their sacrifices and prayers through this time. To my siblings, for always cheering me on. To my son, for giving me the strength to forge ahead. And to my beloved husband, for being there always and giving everything.

May God immensely bless you all.

Publications

Nwaizu, H., Saatchi, R., & Burke, D. (2016). Accelerometer based human joints' range of movement measurement. Paper presented at the *2016 10th International Symposium on Communication Systems, Networks and Digital Signal Processing (CSNDSP)*, 1-6. doi:10.1109/CSNDSP.2016.7573970

Nwaizu, H., Saatchi, R., & Burke, D. (2017). Inertial measurement techniques for human joints' movement analysis. *AAATE 2017: Advancing Assistive Technology and eAccessibility for People with Disabilities and the Aging Population, 242*(Studies in Health Technology and Informatics), 717-724. doi:10.3233/978-1-61499-798-6-717

Ward, O., Nwaizu, H., Saatchi, R., Ramlakhan, S., & Hawley, D. (2018). P36 does thermal imaging correlate with musculoskeletal examination in the identification of inflamed joints in children and young people with juvenile idiopathic arthritis? A prospective diagnostic accuracy study. *Rheumatology, 57* (suppl_8) doi:10.1093/rheumatology/key273.038

Presentations

Nwaizu, H., Saatchi, R., Heller, B., & Burke, D. (2014). Development of inertia measurement techniques for analysing human movement patterns. Poster presented at the 2014 BMRC/MERI winter poster event, Sheffield Hallam University, UK

Nwaizu, H., Saatchi, R., & Burke, D. (2016). Inertial measurement techniques for analysing patterns of human movement. Paper presented at the 2016 MERI Research symposium, Sheffield Hallam University, UK

Nwaizu, H., Saatchi, R., & Burke, D. (2016). Accelerometer based analysis of human joints' range of movement. Poster presented at the 2016 BMRC/MERI winter poster event, Sheffield Hallam University, UK

Table of Contents

Declaration	i
Abstract	ii
Acknowledgments.....	iii
Publications	iv
Table of Contents	v
List of Figures	x
List of Tables.....	xv
List of acronyms	xvii
1 Introduction	1
1.1 Background and purpose of the study	1
1.2 Aim and Objectives.....	2
1.2.1 Objectives.....	2
1.3 Contribution to knowledge	3
1.4 Thesis outline.....	5
1.5 Summary.....	6
2 Literature Review	7
2.1 Current methods for diagnosing JIA.....	7
2.2 Thermal imaging.....	9
2.2.1 Thermography in medicine	9
2.2.2 IRT for diagnosing arthritis.....	9
2.2.3 Image segmentation	12
2.3 Colour analysis for medical diagnosis	13
2.3.1 Colour similarity measurement	14
2.4 Accelerometry based applications	15

2.4.1	Human movement and balance.....	15
2.4.2	Joint Range of Movement.....	18
2.4.3	Assessing arthritis.....	18
2.5	Summary.....	21
3	Relevant Theory.....	22
3.1	Arthritis.....	22
3.2	Juvenile idiopathic arthritis (JIA).....	22
3.2.1	Symptoms.....	23
3.2.2	Causes.....	24
3.2.3	Diagnosis.....	24
3.3	Infrared thermography (IRT).....	27
3.3.1	History.....	27
3.3.2	Fundamentals of infrared thermography.....	28
3.4	Accelerometry for describing movement.....	32
3.4.1	Accelerometers.....	33
3.4.2	Basic accelerometer operation.....	34
3.4.3	Tilt sensing.....	35
3.5	Digital signal processing concepts.....	36
3.5.1	Signal filtering.....	37
3.5.2	Signal analysis.....	38
3.6	Image processing.....	41
3.6.1	Image segmentation.....	41
3.6.2	Image tracking.....	41
3.6.3	Template matching.....	42
3.6.4	Colour feature extraction and similarity index.....	43
3.7	Summary.....	43

4	Research Methodology for the Thermal/Visual Imaging and Accelerometry Study..	45
4.1	Ethical approval	45
4.2	Risk assessment	45
4.3	Recruitment	45
4.3.1	Information sheets	46
4.3.2	Assent / Consent	46
4.3.3	Exclusion criteria	46
4.4	Patients' details	47
4.5	Medical examination of patients.....	48
4.6	Anonymity	51
4.7	Materials.....	51
4.7.1	Camera and associated software	51
4.7.2	Data Processing software.....	52
4.8	Summary.....	52
5	Thermal Imaging for the Clinical Assessment of Juvenile Idiopathic Arthritis	53
5.1	Methodology	53
5.1.1	Setup at the hospital	53
5.1.2	Data collection	54
5.1.3	Image processing procedures	54
5.2	Results and discussion	61
5.2.1	Knee analysis	62
5.2.2	Ankle analysis	72
5.3	Summary.....	80
6	Visual imaging (VI) and its Correlation with Thermal Imaging to Assist with Clinical JIA diagnosis	82
6.1	Methodology	82

6.1.1	Data collection	82
6.1.2	Data processing.....	83
6.2	Results and discussion.....	87
6.2.1	Analysis of the front of the knees (Correlation with TI and consultant's evaluation)	87
6.2.2	Results for the back of the knees (Correlation with consultants' evaluation and TI).....	90
6.2.3	Results for the front of the ankles (Correlation with consultants' evaluation and TI).....	91
6.2.4	Results for the back of the ankles (Correlation with consultants' evaluation and TI).....	92
6.2.5	Summary of the correlation results	93
6.3	Summary.....	94
7	Accelerometry to Aid Assessment of Joint Movement in JIA	96
7.1	Methodology	96
7.1.1	Materials	96
7.1.2	Experimental setup in the University Laboratory	97
7.1.3	Set up at the hospital	101
7.1.4	Participants	102
7.1.5	Clinical Evaluation	102
7.1.6	Measurements	102
7.1.7	Operation of the algorithm	104
7.2	Results and discussion.....	106
7.2.1	Static platform experiment.....	106
7.2.2	Knee model experiment.....	107
7.2.3	Experiment performed on healthy adult knees.....	108
7.2.4	Analysis of data collected from CYP with active JIA on one knee	116

7.3	Summary.....	126
8	Conclusions and Further work	127
8.1	Conclusions.....	127
8.1.1	Thermal/Visual Imaging developments	128
8.1.2	Accelerometry	130
8.2	Further work.....	130
	References.....	xxi
	Appendix 1: Sheffield Hallam University ethical approval.....	xl
	Appendix 2: NHS ethical approval.....	xli
	Appendix 3: Research Passport.....	xliv
	Appendix 4: Introduction to Good Clinical Practice eLearning (Secondary Care)	xlvi
	Appendix 5: Informed consent in paediatric research	xlvii
	Appendix 6: Information sheet for children aged 4 to 11 years (Thermal Imaging) ...	xlviii
	Appendix 7: Information sheet for young persons aged 12 to 16 years (Thermal Imaging).....	lii
	Appendix 8: Information sheet for parent/guardian (Thermal Imaging)	lvi
	Appendix 9: Information sheet for children below 10 years (Accelerometry)	lxi
	Appendix 10: Information sheet for children aged 10 years and above (Accelerometry)	lxv
	Appendix 11: Information sheet for parent/carer (Accelerometry).....	lxix
	Appendix 12: Assent form for children & young people (Thermal Imaging).....	lxxiv
	Appendix 13: Consent form for parent/guardian (Thermal Imaging)	lxxv
	Appendix 14: Assent form for children & young people (Accelerometry)	lxxvi
	Appendix 15: Consent form for parent/guardian (Accelerometry).....	lxxvii
	Appendix 16: Developments in denoising the accelerometer signal	lxxviii

List of Figures

Figure 3-1 International League of Associations for Rheumatology classification of JIA (Boros & Whitehead, 2010)	23
Figure 3-2 Cross section of healthy and JIA affected joint (Chang et al., 2010)	24
Figure 3-3 The electromagnetic spectrum highlighting the visible band (Hickman & Riley, 2010).....	29
Figure 3-4 Block diagram showing the main subunits of a thermal imaging camera (Syed, 2016).....	32
Figure 3-5 A typical 3-axis accelerometer breakout board (Hobby Electronics, 2018) ..	34
Figure 3-6 The broad concept of a capacitive accelerometer (Woodford, 2018)	35
Figure 3-7 Three axis of an accelerometer showing roll, pitch and yaw movements (Ellis et al., 2014)	36
Figure 3-8 Ideal magnitude response of a low-pass filter (Thompson, 2014).....	37
Figure 3-9 Typical responses of a low-pass (LP) Butterworth filter of the 1 st , 2 nd , 3 rd and 6 th order with a normalised cut-off frequency of 0.5	38
Figure 3-10 Discrete wavelet transform decomposition structure (Mathworks, 2018)	40
Figure 3-11 Discrete wavelet transform decomposition tree for three levels (Mathworks, 2018).....	40
Figure 3-12 Wavelet packet decomposition tree down to level 3 (MathWorks, 2019b).	41
Figure 3-13 Normalised cross correlation of two images (Perveen et al., 2013)	43
Figure 4-1 Image of the FLIR T630sc (FLIR, 2019)	51
Figure 5-1 Sample thermal image showing how knee ROI is identified. The patient is facing the camera.....	55

Figure 5-2 Anterior view of the knee (London Knee Specialists, 2019).....	55
Figure 5-3 Sample thermal image showing how ankle ROI is identified (a) Front of the ankle (b) Back of the ankle.....	56
Figure 5-4 Illustration of Skeletal ankle (side view and front view) (OrthoInfo, 2019) ..	56
Figure 5-5 Segmentation process using the knee as an example (a) identified ROI (b) ROI binary mask (c) ROI (d) Extracted ROI	57
Figure 5-6 ROI tracked through right ankle movement from left to right direction	58
Figure 5-7 ROI locations for each image tracked accurately (the image x coordinate is in blue and y coordinate is in red)	59
Figure 5-8 Back of knee showing first image ROI at (20.5, 60.5).....	59
Figure 5-9 Back of knee showing last frame ROI at (29,60).....	60
Figure 5-10 ROI (X, Y image pixel coordinates) tracked through the recorded frames. The starting coordinates were approximated in this Figure to (21, 61).....	61
Figure 5-11 Patient 5 thermal images – (a) Left knee ROI (b) Right knee ROI.....	64
Figure 5-12 Patient 9 thermal image showing the right leg with darker regions (higher temperatures) than the left leg	65
Figure 5-13 Thermal images for front and back of knees for patients’ 1 and 12	66
Figure 5-14 Patient 11 thermal images (a) Front knee (b) back knee	67
Figure 5-15 Chart showing reference temperature (grey bar) lower than the left and right knee temperatures for front of the knee	68
Figure 5-16 Chart showing reference temperature (grey bar) lower than the left and right knee temperatures for back of the knee.....	69
Figure 5-17 Thermal images showing back of knees for category III Patients	71

Figure 5-18 Thermal images for patient 1 showing the (a) front and (b) back of ankles (The warmer regions are the darkest spots as indicated in the colour bar)	73
Figure 5-19: TI for patient 9 showing the front and back of ankles (The hotter regions are the darker regions)	74
Figure 5-20: TI for Patient 13 showing the front and back of ankles (darker regions are warmest)	75
Figure 5-21: TI for patient 7 showing the front and back of ankles (darker regions are warmest)	76
Figure 5-22 Comparing left ankle, right ankle and reference temperatures for front of ankles	77
Figure 5-23 Comparing left ankle, right ankle and reference temperatures for back of ankles	78
Figure 6-1 The cropped knee region and areas under them used to obtain the reference are shown.	83
Figure 6-2 Sample of knee segmented regions after cropping showing the black background of the cropped ROIs in (a) and (b).....	84
Figure 6-3 Sample images used to test similarity algorithm (Keen, 2005)	86
Figure 7-1 ADXL335 accelerometer	96
Figure 7-2 Arduino MEGA 2560 hooked up with accelerometer connections.....	97
Figure 7-3 Experimental setup using four accelerometers for estimating tilt angles	98
Figure 7-4 Model of hinge joint showing attached accelerometer sensors	99
Figure 7-5 Flexible goniometer	99
Figure 7-6 Photo of the accelerometers and microcontroller housed in suitable casings	100

Figure 7-7 Photo of the microcontroller housed in a waist pouch	101
Figure 7-8 Accelerometers strapped to the thighs and shanks of an adult subject	101
Figure 7-9 Flexion and Extension (Global Alliance for Musculoskeletal Health, 2015)	102
Figure 7-10 Typical knee showing accelerometer positions and knee angle, α (Seel, Raisch, & Schauer, 2014).....	103
Figure 7-11: Sample accelerometer signal from characterised with noise	105
Figure 7-12 Sample accelerometer filtered signal	105
Figure 7-13 Accelerometer and protractor measurements.....	107
Figure 7-14 Accelerometer estimated angles from the hinge joint experiment.....	108
Figure 7-15 Measurements from (a) left leg (b) right leg showing relationship between the movement data (Snippets)	109
Figure 7-16 Histograms of data for (a) left and (b) right legs (Nwaizu, Saatchi, & Burke, 2016)	110
Figure 7-17 STFT of movement angles for the (a) left and (b) right legs. Higher amplitudes are shown in bright red up to 40 seconds and the yellow colour thereafter shows reduced relative amplitude (Nwaizu, Saatchi, & Burke, 2016).....	112
Figure 7-18 Angle measurement for (a) left leg (b) right leg, subject laid on his back.	113
Figure 7-19 Short-time Fourier transform of legs' angular movement, subject laid on his back	114
Figure 7-20 Angle measurements from the (a) left and (b) right legs, subject walking	115
Figure 7-21 Short-time Fourier transform of the legs' angular rotation signal, subject walking	116

Figure 7-22 Sample walking signal showing forward swing, backward swing and heel strike region in the oval section	117
Figure 7-23 Lying down ROM	119
Figure 7-24 Movement frequency and data distribution for both legs	119
Figure 7-25 Walking ROM	120
Figure 7-26 Frequency components of the walking signal	120
Figure 7-27 STFT showing the dominant 0.9Hz frequency component	125

List of Tables

Table 4-1 Clinical diagnosis for each patient	49
Table 4-2 Demographic analysis	48
Table 4-3 FLIR T630sc specification (FLIR, 2016)	51
Table 5-1 TI mean temperatures and temperature difference – Category I - Knees	63
Table 5-2 Mean temperatures and PTD for back of knees	65
Table 5-3 Front and back knee temperatures for when both knees are diagnosed with active arthritis	68
Table 5-4 Average PTD for category I and II.....	69
Table 5-5 Front and back knee mean temperatures with no active arthritis.....	70
Table 5-6 Average PTD for category I and III.....	70
Table 5-7 Front ankle results for patients with one active ankle arthritis.....	72
Table 5-8 Back ankle results for patients with one active ankle arthritis.....	73
Table 5-9 Patients with active arthritis in both ankles	77
Table 5-10: Average PTD for Patients in categories I and II.....	79
Table 5-11 Patients with no active ankle arthritis	79
Table 5-12: Average PTD between patients in categories I and III	80
Table 6-1 Correlation between VI using ‘under same knee’ reference, consultant’s evaluation and TI results	88
Table 6-2 Correlation between VI using common reference, consultant’s evaluation and TI results	89
Table 6-3 Back of the knee correlation between VI, consultants’ evaluation and TI	90

Table 6-4 Correlation between VI, consultant’s evaluation and TI results for front of the ankle	91
Table 6-5 Correlation between VI, consultant’s evaluation and TI results for back of the ankle	92
Table 6-6 Correlation results (Techniques compared separately).....	93
Table 6-7 Combined correlation between VI, consultants evaluation and TI	93
Table 7-1 Accelerometer and protractor measurements and the associated absolute errors.....	106
Table 7-2 Estimated goniometer and accelerometer angles.....	108
Table 7-3 Movement information from the left and right legs	111
Table 7-4 Legs' movement's range and frequency for laid down position.....	114
Table 7-5 Legs' movement range and frequency while walking.....	116
Table 7-6 Patient 1 movement information and clinical assessment.....	118
Table 7-7 Patient 2 movement information and clinical assessment.....	122
Table 7-8 Patient 3 movement information and clinical assessment.....	123
Table 7-9 Patient 4 movement information and clinical assessment.....	124
Table 7-10 Correlation between accelerometer and clinical findings.....	126

List of acronyms

°C	Degree Celsius
μm	micrometer
Acc	Accelerometer
E _{Acc}	Accelerometer error
ADC	Analog digital converter
ADXL	The accelerometer series type
ANA	Antinuclear antibody
Anti-CCP	Anticyclic citrullinated peptide
ATD	Absolute temperature difference
cA ₁	Approximation coefficients
cD ₁	Detail coefficients
CBIR	Content-based image retrieval
CE-MRI	Contrast-enhanced magnetic resonance imaging
CF	Complementary filter
CIELAB	Colour space defined by International Commission on Illumination (CIE)
CRP	C-reactive protein
CT	Computed tomography
CYP	Children and young people
DBS	Disclosure and barring service
DFT	Discrete Fourier Transform
DSP	Digital signal processing
DWT	Discrete wavelet transforms
EE	Energy expenditure

EM	Electromagnetic
ESR	Erythrocyte sedimentation rate
F	Force
FFD	Fixed flexion deformity
FFT	Fast Fourier transforms
FIR	Far infrared
FLIR	Forward Looking Infrared/Manufacturers of the thermal camera
RF	Rheumatoid factor
HDI	Heat distribution index
HiD	Highpass decomposition
HRTI	High-resolution thermal imaging
ILAR	International League of Associations for Rheumatology
IMU	Inertial measurement unit
IR	Infrared
IRT	Infrared thermography
JIA	Juvenile idiopathic arthritis
JPEG	Joint photographic experts' group
LoD	Lowpass decomposition
LPF	Low-pass filter
LSM	Level set method
LWIR	Long wave infrared
m	mass
mK	milliKelvin
m/s ²	meter per second squared

MATLAB	Matrix laboratory
MEMS	Micro-electromechanical systems
MSX	Multi-spectral dynamic imaging
MRI	Magnetic resonance imaging
MWIR	Medium wave infrared
NCC	Normalised cross-correlation
NHS	National Health Service
NIR	Near infrared
OI	Osteogenesis imperfecta
pGALS	Paediatric Gait, Arms, Legs, Spine
PA	Physical activity
PDD	Percentage distance difference
PE	Physical examination
P-i-P	Picture-in-picture
PTD	Percentage temperature difference
RA	Rheumatoid arthritis
RGB	Red Green Blue
ROI	Region of Interest
ROM	Range of motion
SAD	Sum of absolute difference
SCH	Sheffield Children Hospital
SD	Standard deviation
SSD	Sum of squared difference
STFT	Short-Time Fourier Transform

SWIR	Short wave infrared
TCM	Traditional Chinese Medicine
TI	Thermal imaging
USB	Universal serial bus
USS	Ultrasound scan
VAS	Visual analog scale
VI	Visual imaging
Wi-Fi	Wireless network technology
WT	Wavelet transform

Chapter 1

1 Introduction

1.1 Background and purpose of the study

Juvenile Idiopathic Arthritis, JIA, is the most common type of arthritis in children (Arthritis Foundation, 2013). Although its causes have not been well established, some research suggests it could have a genetic predisposition (Arthritis Foundation, 2013) which may cause the onset of arthritis when triggered by other environmental factors which may include infection and maternal smoking during pregnancy (Ellis, Munro, & Ponsonby, 2009). It is an auto-immune disease in which the joints' tissues are attacked mistakenly by the body's immune system, thereby making the joints inflamed. Increased temperature, swelling, stiffness, colour changes at the affected joints are some of the clinical diagnostic observations. Early diagnosis and treatment may reduce the likelihood of the joints being permanently damaged and give a more positive outcome. Diagnosis is usually by medical history and physical examinations, which may be supported by laboratory and imaging tests. Although there is no cure for JIA, there are medications to control the progression of the disease and to reduce its symptoms such as joint pain and movement restriction thus improving quality of life (Arthritis Foundation, 2013).

Current assessment of joint inflammation in JIA has limitations. Initial clinical assessment of joint swelling, warmth, and restriction is performed by touch and thus it has subjective variations leading to diagnostic complications and poorer treatment outcomes (Foster et al., 2007; Wallace et al., 2012). A preliminary study demonstrated the variations in the correlation between touch and thermometer measurement of joint skin temperature (Hawley, Offiah, Hawley, & Burke, 2015). Blood inflammatory-marker assessment, although available, they may not be conclusive (NHS, 2016a). Joint ultrasound scanning (USS) has been shown to be useful (Ramos, Ceccarelli, & Jousse-Joulin, 2012; Spalding et al., 2008) but it requires specialist expertise (Lerkvaleekul et al., 2017; Spalding et al., 2008). Contrast-Enhanced Magnetic Resonance Imaging (CE-MRI) is recognised as the 'gold standard' for identifying joint synovitis (Hemke et al., 2014; E. Miller, Uleryk, & Doria, 2009). It can demonstrate early features of arthritis such as bone oedema and is more sensitive than radiography at detecting erosive bone

changes (Ostergaard et al., 2005); however, the cost of CE-MRI can make it inaccessible for routine clinical use (Hemke et al., 2014; Ramos et al., 2012).

There is, therefore, a need for the development of techniques that are cost effective, objective, easily applicable and portable, to assist clinicians in their JIA diagnosis. The purpose of this study is to develop and evaluate thermal and visual imaging and accelerometry techniques to assist clinicians in JIA diagnosis.

High-Resolution Thermal Imaging (HRTI) refers to the technique of accurately measuring and analysing temperatures in a non-contact manner. Its application to arthritic joints potentially provides a non-invasive, portable and inexpensive addition to currently available tools, and may be useful for measuring physiological parameters such as temperature, making a diagnosis, monitoring disease progression and responding to medical treatment. HRTI may be performed more frequently than invasive measures (blood testing) or expensive imaging in Children and Young People (CYP) to track disease progression and thus facilitate a timelier intervention than is currently possible.

In this study, HRTI techniques were developed to measure skin temperature to assess and to determine whether the arthritic joints were warmer than healthy joints. Visual imaging techniques were developed and evaluated to quantify possible skin colour changes at the arthritic joint. An accelerometry system was developed to measure the joint's range of movement restriction.

The study was in collaboration with the Sheffield Children Hospital (SCH). Thermal and visual imaging approaches were evaluated on twenty patients with a JIA diagnosis and the accelerometry technique was evaluated on four patients (of these four, two were part of the thermal and visual imaging study).

1.2 Aim and Objectives

The aim of this study is to evaluate thermal, visual imaging and accelerometry techniques to assist in clinical JIA diagnosis.

1.2.1 Objectives

- i. Develop techniques to segment the thermal imaging (TI) and visual imaging (VI) ROIs from the recorded videos.

- ii. Implement techniques to track the regions of interest (ROIs) in the recorded thermal imaging (TI) videos.
- iii. Develop image processing methods to measure mean temperatures of the TI ROIs and quantify skin colour changes of the VI ROIs.
- iv. Design an accelerometry system and develop techniques to collect, interpret and process the accelerometry data.
- v. Critically evaluate developed systems on CYP at the SCH in comparison with the consultant's evaluation.

1.3 Contribution to knowledge

The study's contributions are:

- i. Development of a new method for identifying the Regions of Interest (ROIs) on the surface of the knees and ankles for segmentation. One of the challenges in this study was identifying the knee and ankle regions to be selected as ROI. A method which uses the curvature of the knees and ankles as a reference was designed. A circle was placed around the curves, and a region 1.5 times the radius vertically up and down the circle was selected for reference. For the back of the ankles, due to the heel bone being immediately under the ankle bone, only the region 1.5 times the radius vertically upwards to the bottom of the circle was considered for ROI. This method for identifying the ROIs was repeated for the knees and ankles of every patient. This identification process introduced a less subjective way to segment the knees and ankles such that about the same region is segmented every time.
- ii. Adaptation of a template matching tracking algorithm in the thermal imaging study to track the segmented ROI in all the images from a patient. A 20-second video recording (frame capture rate=30 frames per second) was performed and due to small body movements, that may be made during the recording (even though patients were advised to stand as still as possible), a means to track the ROI on all images was necessary. A template/ROI was manually selected from the first image, and using the normalised cross-correlation method (which measures the similarity between the template and the image under it), the template was compared with the next image in the recorded file, to produce the correlation coefficients for each pixel in that image. The pixel with the

highest correlation was used to identify the template. This was repeated for all subsequent images in the recording for each patient and the ROIs were tracked effectively. The algorithm was evaluated in the university with a volunteer making instructed body movement in the different directions during a recording session.

- iii. Design of a method to quantify the colour changes on the knees and ankles from the visual imaging study. The colour changes on the knees and ankles of the patients that took part in this study were not visually noticeable, so to compare the ROIs (knees or ankles), a reference image method was adapted. A region mid-way between the knee and ankle was selected for both the left and right side, averaged and used as a common reference image. This reference region was considered as it was visible in the images and was least affected by arthritis. The colour distributions (histogram) of the knees, ankles and reference regions were computed. The similarity between the left and right knees or ankles and the reference image was computed by finding the Euclidean distance between their colour distributions. The knee or ankle with the higher Euclidean distance to the reference image indicated a higher difference to the reference region and so had more colour changes.
- iv. Development of an accelerometry system (hardware/software) to record movements of legs at the knee joint. For each leg, an accelerometer was placed just above and another just below the knee. The recorded accelerometry signals were filtered using a digital Butterworth low pass filter of the 3rd order with a suitable cut-off frequency determined by first finding the frequency spectrum of the signal between 0.5Hz to 3Hz (depending on the movement scenario). The angles of tilt of the thighs and shanks were computed in the range of -180° to 180°. The relative knee angle was obtained by adding the thigh and shank tilt angles and subtracting from 180° and 360° for the lying down and walking scenarios respectively. The angular movement velocity, acceleration, and displacement were also determined, and the results were compared between the left and right knees.
- v. The findings from thermal imaging, visual imaging, and accelerometry developments were correlated against the consultant's assessment in identifying inflamed joints in patients with JIA. Clinical diagnosis of active

arthritis was performed using the validated pGALS (paediatric Gait, Arm, Leg, Spine) approach to check for joint warmth, swelling, and restriction plus history of symptoms. The thermal and visual imaging studies were simultaneously compared with the clinical assessment to determine their correlations. All three techniques were also separately evaluated against the clinical assessment to determine their correlation as well.

1.4 Thesis outline

The outline of the thesis is arranged as follows:

Chapter Two: Literature Review. This chapter reviews previous related studies in relation to arthritis and its diagnosis, thermal, visual imaging and accelerometry techniques.

Chapter Three: Study's related theory. This chapter gives a theoretical explanation of JIA, HRTI, Accelerometry and its operation, signal and image processing.

Chapter Four: Methodology. This chapter discusses the ethical approval, patient recruitment process and details, and the clinical diagnosis.

Chapter Five: Results and Discussion Related to Thermal imaging to assist with Juvenile Idiopathic Arthritis Clinical Assessment. This chapter discusses the developments of the thermal imaging system and the results as compared with the consultant's evaluation.

Chapter Six: Visual imaging (VI) and its correlation with thermal imaging to assist with JIA diagnosis. This chapter discusses the developments of the visual imaging system and the results as compared with both thermal imaging and the consultant's evaluation.

Chapter Seven: Accelerometry to aid assessment of joint movement in JIA. This chapter discusses the accelerometry system developments and the results in comparison with the consultant's evaluation.

Chapter Eight: Conclusions and further work. This chapter summarises the study and recommends some future research.

1.5 Summary

This chapter briefly introduced JIA and the techniques that were investigated in this study. It presented the study's background and purpose, aim and objectives. It further outlined the contributions to knowledge and the arrangement of the thesis chapters.

JIA, which is the most common type of arthritis in children, is an auto-immune disease whereby the immune system mistakenly attacks the joint tissues causing inflammation. Symptoms can include joint warmth, redness, movement restriction etc. Current assessment of JIA has limitations and so research is ongoing to develop techniques that are cost-effective, easily applicable and portable, that may assist clinical diagnosis of JIA.

In this study, High Resolution Thermal Imaging (HRTI), visual imaging and accelerometry techniques were evaluated for clinical JIA assessment. The results obtained were compared against consultants' diagnosis of JIA on twenty-two patients from the Sheffield Children Hospital (SCH).

The next chapter presents a review of literatures related to this study.

Chapter 2

2 Literature Review

Arthritis, which literally means joint inflammation (Arthritis Care, 2016), is a type of disease that affects the joints of the body. The disease is characterised by the progressive breakdown of the cartilage (Taieb, Bruel, & Auges, 2014), the smooth material covering the ends of the bones in the joints to prevent the bones rubbing against each other (Woods, 2004). The symptoms generally include joint pain and stiffness. This condition can cause suffering in a serious manner termed inflammatory flare-up or in a more prolonged manner which can sometimes cause severe disability (Taieb et al., 2014). Without early diagnosis and treatment, this condition can ultimately lead to bone erosion and cartilage damage (Suma, Snehalatha, & Rajalakshmi, 2016).

There are over 100 types of arthritic conditions. Most studies where Infrared thermography (IRT) have been applied for assessing joint inflammation is mainly focused on rheumatoid arthritis (RA) and there is a very limited study on Juvenile idiopathic arthritis (JIA) (Lerkvaleekul et al., 2017). This study, however, focuses on JIA, which is a type of rheumatoid arthritis that affects children, because it is an area of research less developed and our collaboration with Sheffield Children's Hospital.

JIA can be a serious and a disabling condition which may lead to complications such as joint destruction, impaired joint function, limitation of growth and osteoporosis (McMahon & Tattersall, 2011). Early detection and treatment can help alter the natural progression of the disease (McMahon & Tattersall, 2011). A quicker and more effective diagnostic system is therefore essential. This chapter discusses the related literature in arthritis diagnosis. The current methods will be reviewed, followed by studies involving the use of some other alternative methods such as the thermal imaging (TI), IMUs and visual imaging systems, with the aim to show the current state of knowledge.

2.1 Current methods for diagnosing JIA

The existing methods include those outlined in this section. Clinical diagnosis of inflammatory joint (McMahon & Tattersall, 2011) through physical examination (PE).

Features normally looked out for include joint warmth, swelling, and stiffness. These are subjective as it is down to the clinician's experience and expertise, hence disease may not be accurately diagnosed.

Clinicians perform the pGALS (Paediatric Gait Arms Legs Spine) examination, a more validated screening tool, to assess joint inflammation (Foster, Kay, Friswell, Coady, & Myers, 2006). However, this system has its limitations as it requires the expertise of the clinician and sometimes can require further testing using another method such as the MRI scanning to confirm the clinical suspicion.

Routine blood tests can also be used to diagnose the condition, although no blood test on its own, can confirm a diagnosis, however, a few tests can give possible indications of the disease (NHS, 2016a). Full blood count which measures the red cells in the body can show evidence of inflammation with anaemia (as anaemia is common in people with arthritis), raised white cell count and thrombocytosis (McMahon & Tattersall, 2011; NHS, 2016a). Blood tests to check the levels of certain proteins and other chemicals in the blood may also give an indication of the disease. Tests such as erythrocyte sedimentation rate (ESR), c-reactive protein (CRP), antinuclear antibody (ANA), rheumatoid factor (RF), etc. (Arthritis Foundation, 2013).

Imaging technologies which include x-rays, computed tomography (CT) scans, bone scintigraphy, ultrasound scans (US), contrast enhanced magnetic resonance imaging (CE-MRI) are also systems that are used for JIA diagnosis. These systems although effective, have limitations. The CE-MRIs can be expensive (currently about £350 per scan (Fairfield Independent Hospital, 2019)) and may not be well tolerated by younger children as it takes about 15 to 90 minutes to perform (Stanford Health Care, 2019a). There is a risk of an allergic reaction to the contrast dye used (Stanford Health Care, 2019b). MRI machines are also less available (McMahon & Tattersall, 2011). Plain radiographs (X-ray) are not sensitive to early changes in the condition and ultrasound (US) scans, although relatively cost-effective is highly user-dependent as it requires a physician's expertise (Giancane et al., 2016; Lerkvaleekul et al., 2017; Spalding et al., 2008). There is also the radiation effect from the X-rays and CT scans (Mohiyuddin, Dhage, & Warhade, 2014).

Due to the importance of early detection and monitoring of this condition, research is ongoing on alternative methods that can be used for diagnosis that will be accurate, objective, non-invasive and cost-effective. As part of achieving this objective, in this study the effectiveness of thermal imaging, visual imaging and accelerometry is investigated. In the next section, a review of these techniques is provided.

2.2 Thermal imaging

2.2.1 Thermography in medicine

Modern infrared thermography has opened new opportunities in medical diagnosis especially in its use to map surface skin temperature; and since the 1960s, there is now more understanding of the relationship between skin temperature and blood perfusion (Ring, 2010). In a diabetic study, IRT has proved useful in assessing tissue viability and peripheral circulation that could be used to indicate the level of a major limb amputation (Ring, 2010).

Thermal imaging has proved effective as a noncontact real-time method of measuring respiration rate (Alkali, Saatchi, Elphick, & Burke, 2017). In children, IRT has been found to be a well-tolerated technology in the management of children in the emergency unit with acute non-specific limp (Owen, Ramlakhan, Saatchi, & Burke, 2018) and has also been used to detect thoracic vertebral fractures in children and young people with osteogenesis imperfecta (OI) (De Salis, Saatchi, & Dimitri, 2018).

2.2.2 IRT for diagnosing arthritis

Joint warmth is an indication of active inflammation due to arthritis - during active inflammation in deep tissues and joints, the surface skin would normally show changes in thermal behaviour (Mohiyuddin et al., 2014); hence the ability to measure the temperature at these joints can aid the diagnosis of arthritis. Infrared thermography (IRT) or thermal imaging is ideally suited for studying skin temperatures because the human epidermis has a high emissivity (Mohiyuddin et al., 2014).

The association between temperature and disease is centuries old (Ring, 1990). Thermal imaging systems were first developed in the 1930s, and they enable the human eyes to see beyond the short-wavelength red into the far infrared (IR) by making the light naturally emitted by warm objects visible (Lloyd, 2013). They are a fast, passive and non-contact alternative to the existing arthritis diagnostic methods.

There is an enormous interest in the application of thermography in medicine as it has shown good potential to be used as a diagnostic tool for identifying diseases.

The study by Mohiyuddin et al. (2014) successfully applied IRT technique and fuzzy-c-means algorithm to detect rheumatoid arthritis (RA) in various parts of the body. The fuzzy-c means algorithm was used to automatically segment the region of interest (ROI) to be analysed. The Heat Distribution Index (HDI) and skin temperature measurements of subjects with active arthritis were compared with that of unaffected persons. The thermal image where there was active arthritis was seen to be warmer than those of the unaffected subjects.

Another study on RA was conducted by Frize et al. (2011). Thermal images from the hand, wrist, palm, and knee joints were studied. The regions of interest (ROIs) were manually selected for processing and they concluded that RA can be reliably detected in patients using thermal imaging.

Lasanen et al. (2015) investigated IRT technique for screening joint inflammation and rheumatoid arthritis in children focusing on the knee and ankle joints. In analysing the data collected, the mean and maximum surface temperatures were determined for the selected ROIs at the medial and lateral view of the knees and ankles. Their results were compared against clinical evaluations. They observed that in inflamed ankle joints maximum and mean temperatures were significantly higher than in non-inflamed ankles. However, there was no significant difference for the knee joints.

Thermal imaging technique has been compared with ultrasonography with PE for diagnosing wrist arthritis in JIA as seen in the study by Lerkvaleekul et al. (2017). The temperature of the room was maintained at approximately 22° with humidity at 50%. The mean and maximum temperatures in the ROI were observed to be higher in the affected group. The HDI (defined as two standard deviations) of the ROIs were also higher in the moderate to severe group than in the healthy control. They concluded that both IRT and ultrasound were applicable tools for detecting wrist arthritis.

Snehalatha, Anburajan, Sowmiya, Venkatraman and Menaka (2015) tested the ability of some features extracted from the thermographs such as mean, standard deviation, entropy, skewness, kurtosis, etc. to evaluate rheumatoid arthritis. They compared these parameters with measured skin temperature indices such as HDI and

thermographic index and they concluded that the temperature indices correlated significantly with most of the parameters measured.

IRT has been compared with x-ray for evaluating RA using a biochemical method as the standard (Snehalatha, Rajalakshmi, Gopikrishnan, & Gupta, 2017). They observed that the IRT technique was able to detect the disease at an earlier stage than the radiography method.

Varju, Pieper, Renner and Kraus (2004) hypothesized that the surface temperature of the joints could complement the radiographic evaluation of osteoarthritis. Jin, Yang, Xue, Liu and Liu (2013) proposed an automated system for thermal screening of knee osteoarthritis that can provide quantitative information which can further aid in clinical diagnosis. Naz, Ahmad and Karandikar (2015) proposed a thermal image and neural networks method for predicting arthritis in its early stages. Neural networking was used to classify the image inputted into the system as normal or abnormal based on a backpropagation algorithm. Brenner, Braun, Oster and Gulko (2006) monitored inflammatory arthritis activities using thermal imaging in small joints of rat models and concluded the thermal measurements correlated significantly with arthritis activity.

Borojevic et al. (2011) investigated the thermal images of the hands of healthy subjects, patients with rheumatoid arthritis and osteoarthritis and observed there was statistically significant difference in the mean temperature values of healthy, rheumatoid arthritis and osteoarthritis subjects. Ilowite, Walco, and Pochaczewsky (1992) showed that there was significant correlation between pain intensity ratings obtained using the visual analogue scales (VAS) scores from patients, parent and doctor of patients with JIA and joint temperatures obtained from their thermal images. The clinical utility of thermal imaging in assessing arthritis was further demonstrated by Sanchez et al. (2008). Thermal imaging was shown to be effective in identifying inflamed joints by accurately distinguishing between the thermal patterns of normal and synovitis-affected joints (these did not have a normal pattern) (Salisbury, Parr, De Silva, Hazleman, and Page-Thomas, 1983).

Given the findings in the literature, thermal imaging has the potential for evaluating arthritis and so research is ongoing to make the technique more accurate and

adaptable for use in clinics to assist clinicians make a more informed and early diagnosis.

2.2.3 Image segmentation

Image segmentation is one of the vital steps involved in image processing and analysis as the accuracy of diagnosis depends on how well the selection of the ROI is performed (Duarte et al., 2014). It allows for extraction of useful information from images such as finding shapes, identifying colours or measuring object properties. (MathWorks, 2019a). It is also a process used to extract the ROI from an image removing background and noise (Suma et al., 2016).

Segmentation is one of the major challenges faced in processing images as sometimes; region of interest (ROI) is not properly selected without excluding important information or including unwanted noise, such as when using segmentation shapes like rectangles and ellipse which sometimes do not allow selecting the desired ROI.

Improvements in image segmentation techniques have been explored. Duarte et al. (2014) proposed a segmentation technique based on the thresholding method that allows ROIs to be selected independent of its geometric shape for generic applications.

Automated segmentation of hot spots of the hand for evaluation of RA based on the k-means algorithm was developed and was found to be effective in evaluating the disease (Snehalatha et al., 2015).

Qiao, Wei and Zhao (2017) developed an intensity adjustment level set method (LSM) in pedestrian images to address the boundary leakage and intensity homogeneity problems seen in the traditional LSM segmentation method. This LSM method is based on the edge-based active contour model.

Chen, Chen and Ni (2016) developed a semiautomatic segmentation method that involves the use of information from another optical camera which helps to improve the precision of contour sketching of objects in thermal images. Yasaswi, Keerthi, Jainab, Krishna and Sridhar (2015) explored the watershed city-block distance transform segmentation approach for detecting faulty electric circuit.

2.3 Colour analysis for medical diagnosis

Redness around the affected joint is one of the possible indicators of active rheumatoid arthritis, which is when the joint becomes inflamed (Arthritis Foundation, 2013; NHS, 2016b; Versus Arthritis, 2018a).

In this study, the colour of the affected joints was also analysed for evaluation of arthritis to see if the possible redness at the affected joints can be quantified. Although there is not any recorded research on the use of the skin colour parameter for assessing arthritis, however, colour has been used in diagnosing other medical conditions.

Disease diagnosis through inspection of facial and body colour has been in existence for thousands of years in Traditional Chinese Medicine (TCM) but this method is very subjective and qualitative. Due to the benefits of this method, however, which includes being non-invasive, the objectification and quantification of the method in order to be used for clinical diagnosis has been greatly researched (Chen, Zhang, Wu, & Zhang, 2016; Liu & Wang, 2006). Most of the work is focused on using tongue colour and facial colour to diagnose diseases.

Liu and Guo (2008) proposed a method to quantify facial colour diagnosis of TCM (which is normally subjective and down to the human eyes). There is enormous interest in facial colour diagnosis both in clinical medicine and biomedicine because of its role in the diagnosis and treatment of diseases as lesions (such as wound, tumour or ulcer) in the body does change facial colour. They presented a computer-aided diagnosis method for evaluation of hepatitis. Colour feature from the face was extracted from facial images using image processing techniques and their system was able to classify the face colours into healthy, severe hepatitis with jaundice, severe hepatitis without jaundice with accuracy higher than 73%.

Li et al. (2008) proposed a method for classifying tongue colours for TCM using the CIELAB colour space and then developed a numerical method for colour classification based on the TCM and concluded, their system could classify the tongue colours close to those given by human vision and can be used in clinical diagnosis. Zhang, Wang, You and Zhang (2013) developed a tongue colour analysis system for medical diagnosis using the tongue colour gamut. Their system was able to classify a given tongue

sample into healthy or diseased with an accuracy rate of 91.99%. They observed that there was a relationship between the state of the human body and its tongue colour. Tongue colour has also been investigated for assessment of gastroesophageal disease (Kainuma et al., 2015).

Chen et al. (2016) worked on facial colour feature extraction for diagnostic purposes using non-standard colours to represent the facial colour space. Face colour has also been proposed for diagnosing heart diseases (Kim, Lee, Cho, & Oh, 2008).

Wang, Zhang, Guo and Zhang (2013) proposed a computerised facial image analysis system that uses quantitative colour features extracted by fuzzy clustering method for disease diagnosis applications. They evaluated three types of health conditions - healthy, icterohepatitis (inflammation of the liver with marked jaundice), and severe hepatitis. Experiments conducted were compared with a database of more than 300 images and they concluded the system could classify these images into these conditions with an accuracy of more than 88%.

These studies show that the colour feature technique is useful and may potentially be an effective tool in medical diagnosis.

2.3.1 Colour similarity measurement

In this study, the regions of interest from the visual images were compared based on their colour features to determine which joint had more colour changes.

Colour histograms, which represents the colour distribution of the three colour channels, RGB (Red Green Blue) is the simplest and the most often used colour feature, and it is frequently used with the Euclidean distance as the colour metric to give an efficient and undemanding colour similarity retrieval method (Mojsilovic, Hu, & Soljanin, 2002).

Narwade and Kumar (2016) applied colour histogram colour feature method in image retrieval applications. The colour features of the reference image and images in the database were computed using the local colour features combined to represent the colour histogram. The Euclidean distance metric was then used to determine the similarity between the reference image and the images in the database.

Mali and Tejaswini (2014) also developed a technique based on the low-level image histogram feature for image retrieval application. They have adopted this method because histogram-based systems are quick and simple to compute. They have also applied the Euclidean distance metric to measure the similarity between the images. The higher the distance between the images, the greater the difference between them.

Kodituwakku and Selvarajah (2004) performed an experimental comparison of some colour descriptors – colour histograms, colour moment and colour coherent vector (CCV) for content-based image retrieval (CBIR) applications to determine which was more efficient in representing similarity of colour images in the RGB colour space. They concluded the performance of the techniques depended on the distribution of the images.

The colour histogram – Euclidean distance method was implemented in this study to compare the colour images as it has been reported to be computationally simple and efficient.

2.4 Accelerometry based applications

2.4.1 Human movement and balance

The third approach considered in this study for evaluating arthritis is the accelerometry system to quantify joint movements. Arthritis is a joint disease that can cause stiffness at the joints; hence the ability to measure movements at the joints such as the range of motion (ROM) will assist in clinical diagnosis and rehabilitation (Nwaizu, Saatchi, & Burke, 2016).

The conventional gold standard for measuring and monitoring general human movements including joints' angle is optically based. Its setup involves placing several cameras around a walkway, and reflective markers on the joints. As the subject moves, the system produces the 3D spatial movements of the markers, while a software determines an estimate of joints' angles or the gait parameters (Djurić-Jovičić, Jovičić, & Popović, 2011; Nwaizu, Saatchi, & Burke, 2016). However, this approach is restricted to monitoring in specific gait laboratories as it requires an expensive setup and so it is not very practical for routine clinical use or assessment of patient's activities in their home environment. An alternative method for measuring joint range of motion is with

electrogoniometers. However, this approach requires a trained clinician to operate; it is time-consuming to perform and is not sufficiently robust for daily clinical use (Bakhshi, Mahoor, & Davidson, 2011; Djurić-Jovičić et al., 2011; Nwaizu, Saatchi, & Burke, 2016).

To overcome these limitations, researchers have been exploring alternative methods of measuring human movements and balance. Recent developments in micro-electromechanical systems (MEMS) have resulted in portable, relatively affordable and wearable sensors such as accelerometers, gyroscopes, magnetometers. These can be used either individually or they can be integrated into a single chip as an inertial measurement unit (IMU), for measuring movements in three orthogonal axes, typically referred to as x , y , and z . Extensive research has been carried out in developing these sensors as they have the potential to provide more practical solutions for clinical use and for patient's movement monitoring in their home environments (Nwaizu, Saatchi, & Burke, 2016).

The challenges in using the combined accelerometer and gyroscope unit are computational problems for determining the angles (Djurić-Jovičić et al., 2011) also, the effect of offset errors on the gyroscope's output, as a gyroscope provides a rate of rotation and integration of its output is needed to determine the amount of an object's rotation (Fisher, 2010).

Accelerometers are types of inertial sensors and have been generally accepted as useful and practical sensors to measure and assess movement (Yang & Hsu, 2010). Researchers have shown enormous interest in this subject due to the many benefits of using inertial sensors to measure and monitor human movement and balance such as the low cost, small size, low power consumption, remote monitoring capabilities, etc. This approach involves strapping the sensor in some way to the body part of interest and taking measurements. It is non-invasive and so very practical for clinics, remote monitoring in the community and during activities of daily living.

Accelerometers have been reported to be highly reliable in distinguishing posture and motion for detecting cyclical movements and conditions of daily living (Foerster, Smeja, & Fahrenberg, 1999; Veltink et al., 1993).

Martinez-Mendez, Sekine and Tamura (2012) evaluated the sensitivity of accelerometry signals attached to the trunk of subjects to distinguish changes in postural balance related to age - elderly vs. young; and changes in visual conditions, and reported the results were better than the typical force plate signals. The measurements obtained from accelerometers have also been used to develop an efficient system for assessing static and dynamic balance and postural sway (Kamen, Patten, Du, & Sison, 1998).

Hendelman, Miller, Baggett, Debold and Freedson (2000) examined its ability to assess intensity levels/Energy Expenditure (EE) during different physical activities to evaluate the metabolic cost of various recreational and household activities using the accelerometer counts recorded during these activities. Chen and Bassett (2005) compared accelerometry-based activity monitors between first-generation devices and emerging technologies to predict EE. Yang and Hsu (2010) reviewed the use of accelerometry-based wearable motion detectors for physical activity (PA) monitoring and reported they allow for automatic, continuous and long-term measurement of people in free-living conditions. Accelerometers can be used to estimate EE as activity counts from the accelerometer is related to EE, can detect postural sway and important gait parameters, and detect unusual movement such as falls.

Luinge and Veltink (2004) used 3D accelerometers attached to the back of the trunk at T4/T5 level and the pelvis to estimate the inclination of the body segments for monitoring daily life task focusing on the task of lifting and stacking objects. Karantonis, Narayanan, Mathie, Lovell and Celler (2006) implemented a real-time system for classifying types of human movement associated with data obtained from a single waist-mounted triaxial accelerometer and could distinguish periods of rest and activity as well as detect different events. Kavanagh and Menz (2008) reviewed literatures that have used accelerometry for quantifying human movement during walking and concluded that the technique was accurate and reliable and could provide useful information regarding the motor control of normal walking and gait patterns.

Yeoh, Pek, Yong, Chen and Waluyo (2008) looked at the use of accelerometers for detecting posture and walking speed using a rule-based Heuristic system that can be used for real-time ambulatory monitoring and observed the results were promising. The speed of walking was the parameter used to distinguish between different types

of movement activities such as running, jogging, etc. Lyons, Culhane, Hilton, Grace and Lyons (2005) investigated techniques that allow accelerometers to distinguish between static and dynamic activities using a thresholding method. Experiments were performed in an uncontrolled environment for long hours to achieve long term ambulatory monitoring.

2.4.2 Joint Range of Movement

Willemsen, Van Alste and Boom (1990) used eight uniaxial accelerometers to determine knee angle without the need for integration, to reduce the effect of offset drift. Kurata, Makikawa, Kobayashi, Takahashi and Tokue (1998) monitored upper limb motion -elbow and shoulder joints- in daily activities using two accelerometers set at “both-near-sides” around the joints and they concluded the system was effective for one axis motion monitoring, though the accuracy of the three axes joint movement was not confirmed in the study.

Djurić-Jovičić et al., (2011) used accelerometers to estimate angles of leg segments and joints during gait, with the focus on the knee and ankle joints based on a second-order low-pass digital filter. This method did not require double integration which introduces drift effect on the results as seen with gyroscopes. The effectiveness of the developed system was compared with the results obtained from flexible goniometers and they concluded the technique was good enough for quick diagnostics of gait and its applications. Dong, Chen, Lim and Goh (2007) used four biaxial accelerometers to measure flexion-extension angles, and the system was more accurate when sensors were placed parallel to the sagittal plane.

Researchers have also considered the use of IMUs combining accelerometers and gyroscopes for measuring joint angles. Bakhshi et al. (2011) focused on measuring knee joint range of movement using two IMUs placed near the joint. Bennett, Odom and Ben-Asher (2013) developed an algorithm to measure knee angles using two IMUs and artificial neural networks. Their system was validated against the results obtained from an electro-goniometer.

2.4.3 Assessing arthritis

Accelerometers have been evaluated for distinguishing arthritis and other joint-related conditions. Reddy, Rothschild, Mandal, Gupta, and Suryanarayanan (1995) used

accelerometers to distinguish normal knees from knees affected by osteoarthritis (OA), RA and chondromalacia using the acceleration measures obtained from the knees during a leg rotation. In later research, Reddy, Rothschild, Verrall, & Joshi (2001) further applied accelerometry to distinguish knee RA and spondyloarthropathy (chronic diseases of the joints) as the subjects performed a flexion-extension rotation of the leg. They used the mean power of the signal as a parameter to characterise the disease. Significant differences were observed between RA and spondyloarthropathy patients.

Accelerometers have also been applied for monitoring the physical activities (PA) in arthritis patients in order to give an objective means of assessing the effect of the disease activity, to help clinicians make more informed recommendations to improve the health status of these patients (Hernandez-Hernandez & Diaz-Gonzalez, 2017).

Previous studies have shown accelerometers to be reliable in assessing and monitoring PA in persons with arthritis (Semanik et al., 2010; Norgaard, Twilt, Andersen, & Herlin, 2016; Pioreschi, Hodkinson, Avidon, Tikly, & McVeigh, 2013).

Hernandez-Hernandez, Ferraz-Amaro, & Diaz-Gonzalez (2014) applied accelerometry to assess the effects of RA activity on the PA of patients with rheumatoid arthritis. They concluded that RA patients spent less time (fewer minutes per day) doing moderate and vigorous PA than the healthy subjects and that the disease activity interfered significantly with the PA time of RA patients.

The impact of obesity and other modifiable factors of physical inactivity (weight, diet, smoking, knee pain, etc.) in OA patients were evaluated using accelerometers to measure their PA (Lee et al., 2013).

The daily monitoring of PA in children with JIA has also been achieved using accelerometers to determine the correlation between daily PA diary and accelerometry measures (Armbrust et al., 2017), the relationship between accelerometer-assessed PA and disease activity, report of pain intensity, use of pain coping strategies in children with JIA (Norgaard et al., 2017).

This review shows accelerometers can potentially be a useful tool to assess arthritis; however, work is ongoing to improve its functionality and make it practical for use in clinics.

In our study, the use of four triaxial accelerometers placed at the right and left thighs and shanks of a patient to measure knees' angle, velocity, acceleration, and displacement to assist JIA diagnosis was explored.

2.5 Summary

In this chapter, arthritis, which is a condition that causes pain and inflammation in a joint (NHS, 2017), was briefly discussed. The current diagnostic methods, which include clinical examination, blood tests, imaging technologies such as CT scans, US scans and CE-MRI were outlined.

Related literatures in the alternative methods of diagnosing medical conditions such as thermal imaging, colour analysis, and accelerometry were reported. TI was shown to be useful for screening joint inflammation and Rheumatoid Arthritis (RA) at the knees and ankles of children (Lasanen et al., 2015). TI was found to be applicable for detecting wrist arthritis in comparison with ultrasonography and physical examination (Lerkvaleekul et al., 2017). TI was also able to successfully detect RA at an earlier stage than the radiography method (Snehalatha et al., 2017). Body and facial colour were used to diagnose medical conditions (Chen et al., 2016; Liu & Wang, 2006) such as hepatitis (Liu & Guo, 2008), heart diseases (Kim et al., 2008). Accelerometry was proved reliable for assessing physical activities of persons with RA (Semanik et al., 2010) and for measuring joints range of motion (Djurić-Jovičić et al., 2011).

In this study, these methods have been applied for the evaluation of JIA.

In the next chapter, the theories relevant to this study are presented.

Chapter 3

3 Relevant Theory

In this chapter, the relevant theories on Juvenile idiopathic arthritis (JIA), infrared thermography, accelerometry, signal and image processing techniques, visual image processing are presented. The patients included in this study were referred to the hospital suspected of having JIA. Thermal imaging was the main tool used in this study to assist with diagnosing JIA. Accelerometry was used to investigate joint movement. Signal processing was primarily used to process the accelerometry signal. Image processing was needed for thermography and visual imaging.

3.1 Arthritis

Arthritis can be generally defined as the presence of joint inflammation with reduced range of motion, pain on movement and/or warmth of the joint (Boros & Whitehead, 2010). There are more than 100 types of arthritis with the most common being osteoarthritis, the next common is rheumatoid arthritis. Osteoarthritis normally occurs with age, whereas rheumatoid arthritis is an autoimmune disorder in which the immune system attacks the body's own tissues causing an inflammatory response - which is a normal reaction of the body to injury or infection of living tissues (Versus Arthritis, 2018b). JIA is a type of rheumatoid arthritis.

3.2 Juvenile idiopathic arthritis (JIA)

JIA is a broad term used to describe all forms of arthritis that begin before the age of 16 years, persist for more than 6 weeks and are of unknown cause (Ravelli & Martini, 2007). It is the most common childhood chronic rheumatic disease affecting about 1 in 500 children and can cause much disability (Boros & Whitehead, 2010; Prakken, Albani, & Martini, 2011). To facilitate research and treatment, the disease is generally classified based on the number of joints affected and the presence of systemic symptoms and signs (Borchers et al., 2006). The International League of Associations for Rheumatology (ILAR) classified JIA into seven categories (Boros & Whitehead, 2010) shown in Figure 3-1.

Category	Diagnostic criteria
Systemic arthritis (10–20%)	Fever of at least 2 weeks duration (daily for at least 3 days) and arthritis in one or more joints, plus one of the following: <ul style="list-style-type: none"> • erythematous rash • generalised lymph node enlargement • hepatomegaly and/or splenomegaly • serositis
Oligoarthritis (50–60%)	Arthritis affecting ≤ four joints during the first 6 months of the disease. If after 6 months more than four joints are involved the term extended oligoarthritis is used
Polyarthritis (20–30%) (rheumatoid factor negative)	Arthritis affecting ≥ five joints during the first 6 months of the disease with rheumatoid factor negative
Polyarthritis (5–10%) (rheumatoid factor positive)	Arthritis affecting ≥ five joints during the first 6 months of disease with rheumatoid factor positive on at least two occasions at least 3 months apart
Psoriatic arthritis (2–15%)	Arthritis and psoriasis or arthritis and at least two of the following: <ul style="list-style-type: none"> • dactylitis • nail pitting or onycholysis • psoriasis in a first degree relative
Enthesitis related arthritis (1–7%)	Arthritis and enthesitis or arthritis or enthesitis with at least two of the following: <ul style="list-style-type: none"> • presence/history of sacroiliac joint tenderness and/or inflammatory lumbosacral pain and HLA-B27 positive • onset of arthritis in a male over 6 years of age • acute (symptomatic) anterior uveitis • history of ankylosing spondylitis, enthesitis related arthritis, sacroiliitis with inflammatory bowel disease or acute anterior uveitis in a first degree relative
Undifferentiated arthritis	Arthritis that fulfils criteria in no category or in two or more of the above categories

Figure 3-1 International League of Associations for Rheumatology classification of JIA (Boros & Whitehead, 2010)

3.2.1 Symptoms

The symptoms include (Chang, Burke, & Glass, 2010): morning stiffness, pain, swelling, and tenderness in the joints; limping, fever, rash, weight loss, fatigue or irritability; and eye redness, pain, or blurred vision. Chronic eye inflammation occurs in 10% to 20% of all patients; of these, 30% to 40% have a severe loss of vision. Redness around the affected joint is also a possible symptom of joint inflammation (Arthritis Foundation, 2013). If untreated, this condition can cause complete loss or impaired vision, permanent damage and loss of function at the joints, interference with the growth of

the bone and inflammation of membranes around the heart and lungs (Chang et al., 2010).

3.2.2 Causes

The cause of the disease is unknown. It is, however, an autoimmune disease, whereby, the immune system attacks the lining of the joints called the synovium (Bailey, 2014) thereby causing inflammation and swelling of the lining and fluid in the joints. Figure 3-2 shows a cross-section of a healthy and JIA- affected knee joint.

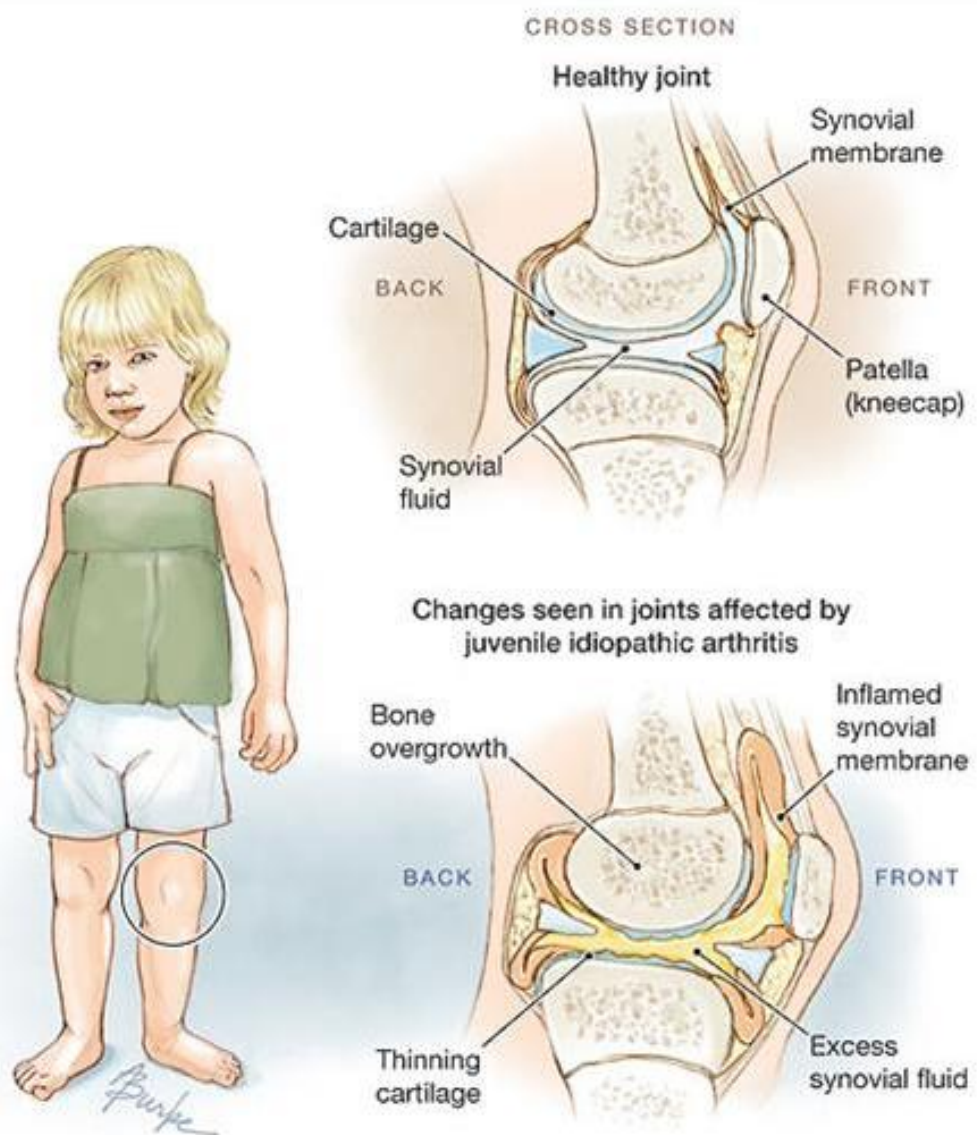


Figure 3-2 Cross section of healthy and JIA affected joint (Chang et al., 2010)

3.2.3 Diagnosis

Once the disease is suspected, diagnosis normally includes the methods listed in the next subsections (Giancane et al., 2016):

3.2.3.1 Clinical evaluation

This involves a detailed physical examination of all body joints where the clinician checks for joint swelling, warmth, redness, and restriction. The clinician also takes a family history, personal history and recent arthritis symptoms/pathologic events with specific attention to pain and morning stiffness. Family history is taken as it can indicate one's risk of developing RA. After the examination, the clinician normally gives an overall rating of the disease activity ranging from zero (no activity) to ten (maximum activity) on a visual analog scale (VAS). For systemic JIA, diagnosis may be difficult as arthritis is often not present at the onset. However, this method is subjective.

3.2.3.1.1 pGALS

Foster and Jandial (2008) describe pGALS (Paediatric Gait, Arms, Legs, Spine) as an evidence-based musculoskeletal (MSK) screening assessment tool that has been validated for school-aged children. The assessment normally involves simple manoeuvres that are commonly used in clinics and is quick to perform (takes about 2 minutes) and well tolerated by the child and parent/carer. pGALS has been shown to be highly sensitive in detecting movement anomalies. The assessment is performed when the child presents one or more of the following symptoms (Foster & Jandial, 2008):

- Muscle, joint or bone pain
- Unwell with pyrexia (fever)
- Limping
- Delay in achieving or a regression of motor milestones
- Clumsiness with no known neurological disease.
- Presence of a chronic disease that has MSK presentations.

Three screening questions relating to pains and problems with dressing themselves or walking are initially asked by the clinician before full examination of the Gait, arms, legs and spine of the child is performed while checking for any appearance or movement abnormality (Foster & Jandial, 2008).

3.2.3.2 Imaging

Radiography: Also known as the plain X-rays are the conventional gold standard imaging method for diagnosing arthritis. X-rays are a type of radiation that can pass through the body to produce images of the inside of the body (NHS, 2015a). At the first instance, they can help to exclude other causes of pains and swelling at the joints; they can also detect late complications of JIA (Sheybani, Khanna, White, & Demertzis, 2013). However, this method exposes the body to ionising radiation, has poor sensitivity in identifying active synovitis (inflammation of the synovial membrane) and limited ability to detect erosive changes in the joint at the onset of the disease.

Contrast-Enhanced Magnetic Resonance Imaging (CE-MRI): CE-MRI is a type of scan that uses strong magnetic fields and radio waves to produce detailed images of the inside of the body (NHS, 2018) with contrast enhancement to improve the image quality. This method is the most sensitive for detecting active synovitis at the early stages of the disease. It is also able to identify bone marrow Oedema (abnormal accumulation of fluid) which is considered a pre-erosive abnormality and therefore an indication to begin early treatment. It does not expose the body to x-ray radiation and so is a more preferred technique. However, despite these benefits, CE-MRI examinations are very lengthy and costly; require intravenous administration of the contrast material (dye) to maintain sensitivity and frequent sedation of the patient (Sheybani et al., 2013). The contrast-medium for enhancing the image quality also has to be carefully selected based on criteria of safety, tolerability, and efficacy, as seen in in age-specific clinical trials and personal experience (Bhargava et al., 2013)

Ultrasonography (US): This procedure uses high- frequency sound waves to create an image of part of the inside of the body; the technique is very safe and does not involve exposure to radiation (NHS, 2015b). It is relatively inexpensive and more readily available than the MRI machines; it can reliably detect synovitis, joint effusion, cartilage damage and does not require sedation of the patient. However, this procedure is highly operator dependent (Sheybani et al., 2013) and requires training and a careful interpretation of the abnormalities (Giancane et al., 2016).

3.2.3.3 Laboratory blood test

A test for certain proteins in the blood can aid an RA diagnosis. Most patients with RA would test positive to rheumatoid factor (RF) and anticyclic citrullinated peptide (anti-

CCP) antibodies, as well as have an elevated erythrocyte sedimentation rate (ESR) and C-reactive protein (CRP) (Pincus & Sokka, 2009). However, more than 30% of RA patients have a negative test for RF and anti-CCP antibodies and more than 40% have a normal ESR and CRP. These findings show that though the blood tests can aid in diagnosing certain patients, it is not a definitive measure for RA diagnosis and management (Pincus & Sokka, 2009).

3.1.4 Treatment

Treatment of JIA is aimed at managing the symptoms in order to allow the child to live an active and independent life (Arthritis Research, 2018). For optimal management, the treatment methods involve a multidisciplinary team which includes; paediatric rheumatologist, ophthalmologist, orthopaedic surgeon, specialist nurse, physical therapist, occupational therapist, and psychologist. Treatment options can either be via pharmacological or non-pharmacological interventions (Giancane et al., 2016).

The pharmacological interventions include painkillers e.g. paracetamol, codeine, etc.; non-steroidal anti-inflammatory drugs (NSAIDs) such as ibuprofen, indomethacin, etc.; disease-modifying anti-rheumatic drugs (DMARDs) e.g. Methotrexate; biological therapies such as etanercept, others include infliximab and adalimumab; steroids, which can be administered as tablets or injections; eye drops, if eye inflammation is also diagnosed (Arthritis Research, 2018).

Non-pharmacological interventions include physiotherapy and occupational therapy which include using pain relief method such as acupuncture, massage, etc.; exercising daily, posture improvement, using splints and insoles, joint protection by using supports if needed, and also mobility support to aid movement (Arthritis Research, 2018).

3.3 Infrared thermography (IRT)

3.3.1 History

Human body temperature has been very key to medicine since early times, however, till the 16th century when the thermometer was developed, there was no objective way of measuring it; and in recent times, infrared thermal imaging has been explored in medicine for measuring body surface temperature to better understand health and diseases and the technique is now more affordable and reliable (Ring, 2006).

The history behind infrared radiation started in 1800 when Sir William Herschel, an astronomer, detected heating rays beyond the visible red of the sun's spectrum and in 1840, his son, John Herschel made the first thermal image from sunlight using the evaporograph technique (Ring, 2004) - where infrared image is converted into a visible image by differential evaporation or condensation of oil on a thin membrane (McDaniel & Robinson, 1962).

About a hundred years later, in 1940, the first thermal imaging devices were developed and only became available to industry and medicine between 1959 -1962; however, the thermograms were very crude and the mechanical scanning was slow with each image needing about 2-5 minutes to record (Ring, 2007). During this time, the potential for thermal imaging in medicine was attaining significant interest as the human skin is an efficient radiator with an emissivity of 0.98 which is close to that of a perfect black body (Ring, 2007). By the mid-1970s, computerisation was introduced for processing these images and thereafter, associations were formed to come up with guidelines for good practise including the requirement for patient preparation, conditions for thermal imaging and criteria for the use of thermal imaging in medicine and pharmacology (Ring, 2007).

3.3.2 Fundamentals of infrared thermography

Infrared thermography is a measurement technique that can quantitatively measure surface temperatures of objects (Vollmer & Möllmann, 2010). It is a non-contact technology that measures or sees infrared wavelengths emitted from objects and then converts the temperature information into an image (Davis Instruments, 2012). When a piece of equipment malfunctions, or when a disease is suspected in the human body, there is usually an increase in temperature in the affected region. A more accurate diagnosis can be made about the fault or disease by observing the heat patterns in these regions (Land Instruments International, 2004).

The most important process for thermography is the thermal radiation which implies that all matter at a temperature above the absolute zero (-273.15°C) emits electromagnetic radiation (Vollmer & Möllmann, 2010).

The next subsections will discuss the terms and theories associated with infrared (IR) thermal imaging.

3.3.2.1 Electromagnetic (EM) spectrum

The electromagnetic (EM) spectrum comprises all sources of radiation including X-rays, visible light, radio waves, etc. and these radiation types are mainly differentiated by their wavelengths (Hickman & Riley, 2010). Figure 3-3 illustrates the EM spectrum highlighting the visible band:

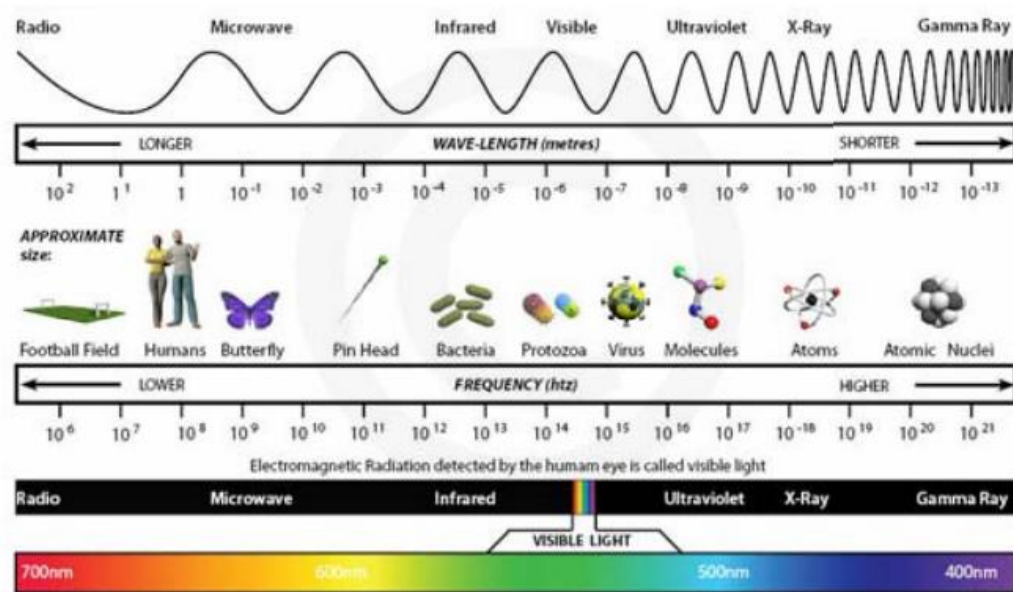


Figure 3-3 The electromagnetic spectrum highlighting the visible band (Hickman & Riley, 2010)

The visible band is the range over which the human eye is sensitive. It covers the wavelength range of $0.4\mu\text{m}$ to $0.7\mu\text{m}$. The infrared spectrum, on the other hand, is invisible to the human eye and corresponds to radiation whose wavelength is found between the end of the visible band ($0.7\mu\text{m}$) and the start of the microwave band (1mm) and is sensitive to lower temperatures including objects at room temperature (about 300K) (Hickman & Riley, 2010).

According to Hickman and Riley (2010), the IR spectrum comprises of relatively discrete bands which are often used to distinguish TI cameras. They include the near IR (NIR), short wave IR (SWIR), medium wave IR (MWIR), long wave IR (LWIR) and the far IR (FIR), and images from the same scene can look very different depending on the

band of the TI camera. An SWIR image would look more like a visual band image than an LWIR image.

3.3.2.2 Thermal radiation

Thermal radiation is EM radiation emitted from a material due to the heat of the material, the characteristics of which depends on the temperature. This type of radiation is generated when heat from the movement of charges in the material (electrons and protons) is converted to electromagnetic radiation (Miller, 2012). Examples of such EM radiation include microwave, radio frequency, X-rays, infrared, etc. with different wavelengths and can be transmitted through atmosphere, space, vacuum, etc. (Sha, Jhuo, Chen, & Wang, 2013). Radiation transfers heat directly from surface to surface; it does not require any medium to transfer heat. A campfire's heat felt by the human body is an example of radiation.

A body that absorbs all incident EM radiation upon it is known as a black body. The total power (energy per unit time) radiated from a black body is given by the Stefan-Boltzmann law which states that the total energy radiated per unit surface area of a black body per unit time across all wavelengths is directly proportional to the fourth power of the black body's thermodynamic temperature, T in Kelvin, as shown in Equation 3-1 (Hanania, Stenhouse, & Donev, 2017):

$$P = \sigma AT^4 \quad (3-1)$$

Where P : Total power radiated per unit surface area (watt)

σ : Stefan – Boltzmann constant, $5.676 \times 10^{-8} \text{ W/m}^2\text{K}^4$.

A : Surface area (m^2)

T : Absolute temperature (K)

A body that does not absorb all the incident radiation is known as a grey body and is characterised by an emissivity, ε less than 1 ($\varepsilon < 1$). Emissivity indicates the effectiveness of a body's surface to emit energy as thermal radiation. For a perfect black body, $\varepsilon = 1$ and for a human body, $\varepsilon = 0.98$, hence a very good emitter of thermal radiation. The closer the body is to black/dark colour, the higher the emissive power (Sha et al., 2013).

The total energy per unit time (*watt*), radiated by a grey body is then given in Equation 3-2 as (Sha et al., 2013):

$$P = \sigma \varepsilon AT^4 \quad (3-2)$$

Radiant energy that reaches a body's surface can either be absorbed (α), reflected (τ) or transmitted (ρ) and is described with Equation 3-3 (Miller, 2012)

$$\alpha + \rho + \tau = 1 \quad (3-3)$$

For an opaque body, there is no transmitted energy, so $\tau = 0$ and Equation 3-3 then reduces to Equation 3-4 (Sha et al., 2013).

$$\alpha + \rho = 1 \quad (3-4)$$

3.3.2.3 Thermal imagers

Thermal imaging systems enable the eye to see beyond the visible band of the EM spectrum into the far infrared of the EM spectrum by making the light naturally emitted by warm objects visible (Lloyd, 2013). Thermal imagers enable accurate non-contact measurement of temperature for a quick inspection of faults and objects can be viewed in total darkness (Hickman & Riley, 2010).

A thermal imager (TI) or a thermal camera is used to capture thermal images. It mainly consists of an optical system which is an infrared lens system that focuses the infrared light emitted by all of the objects in view onto the detector; one or more infrared detector elements that scans the focused light creating a very detailed temperature pattern called a thermogram, which is then translated to electrical signals; an electronic processor to process the outputs from the detector and converts them into data for the display; then a display unit that outputs the data, a combination of the electrical signals from all of the detector elements, as visual images (Tyson, 2001; Williams, 2009). The main subunits of a thermal camera are shown in Figure 3-4:

There are two common types of thermal imagers classed as cooled and uncooled (FLIR Systems, 2015):

- Cooled thermal imagers have an imaging sensor integrated with a cryocooler which lowers the sensor temperature to cryogenic temperatures. This helps to reduce the thermally induced noise to a level below that of the signal being acquired. They are highly sensitive and can detect very small temperature changes between objects. However, the cryocooler have movable parts and so wear out over time. They are also more expensive than the uncooled version.
- Uncooled thermal imagers are the most common and their IR (infrared) detector design is based on a microbolometer, a tiny vanadium oxide resistor with a low heat capacity and good thermal isolation. Changes in scene temperature cause changes in the bolometer temperature, which are converted to electrical signals and processed into an image. They are relatively cheaper, consume less power, have longer durability, and can work for many years without needing maintenance.

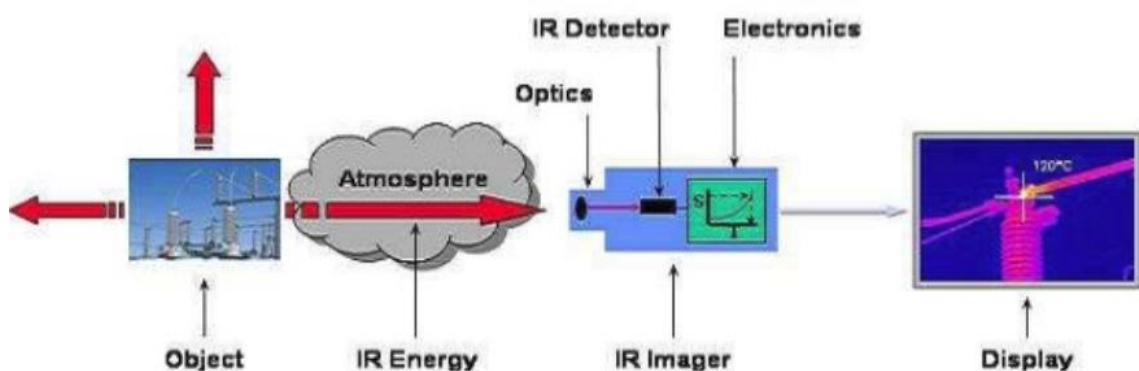


Figure 3-4 Block diagram showing the main subunits of a thermal imaging camera (Syed, 2016)

3.4 Accelerometry for describing movement

Accelerometry, in this context, refers to techniques in which accelerometer-based systems are used to quantify and measure movement. In this study, accelerometry data from the knees were studied. The types of movement that were focused on at the knee joints were the flexion and extension movements. These are briefly described (Hamill, Knutzen, & Derrick, 2014):

Flexion - This is a bending movement in which the relative angle of joint between the two adjacent segments decreases e.g. bending of the knee.

Extension - This is a straightening movement in which the relative angle between the two adjacent segment increases as the joint returns to the reference position e.g. straightening of the knee.

3.4.1 Accelerometers

There are many types of accelerometers, but the most popular and modern types are the microelectromechanical systems (MEMS) accelerometers due to their compactness.

MEMS combine mechanical and electrical components into small structures in sizes of micrometres to millimetres (Dadafshar, 2014). MEMS sensors are characterised by small size, low power consumption, low costs, high precision and integration etc.

Accelerometers are electromechanical devices that measure forces of acceleration. Acceleration is simply defined as the rate at which an object is speeding or slowing down. These acceleration forces may be static such as the constant force of gravity pulling at your feet or dynamic, caused by vibrating or moving the accelerometer (Andrejasic, 2008).

MEMS accelerometers can be found in numerous applications such as in inertial navigation systems, gaming, smartphones, mobile devices (Zhang, Su, Shi, & Qiu, 2015). They are also widely applied in medicine and sports as step counters, physical activity monitors, human movement monitors (gait analysis) etc. In laptops, accelerometers are used to prevent damage to the hard drive in the event of a fall while in use as the device can detect the sudden free fall and immediately turn the hard drive off. A typical 3-axis accelerometer board is shown in Figure 3-5.



Figure 3-5 A typical 3-axis accelerometer breakout board (Hobby Electronics, 2018)

3.4.2 Basic accelerometer operation

The principle of operation of the accelerometer is based on Newton's second law of motion which states that the acceleration, a (m/s^2) of a body is directly proportional to and in the same direction as the net force, F (*Newton*) acting on the body and inversely proportional to its mass, m (*gram*) as shown in Equation 3-5 (Dadafshar, 2014).

$$a = \frac{F}{m} \quad (3-5)$$

From Equation 3-5, acceleration can be further explained as the amount of force required to move each unit of mass, which means if the force acting on an object is known, and the mass of the object is also known, then the acceleration can be determined without the need to measure speed and time. So, accelerometers measure acceleration by measuring force. This is done by sensing how much a mass presses on an object when a force acts on it (Woodford, 2018).

MEMS accelerometers are mainly of two types; the piezoresistive and the capacitive accelerometers. The most common sensing method is however, the capacitance sensing method such as the ADXL series from Analog Devices (Albarbar & Teay, 2017) and it is discussed further.

In the capacitance sensing approach, acceleration is related to change in the capacitance of a moving mass. This approach has high accuracy, stability, low power

dissipation and is simple to build. It is not prone to noise and variation with temperature (Dadafshar, 2014).

A typical capacitive acceleration sensor essentially contains a stationary plate, connected to the housing and a second plate attached to the inertial mass that moves freely within the housing. These plates form the capacitor, whose capacitance value (in Farads) is a function of the distance, d , between the plates as shown in Equation 3-6 (Fraden, 2004):

$$C = \frac{\epsilon_0 \epsilon A}{d} \quad (3-6)$$

Where ϵ_0 is permittivity of free space/vacuum or the electric constant with an approximate value of $8.85 \times 10^{-12} \text{ F/m}$, ϵ is the permittivity of the material separating the electrodes, A is the area of the two electrodes.

The movement of the proof mass due to an acceleration of the device changes the distance between the plates, thereby changing the capacitance value between them as well. The difference in the capacitance can then be used to determine the acceleration (Albarbar & Teay, 2017). Figure 3-6 further illustrates this concept. As the accelerometer box moves to the right, the mass is left behind and pushes the metal plates closer together, changing their capacitance (Woodford, 2018).

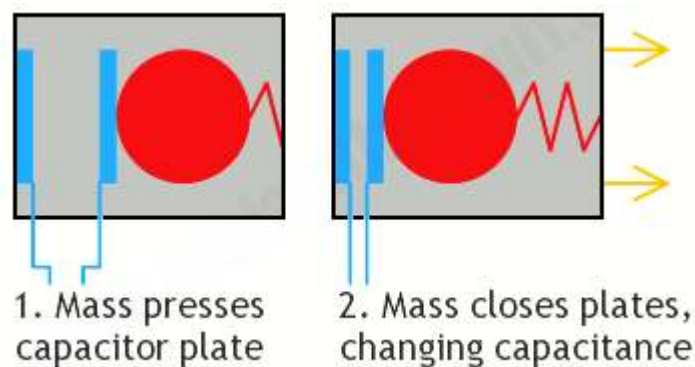


Figure 3-6 The broad concept of a capacitive accelerometer (Woodford, 2018)

3.4.3 Tilt sensing

Pitch and roll angles can be determined with the aid of accelerometers. Accelerometers can measure static forces of acceleration. Tilt is a static measurement

where gravity is the only acceleration being measured and for accurate measure of tilt, a low-g, high-sensitivity accelerometer is required (Clifford & Gomez, 2005).

For a three-axis accelerometer as shown in Figure 3-7, the pitch and roll angles can be estimated using Equations 3-7 and 3-8 where A_x , A_y and A_z are measured accelerations sensed at the x , y and z - axes respectively.

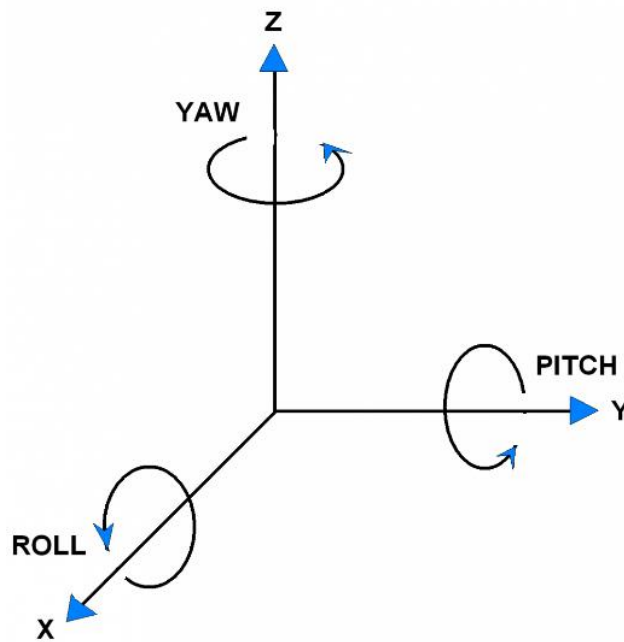


Figure 3-7 Three axis of an accelerometer showing roll, pitch and yaw movements (Ellis et al., 2014)

$$\text{Roll} = \text{arctangent2}(A_x, A_z) \quad (3-7)$$

$$\text{Pitch} = \text{arctangent2}(A_y, A_z) \quad (3-8)$$

The arctangent2 function returns the angle in the correct quadrant based on the signs of the two arguments i.e. $[-\pi, \pi]$, in contrast to the arctangent function that limits results to the interval $[-\pi/2, \pi/2]$.

3.5 Digital signal processing concepts

Signals are carriers of information, both wanted and unwanted, so the ability to extract the useful information from the signal is necessary. Digital signal processing (DSP) can therefore be defined as the extraction, enhancing, storing and transmission of useful

information (Ingle & Proakis, 2012) using digital processing such as by computers or more specialised digital signal processors.

Most DSP operations can be categorised as signal filtering or signal analysis tasks.

3.5.1 Signal filtering

This is the process of removing unwanted components or background noise without affecting the main information from a signal and can be majorly classed into low-pass, high-pass or band-pass filters.

Movement signals from accelerometers are associated with high-frequency noise components. Low-pass filters (LPFs) can be used to reduce or completely remove these unwanted components. The Butterworth filter was used in this study for signal filtering.

LPFs are electrical networks that allow signals with a frequency lower than the cut-off frequency (ω_c) to pass through (pass bands) and rejects/stops signals with frequencies higher than the ω_c (stop bands). An ideal magnitude response of the LPF is shown in Figure 3-8 where $|H(j\omega)|$ is the amplitude of the signal and ω is the frequency (Thompson, 2014).

However, the ideal filter cannot be achieved in reality using electric circuits so the magnitude response of a real or practical filter, such as the Butterworth filter has a maximally flat magnitude response in the passband (Butterfield & Szymanski, 2018; Mahata, Saha, Kar, & Mandal, 2018) and steep slope soon after f_c in the stopband depending on the filter order number. Figure 3-9 shows a typical Butterworth magnitude response of the 1st and 2nd order with cut-off frequency of 1 rad/s.

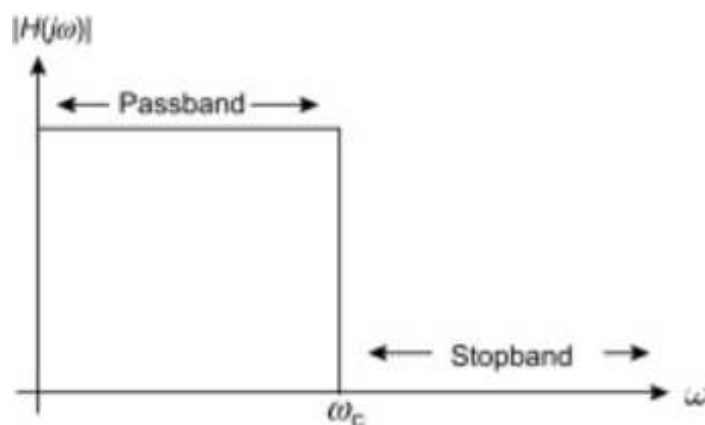


Figure 3-8 Ideal magnitude response of a low-pass filter (Thompson, 2014)

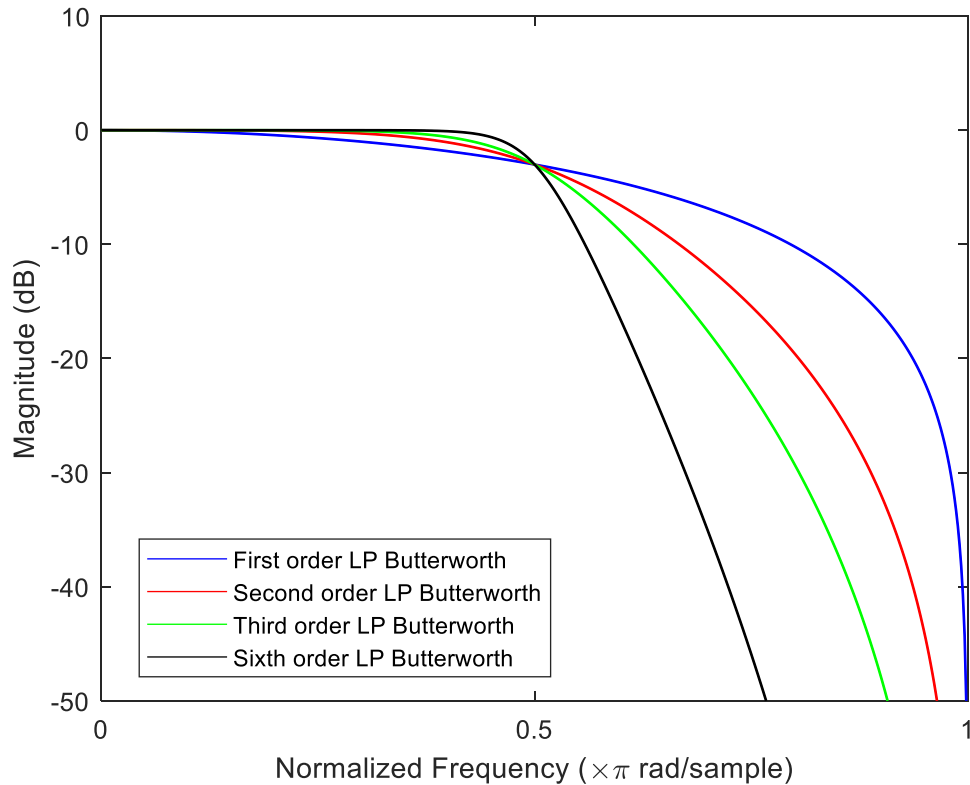


Figure 3-9 Typical responses of a low-pass (LP) Butterworth filter of the 1st, 2nd, 3rd and 6th order with a normalised cut-off frequency of 0.5

3.5.2 Signal analysis

This deals with the measurement of signal properties and is mostly a frequency-domain operation (Ingle & Proakis, 2012), such as spectrum analysis using transforms. Transformation of signals from time domain to frequency domain is widely used in signal processing as they provide information about the frequency components of the signal (Williston, 2009).

3.5.2.1 Discrete Fourier Transform (DFT) and Fast Fourier transform (FFT)

Discrete Fourier transform (DFT) is simply a transform that takes a signal in time domain and computes the frequency content of the signal (Parker, 2010).

The DFT $X[k]$ of an N -point signal $x[n]$ is given by (Williston, 2009) in Equation 3-9:

$$\begin{cases} X[k] = \sum_{n=0}^{N-1} x[n] W_N^{nk}, k = 0, 1, \dots, N-1 \\ x[n] = \frac{1}{N} \sum_{k=0}^{N-1} X[k] W_N^{-nk}, n = 0, 1, \dots, N-1 \end{cases} \quad (3-9)$$

Where $W_N = e^{-j2\pi/N}$.

However, the above transform equations are computationally intensive and direct computation is not efficient. For a faster, more efficient and real-time computation of DFT, a fast Fourier transform (FFT) algorithm is used. Rather than the N^2 complex multiplications and additions required by the DFT, the FFT requires $N \cdot \log_2 N$ complex multiplication and addition operations (Parker, 2010).

3.5.2.2 Short-Time Fourier Transform (STFT)

Short-time Fourier transform (STFT) provides the time-localised frequency information of signals whose frequency components vary over time. It is a sequence of Fourier transforms performed on windowed signals. There is a trade-off between time and frequency resolution in STFT. A window with narrow-width results in a better resolution in the time domain and a poor resolution in the frequency domain and vice versa. A spectrogram is used to visualise the STFT of a signal (Williston, 2009).

3.5.2.3 Wavelet transform (WT)

Wavelet transform (WT) offers time-frequency analysis that decomposes a signal in terms of a family of wavelets which have a fixed shape but can be shifted and dilated in time (Tan & Jiang, 2013). Wavelet transform provides high frequency resolution at low frequencies and high time resolution at high frequencies (Williston, 2009).

A. Discrete wavelet transforms (DWT)

The discrete wavelet transforms (DWT) of a signal is defined based on some approximation coefficients and detail coefficients using the filter bank structure (Williston, 2009) shown in Figure 3-10. For a signal, s , the first step involves convolving s with a lowpass (LoD) and highpass (HiD) decomposition filters, followed by down sampling by two (keep the even indexed elements) to give the approximation (cA_1) and detail (cD_1) coefficients as shown in Figure 3-10. In the subsequent steps, the new approximation coefficients at a higher level are split into two parts using the same approach, to compute the approximation and detail coefficients at a lower level. This

structure is then repeated for a multi-level decomposition as shown in Figure 3-11. The successive details are not re-analysed (Mathworks, 2018).

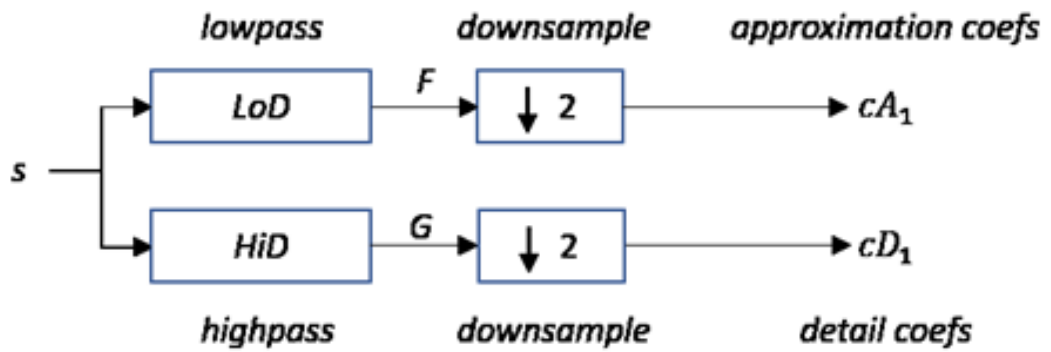


Figure 3-10 Discrete wavelet transform decomposition structure (Mathworks, 2018)

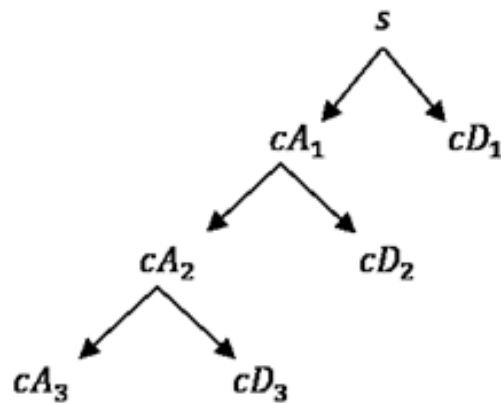


Figure 3-11 Discrete wavelet transform decomposition tree for three levels (Mathworks, 2018)

B. Wavelet packet transform

This method is a generalization of wavelet decomposition that allows for richer signal analysis. Contrary to the DWT method described above, this procedure splits both the approximation and detail vector into two parts at every step/level i.e. the detail vector is further analysed as well as shown in Figure 3-12. Signal is reconstructed using the coefficients identified to contain the desired information (MathWorks, 2019b).

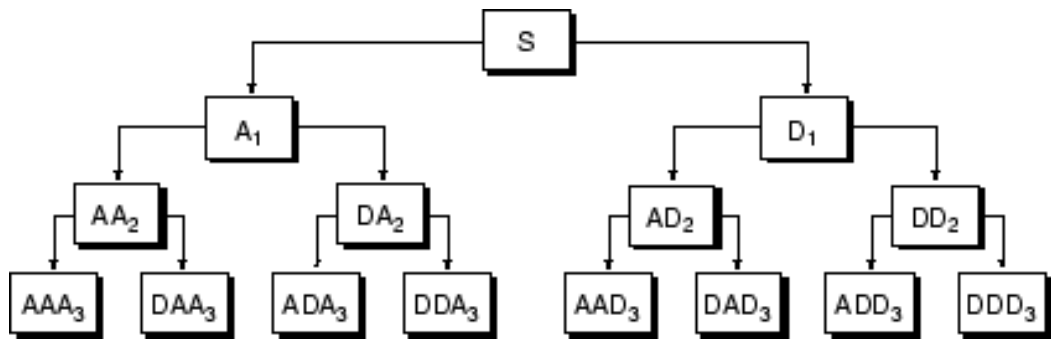


Figure 3-12 Wavelet packet decomposition tree down to level 3 (MathWorks, 2019b).

3.6 Image processing

3.6.1 Image segmentation

This process allows sections of images referred to as regions of interest (ROIs) to be defined and selected from the background for further analysis.

The ROIs can be of any shape using the MATLAB[®] *drawpolygon* function. The ROI, once determined, can be used to create a binary mask image. In the mask image, pixels belonging to the ROI are set to 1 and all other pixels (outside the ROI) are set to 0 (MathWorks, 2019a).

3.6.2 Image tracking

Image tracking refers to the ability for an algorithm to detect a region of interest in an image and recognise the same in subsequent images. The main objective of image tracking is to deal with the streams of images that change with time (Reddy, Priya, & Neelima, 2015).

Several image tracking algorithms have been reported in literatures and one that has gained much attention, and which was also used in this study is the template matching method (Pan, Hu, & Zhang, 2006).

3.6.3 Template matching

Template matching is a technique for finding areas of an image that could either match or be similar to the template (ROI) image (Munsayac, Alonzo, Lindo, Baldovino, & Bugtai, 2017) using a suitable template matching algorithm.

Template matching by normalised cross-correlation (NCC)

The correlation between two signals is a standard approach for feature detection. This method has been extensively used for evaluating similarity between images and its main advantage over the ordinary cross correlation method is that it is less sensitive to changes in background intensity and brightness i.e. changes in the brightness or darkness of the images does not affect the result (Perveen, Kumar, & Bhardwaj, 2013) NCC has been reported to be more accurate than other methods such as the sum of absolute difference (SAD) and sum of squared difference (SSD); however, the computational load is heavier (Munsayac et al., 2017).

The NCC method can be used to measure the similarity between image and template (ROI) as the template (ROI) is compared with image. The NCC of the region of image under the template (u, v) and the template image $t(x, y)$ can be computed with Equation 3-11 (Lewis, 1995):

$$NCC(u, v) = \frac{\sum_{x,y}[f(x, y) - \bar{f}_{u,v}][t(x - u, y - v) - \bar{t}]}{\sqrt{\sum_{x,y}[f(x, y) - \bar{f}_{u,v}]^2 \sum_{x,y}[t(x - u, y - v) - \bar{t}]^2}} \quad (3-11)$$

Where f is the image, \bar{t} is the mean of the template image, $\bar{f}_{u,v}$ is the mean of $f(x, y)$ in the region under the template image (Lewis, 1995).

The larger the NCC value, the more similar the two images are. Generally, NCC values can range from -1.0 to 1.0 such that NCC of two identical images equals 1.0 and NCC of an image and its exact negative (inverted grayscale values) equals -1.0 (O'Dell, 2005; Perveen et al., 2013). Figure 3-15 illustrates the NCC of two images. It shows the NCC values of image1 and image2, with the highest NCC value (0.844) shown for the most identical of the two images (Perveen et al., 2013).







Image1	Image2	NCC
		0.417
		0.553
		0.844

Figure 3-13 Normalised cross correlation of two images (Perveen et al., 2013)

3.6.4 Colour feature extraction and similarity index

In this study, the Euclidean distance metric method was implemented to measure the similarity between the colour histograms of the visual images.

Colour histogram is a colour feature extraction method that represents the distribution of the number of pixels in an image (Kodituwakku & Selvarajah, 2004).

Euclidean distance is the most commonly used image metric because of its simple computation. If x and y are two M by N images, $x = (x^1, x^2, \dots, x^{MN})$, $y = (y^1, y^2, \dots, y^{MN})$, then for $k = 1$ to MN pixels, the Euclidean distance, $d_E(x, y)$ is given by Wang, Zhang, & Feng (2005) in Equation 3-12 as:

$$d_E(x, y) = \sqrt{\sum_{k=1}^{MN} (x_k - y_k)^2} \quad (3-12)$$

where M by N is the size of the image

MN ($M \times N$) is the total number of pixels in each image

3.7 Summary

In this chapter, the relevant theory of the study was briefly discussed to give some background understanding of the work, basic definitions and formulas.

JIA refers to all types of arthritis that begin before the age of 16, persist for more than 6 weeks and are of unknown cause and the symptoms can include stiffness, warm and redness around the affected joint. Disease diagnosis can be through clinical evaluation

(pGALS), imaging technologies (radiography, CT, ultrasound, CE-MRI), tests for certain proteins in the blood. There is no cure for the disease, so treatment is aimed at management of the symptoms.

Brief explanations of signal and image processing concepts such as signal filtering (low pass filters) and analysis (FFT and STFT), image segmentation, image tracking, template matching technique (using normalised cross correlation method), and colour feature extraction method were also given.

In the next chapter, the research methodology for the thermal/visual imaging and accelerometry study is presented.

Chapter 4

4 Research Methodology for the Thermal/Visual Imaging and Accelerometry Study

In this chapter, the research methodologies that are common to the results obtained in the following results chapter are explained. To improve clarity and ease of reading, research methodologies that are only specific to studies in specific chapters are explained in the related chapters.

4.1 Ethical approval

Full ethical approvals from Sheffield Hallam University (Appendix 1) and National Health Service (NHS) (Appendix 2) were obtained prior to the start of the study. As part of the approvals process, a health check and Disclosure and Barring Service (DBS) check was also carried out by the authorised bodies to certify the researcher was fit for performing NHS related tasks such as data recordings from children. These led to the researcher being awarded a Research Passport (Appendix 3) by the hospital to give access to the hospital for data recording purposes. Further, the NHS courses on the Good Clinical Practice (Appendix 4) and Informed Consent in Paediatric Research were studied and passed (Appendix 5).

4.2 Risk assessment

An assessment of the risks that could be involved in the study was fully considered and the appropriate forms were completed and submitted to the designated authorities.

4.3 Recruitment

Children and young people (CYP) diagnosed with Oligoarticular (affecting four or fewer joints for the first 6 months in the persistent case, and more than four joints after the first 6 months in the extended case (Ravelli & Martini, 2007) or Polyarticular JIA (affecting five or more joints during the first 6 months) were recruited for the study from the routine rheumatology clinics or steroid injection lists held at the Sheffield Children's Hospital (SCH).

The knee and ankle joints were investigated as these joints have the most flares in practice and thus were more available to test.

4.3.1 Information sheets

After identifying eligible patients, purpose designed information sheets explaining the study for parent/guardian and CYP were provided before the routine clinic appointment.

For the thermal/visual imaging study, there were separate information sheets for

- Children aged 4 to 11 years (Appendix 6)
- Young persons aged 12 to 16 years (Appendix 7)
- Parent/guardian (Appendix 8)

Likewise, for the accelerometry study, there were different information sheets for

- Children below 10 years (Appendix 9)
- Children 10 years and above (Appendix 10)
- Parent/guardian (Appendix 11)

The information sheets were prepared clearly in a manner that would be well understood by patients of a specific age. The study was also verbally outlined with the patients and their parent/guardian at the appointment by a member of the clinical team and any question answered.

4.3.2 Assent / Consent

Once the study was informed to the patients and their rights to withdraw were explained, interested patients and their parent/guardian were given the assent and consent forms respectively to sign. These were duly obtained before taking part in the study (Sample assent (for CYP) and consent forms (for parent/guardian) are provided in Appendices 12 to 15 for the thermal/visual imaging and accelerometry studies).

4.3.3 Exclusion criteria

Exclusion criteria for the TI study included:

- CYP below 4 years of age
- CYP with active/chronic infection that required hospitalisation or treatment with intravenous antibiotics within 30 days of recruitment or oral antibiotics within 14 days of recruitment.

- CYP with history of active tuberculosis of less than 6 months treatment or untreated latent tuberculosis.
- CYP with soft tissue infection, injury or fracture of the affected joint which could affect the TI reading
- CYP with any inflammatory skin condition which may be near the affected joint
- Non-consenting CYP, or parent(s)/guardian(s)

Exclusion criteria for the Accelerometry study included:

- CYP aged below 8 years (this is to ensure that the participant is old enough to co-operate with attaching the accelerometry device to the lower limb and follow flexion and extension movements as demonstrated).
- Diagnosis of any previous joint condition (other than JIA) affecting lower limbs
- Fracture of any bone in the previous 4 months
- Diagnosis of any muscle condition or chronic pain syndrome
- Any concerns from parent(s)/guardian(s) regarding the patient's ability to complete the data recording session

Recordings were performed in the presence of a medical supervisor.

4.4 Patients' details

The pilot study focused on rheumatoid arthritis of the knees primarily because of the ease of thermal image recording for the region and the relative availability of patients with knees rheumatoid arthritis. However, the ankles were also analysed. Twenty-two patients aged 4 to 16 years (age: mean=10.6 years, SD = 2 years) with diagnosis of JIA were recruited for the studies from the patients referred to Sheffield Children's Hospital (Sheffield, United Kingdom). Twenty patients participated in the thermal/visual imaging study and four patients in the accelerometry study (2 patients from the thermal/visual imaging study were part of the 4 that partook in the accelerometry study, making a total of 22 patients recruited). The patients' demographic details are included in Table 4-2. The study did not interfere with the manner the patients were medically treated.

Table 4-1 Demographic analysis

Parameter	Value
Mean age (SD) (years)	10.6 (2.3)
Sex	Male: 9 (41%), Female: 13 (59%)
Mean weight (SD) (kg)	42.05 (14.91)
Mean height (SD) (cm)	142.77 (14.34)
Patient Categories	<ul style="list-style-type: none"> • Knee: 10 patients clinically diagnosed with active arthritis on one knee, 8 patients had on both knees, while 4 patients had no active knee arthritis at the time of clinical assessment • Ankle: 9 patients clinically diagnosed with active arthritis on one ankle, 4 had on both ankles and 7 with no active arthritis in the ankles at the time of clinical assessment
Medication of patients with JIA. Values in parenthesis are the number of cases	<ul style="list-style-type: none"> • Systemic immunosuppression (10) • Course of oral steroid (1) • Systemic immunosuppression + Ibuprofen (4) • Regular Ibuprofen (2) • Regular Naproxen (1) • Methotrexate, Adalimumab (1) • No medication (3)

The patients included had active arthritis on either one or both knees or ankles at the time of clinical assessment. Data recordings were performed within half an hour before or after the clinical assessment.

4.5 Medical examination of patients

All patients were evaluated by an experienced paediatric rheumatologist. Diagnosis of JIA was clinically made by performing a musculoskeletal examination which checked for joint warmth, swelling and restriction using the pGALS (paediatric Gait Arms Legs and Spine) tool plus history of the symptoms i.e. persistence of the symptoms (joint swelling and early morning joint stiffness) for 6 weeks or more lasting for 30 minutes or more.

pGALS is a validated screening tool of the musculoskeletal system for inflammatory disease to distinguish abnormal from normal joints and can be completed within two minutes (Foster & Jandial, 2013). A summary of the symptoms observed in all patients is provided in Table 4-1. (For thermal/visual imaging and Accelerometry studies).

Table 4-2 Clinical diagnosis for each patient (presence of symptoms are highlighted)

Patient No	Diagnosis	Joint	Symptoms			How diagnosis was made
			Warm	Swollen	Restricted	
1	Extended Oligoarticular JIA	Right Knee	No	No	No	All Musculoskeletal examination and history taken by experienced clinician prior to completion of joint injections. <u>Examination:</u> Clinically suspected warmth, swelling, and restriction. <u>History:</u> confirmed diagnosis of arthritis due to persistent unexplained symptoms lasting more than 6 weeks, 30 mins or greater of early morning joint stiffness
		Left Knee	Yes	Yes	Yes	
		Right Ankle	No	No	No	
		Left Ankle	No	Yes	No	
2	Polyarticular JIA	Right Knee	No	Yes	No	
		Left Knee	No	Yes	No	
		Right Ankle	No	No	No	
		Left Ankle	Yes	No	No	
3	Oligoarticular JIA	Right Knee	Yes	Yes	Yes	
		Left Knee	No	No	No	
		Right Ankle	No	No	No	
		Left Ankle	No	No	No	
4	Polyarticular JIA	Right Knee	No	No	No	
		Left Knee	No	No	No	
		Right Ankle	No	No	No	
		Left Ankle	No	No	No	
5	Oligoarticular JIA	Right Knee	Yes	Yes	Yes	
		Left Knee	No	No	No	
		Right Ankle	No	No	No	
		Left Ankle	No	No	No	
6	Extended Oligoarticular JIA	Right Knee	Yes	Yes	Yes	
		Left Knee	No	No	No	
		Right Ankle	Yes	Yes	Yes	
		Left Ankle	No	No	No	
7	Extended Oligoarticular JIA	Right Knee	Yes	Yes	Yes	
		Left Knee	Yes	Yes	Yes	
		Right Ankle	Yes	Yes	Yes	
		Left Ankle	No	No	No	
8	Oligoarticular JIA	Right Knee	Yes	Yes	Yes	
		Left Knee	Yes	Yes	Yes	
		Right Ankle	Yes	No	No	
		Left Ankle	No	No	No	
9	Extended Oligoarticular JIA	Right Knee	No	No	No	
		Left Knee	No	Yes	Yes	
		Right Ankle	No	No	No	
		Left Ankle	No	Yes	Yes	
10	Oligoarticular JIA	Right Knee	No	Yes	No	
		Left Knee	No	No	No	
		Right Ankle	No	Yes	Yes	
		Left Ankle	No	No	No	
11	Oligoarticular JIA	Right Knee	No	No	No	
		Left Knee	Yes	Yes	Yes	

		Right Ankle	No	No	No
		Left Ankle	No	No	No
12	Oligoarticular JIA	Right Knee	No	No	No
		Left Knee	No	Yes	No
		Right Ankle	No	Yes	No
		Left Ankle	No	Yes	No
13	Polyarticular JIA	Right Knee	No	No	No
		Left Knee	No	No	No
		Right Ankle	No	Yes	Yes
		Left Ankle	No	No	No
14	Extended Oligoarticular JIA	Right Knee	Yes	No	No
		Left Knee	Yes	No	No
		Right Ankle	Yes	Yes	No
		Left Ankle	Yes	Yes	Yes
15	Oligoarticular JIA	Right Knee	Yes	Yes	Yes
		Left Knee	Yes	No	No
		Right Ankle	No	No	No
		Left Ankle	No	No	No
16	Oligoarticular JIA	Right Knee	Yes	Yes	No
		Left Knee	Yes	Yes	No
		Right Ankle	No	No	No
		Left Ankle	No	Yes	No
17	Oligoarticular JIA	Right Knee	Yes	Yes	Yes
		Left Knee	Yes	Yes	Yes
		Right Ankle	No	No	No
		Left Ankle	No	No	No
18	Oligoarticular JIA	Right Knee	No	No	No
		Left Knee	No	No	No
		Right Ankle	Yes	Yes	No
		Left Ankle	Yes	Yes	No
19	Polyarticular JIA	Right Knee	Yes	Yes	Yes
		Left Knee	Yes	Yes	Yes
		Right Ankle	No	No	No
		Left Ankle	No	No	No
20	Oligoarticular JIA	Right Knee	No	No	No
		Left Knee	No	No	No
		Right Ankle	Yes	Yes	Yes
		Left Ankle	Yes	Yes	Yes
21	Polyarticular JIA	Right Knee	No	Yes	No
		Left Knee	No	No	No
		Right Ankle	No	No	No
		Left Ankle	No	No	No
22	Oligoarticular JIA	Right Knee	No	Yes	Yes
		Left Knee	No	No	No
		Right Ankle	No	No	No
		Left Ankle	No	No	No

4.6 Anonymity

In order to protect the identity of the participating patients in line with the ethics approval, unique identifier numbers were used to identify each patient.

4.7 Materials

4.7.1 Camera and associated software

A FLIR T630sc portable thermal camera which also has an integrated visible camera was used for the thermal/visual imaging study. The camera image is displayed in Figure 4-1. The camera specifications are provided in Table 4-3.

The associated FLIR ResearchIR Max software was used to operate the camera through a laptop.



Figure 4-1 Image of the FLIR T630sc (FLIR, 2019)

Table 4-3 FLIR T630sc specification (FLIR, 2016)

Parameter	Specification
Detector type	Uncooled microbolometer
Spectral Range	7.5 – 13.0 μm
Resolution	640 \times 480 pixels
Operating Temperature Range	-15°C to 50°C
Visible Image	5.0 Megapixel from Integrated Visible Camera
Object Temperature Range	-40°C to 650°C
Accuracy	$\pm 2^\circ\text{C}$ or 2%
Focus	Continuous Automatic or Manual
Frame Rate	30 Hz
Sensitivity	<40mK
Command & Control	USB, Wi-Fi
MSX [®] Enhancement/Picture in Picture	Adds Visible Detail to Thermal/P-i-P Overlays Thermal on Visible Image
Size (L \times W \times H)	143 \times 195 \times 95 mm

4.7.2 Data Processing software

Data collected from this study was processed using MATLAB®.

4.8 Summary

In this chapter, the ethical approval and recruitment procedure for the study were discussed. Twenty-two patients aged 4 to 16 years with either Oligoarticular or Polyarticular JIA diagnosis were recruited from the routine clinics at the Sheffield Children Hospital (SCH). Purpose designed information sheets for eligible patient/guardian were provided and duly signed assent/consent forms were obtained from the patient/guardian before partaking in the study. The knees and ankles were investigated in this study.

The medical diagnosis and symptoms observed by the clinician for each patient were also presented. The specific procedures followed for each study (thermal imaging, visual imaging and accelerometry) are presented in the relevant chapters.

In the next chapter, the results related to the thermal imaging study are presented and discussed.

Chapter 5

5 Thermal Imaging for the Clinical Assessment of Juvenile Idiopathic Arthritis

In this chapter, thermal imaging (TI) methods are developed and compared with routine clinician musculoskeletal examination in assessing knees and ankles with active arthritis in children and young people (CYP) with Juvenile idiopathic arthritis (JIA). An increase in the joint temperature may indicate inflammation due to active rheumatoid arthritis hence accurate means to measure temperature at these joints may assist with the clinical assessment and diagnosis of JIA.

TI techniques were developed to determine whether they can detect the changes in temperature (caused by alterations in blood flow patterns) of the skin overlying joints which may be inflamed. Thermal videos of the front and back of the knees and ankles of twenty patients were recorded. A technique to locate the regions of interest (ROIs) enclosing the affected area was developed to allow consistency of analysis across patients. The ROI used polygon segmentation method to best follow the contour of the affected area. The ROIs centred on the knees and ankles were manually segmented from the images for further processing. These were analysed and interpreted as described in the following sections

5.1 Methodology

5.1.1 Setup at the hospital

Thermal image recording was performed in a room with consistent temperature and humidity and free of draught. The average room temperature and relative humidity were 23.6°C (standard deviation (SD) 1.26°) and 33% (SD 2.4%) respectively.

The patient on arrival sat on a chair draped with towel and placed their feet on the ground, equally draped with towel. They sat for approximately 10 minutes, ensuring no contact with the knees, to acclimatise with the room temperature and ensure even skin blood flow. Thermal recordings of the front and back of the knees and ankles were then taken while the patient stood on a towel to isolate the feet from ground.

The FLIR T630sc infrared camera and the associated FLIR ResearchIR software from FLIR systems were used for the thermal recording. The camera's features included high thermal sensitivity of less than $40mk$, pixel resolution of $640 \times 480 \text{ pixels}$. Emissivity of the camera was set to 0.98 as is required for the human skin. The thermal camera was located one meter away from the patient. The camera was connected to a laptop to display the image as well as store the recorded image.

5.1.2 Data collection

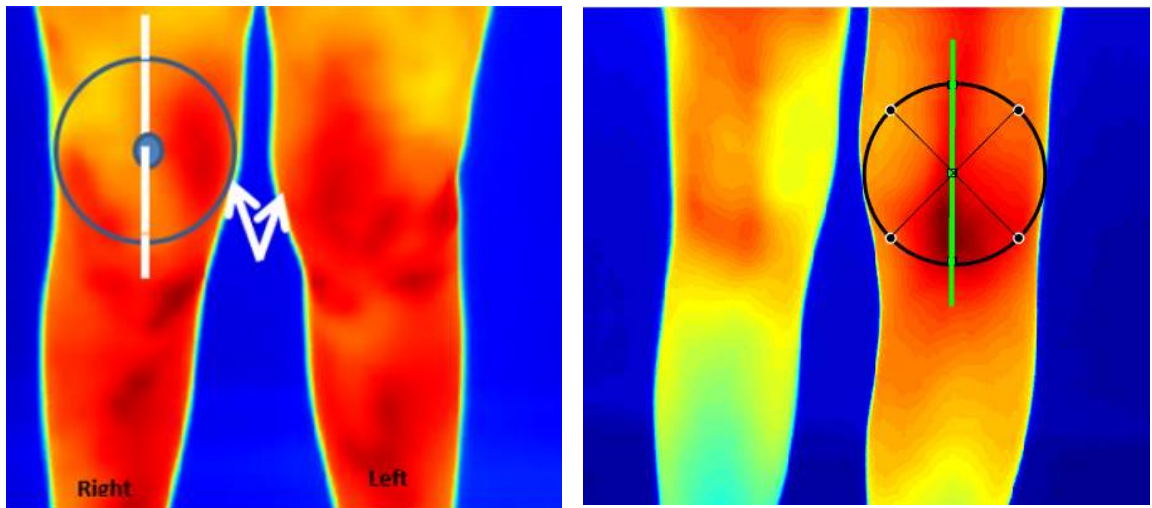
A 20-second thermal video recording of the front and back of knees and ankles was collected at 30 frames per second in order to allow the temperature measurement over a time period rather than just a single image. Recorded data were processed offline using the MATLAB[®] package (The recorded file was converted from sequence to mat file). The team that processed the data was unaware of the clinical diagnosis for the patients to ensure the unbiased processing.

5.1.3 Image processing procedures

For segmenting the images, identifying the location of the knees and ankles was very key for this process. A repeatable method to locate the joints was adopted (described in the next section).

5.1.3.1 Segmenting the knee

Using MATLAB[®] the first thermal image of the recorded video (containing 20 seconds \times 30 frames per seconds = 600 frames) was displayed on computer screen. Using the polygon cropping tool available in MATLAB[®], a region centred on the knees was manually segmented from the image (see Figure 5-1). The knee region was visually located. This was assisted by considering the curvature at the point of the knee region (see white arrows in Figure 5-1(a)). A circle was fitted at the location of curve in such a manner to best fit into the curve of the knee. The centre of the circle was located. From the centre of the circle, an area that covers vertically, 1.5 of the radii of the circle forms the ROI (Figure 5-2 shows the anterior view of the knee describing the bone make-up of the knee to include the femur/ thigh bone through to the tibia/shin bone).



(a) Front knee

(b) Back knee

Figure 5-1 Sample thermal image showing how knee ROI is identified. The patient is facing the camera

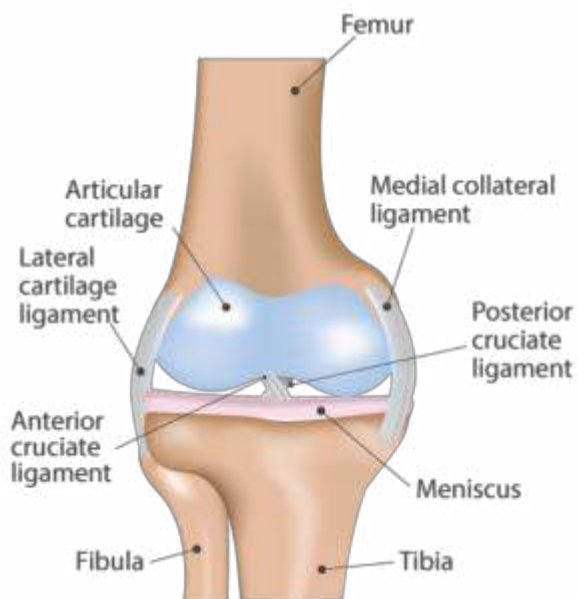


Figure 5-2 Anterior view of the knee (London Knee Specialists, 2019)

5.1.3.2 Segmenting the ankle

The front of the ankle ROI was identified using the same principle as that used to locate the knee ROI (see Figure 5-3). From Figure 5-3(a), the identified ROI is the area covering the blue line from top to bottom.

For the back of the ankles, however, because the ankle joint sits on the heel bone (calcaneus - which was observed to be much cooler than the rest of the leg on most patients), after fitting the circle around the ankle curve, an area that covered from 1.5

of the radii vertically upwards to the bottom of the circle was selected as ROI (basically, the blue line in Figure 5-3(b)). Figure 5-4 illustrates the skeletal ankle joint which shows the ankle joint to be made of the tibia (shin bone), fibula, and the talus (ankle bone).

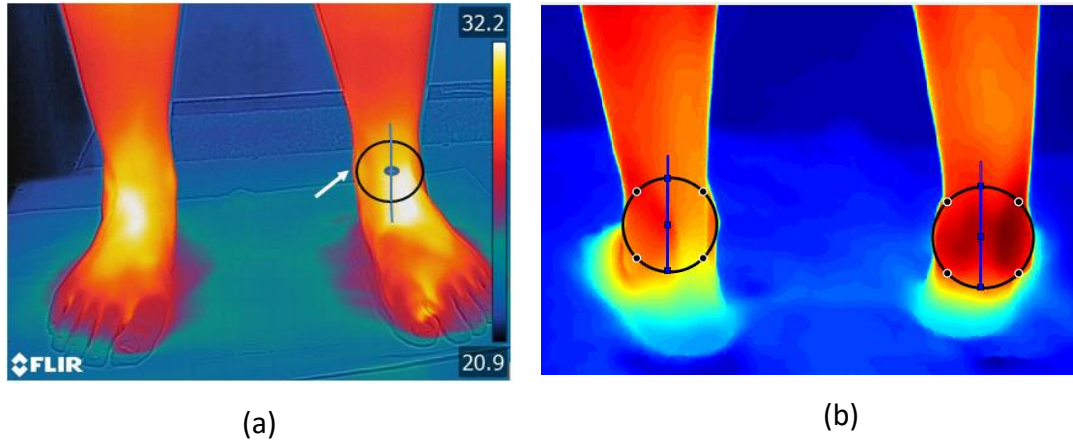


Figure 5-3 Sample thermal image showing how ankle ROI is identified (a) Front of the ankle (b) Back of the ankle

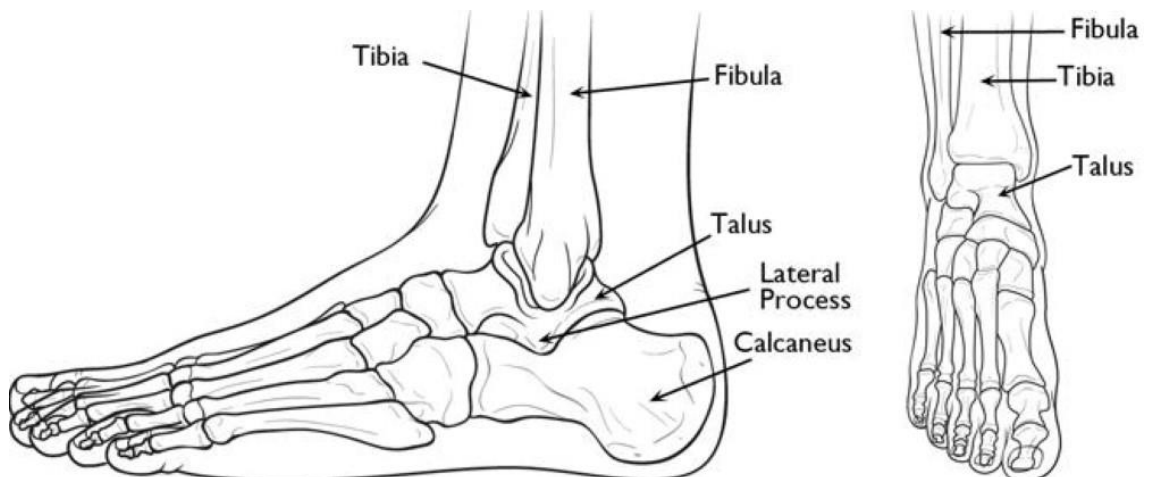
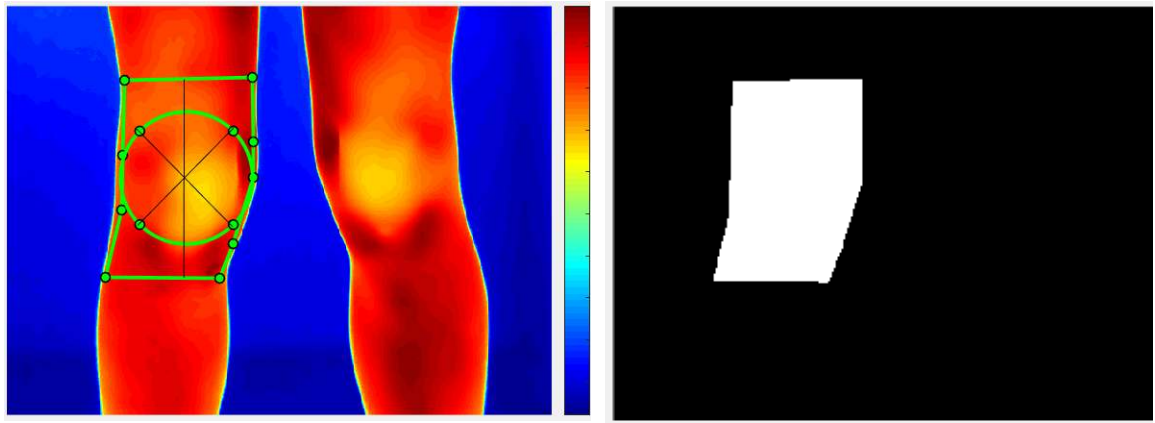


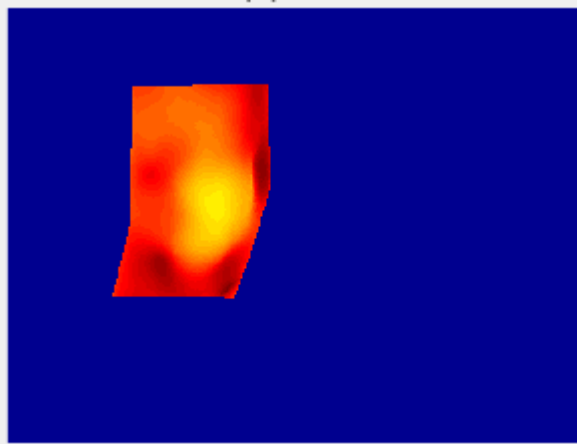
Figure 5-4 Illustration of Skeletal ankle (side view and front view) (OrthoInfo, 2019)

The segmentation process using the knee as an example is described in Figure 5-5. After the ROI was identified, a mask of the region was generated and mapped over the original image, rectangular cropping was then performed to extract the ROI from the full image.

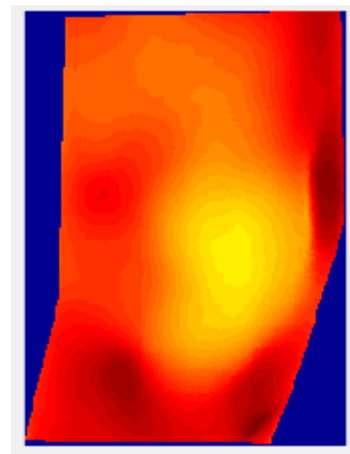


(a) Identified ROI

(b) The binary mask of ROI



(c) ROI



(d) ROI cropped out

Figure 5-5 Segmentation process using the knee as an example (a) identified ROI (b) ROI binary mask (c) ROI (d) Extracted ROI

The thermal images described are shown in colour images for visual display and for visually cropping the first image in the algorithm. However, the images processed were not RGB (Red Green Blue) but each pixel represented the actual temperature in degree centigrade.

5.1.3.3 Tracking by template matching

The ROIs for the remaining images in the same recording were then determined using a template matching algorithm based on normalised cross correlation (NCC) (Lewis, 1995). A tracking operation was needed as the small body movements during the recording caused the ROI to appear in different locations for each recorded image.

The converted sequence file loaded into MATLAB[®] as a mat file read approximately 600 files into the system. The operation of the algorithm is explained in the next steps (Griffin,2009).

- The first image, A, was displayed and the template (ROI) was selected and cropped out.
- For the next image, B, the NCC matrix of the template and image B was determined. The NCC matrix is in the value range of -1 to 1(The NCC function scans the template over the image to find the best match).
- The $(row, column)$ coordinates of the position of the highest NCC value was obtained as the location of the best match in the NCC matrix and used to determine the best match in the image B.
- The coordinates of the best match in image B were then used to identify the new template in image B, using the width and height of the first template.
- This process is repeated for the subsequent images to determine the new ROIs.

Figure 5-6 illustrates an example performed in the laboratory to test the NCC-based tracking algorithm implemented in this study. This example shows a right ankle moving from left to right and the ROI marked by the box, maintaining its original position at the back of the ankle, irrespective of the ankle movement. Figure 5-7 shows the starting location (x, y) of the ROI in each image for the entire recording. Figure 5-7 shows the x and y axes, changing position as it tracks the ROI, verifying the algorithm could match the ROI template as it moves. The x and y axes record the horizontal and vertical movement respectively.

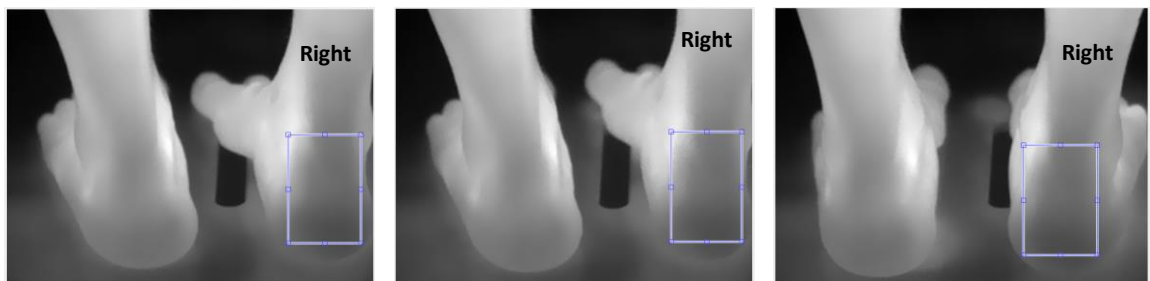


Figure 5-6 ROI tracked through right ankle movement from left to right direction

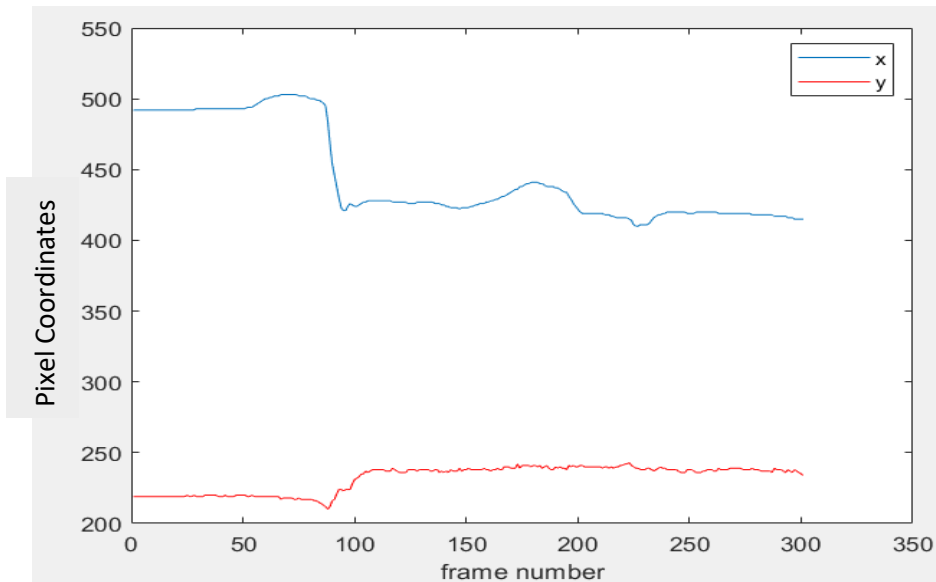


Figure 5-7 ROI locations for each image tracked accurately (the image x coordinate is in blue and y coordinate is in red)

An example to illustrate the tracking of the knee is shown in Figures 5-8 to 5-10. The first image has ROI starting at the (20.5, 60.5) point (see Figure 5-8).

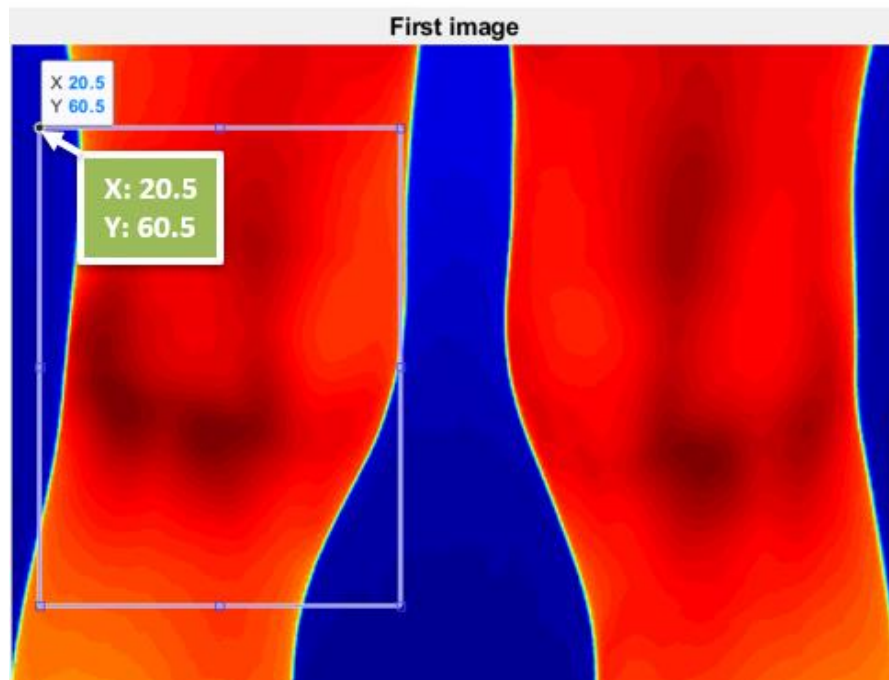


Figure 5-8 Back of knee showing first image ROI at (20.5, 60.5)

At the end of the tracking algorithm, the last image shows the ROI at the (29, 60) point, (see Figure 5-9) showing that the patient had moved in the course of the recording. Despite the movement, the tracking algorithm was still able to identify the ROI. The ROI co-ordinates for all the frames is shown in Figure 5-11 showing movements in both the x and y axes.

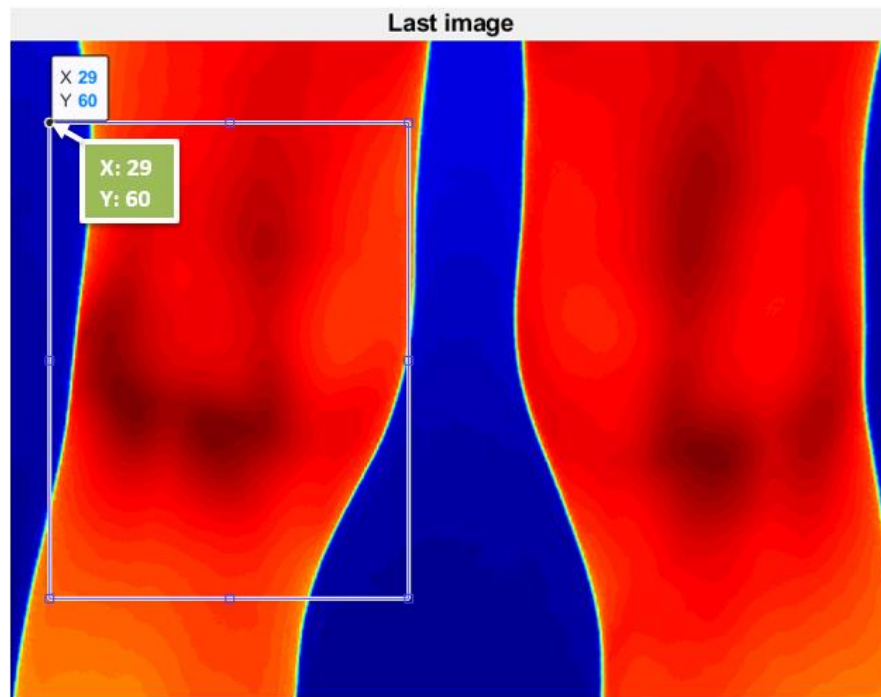


Figure 5-9 Back of knee showing last frame ROI at (29,60)

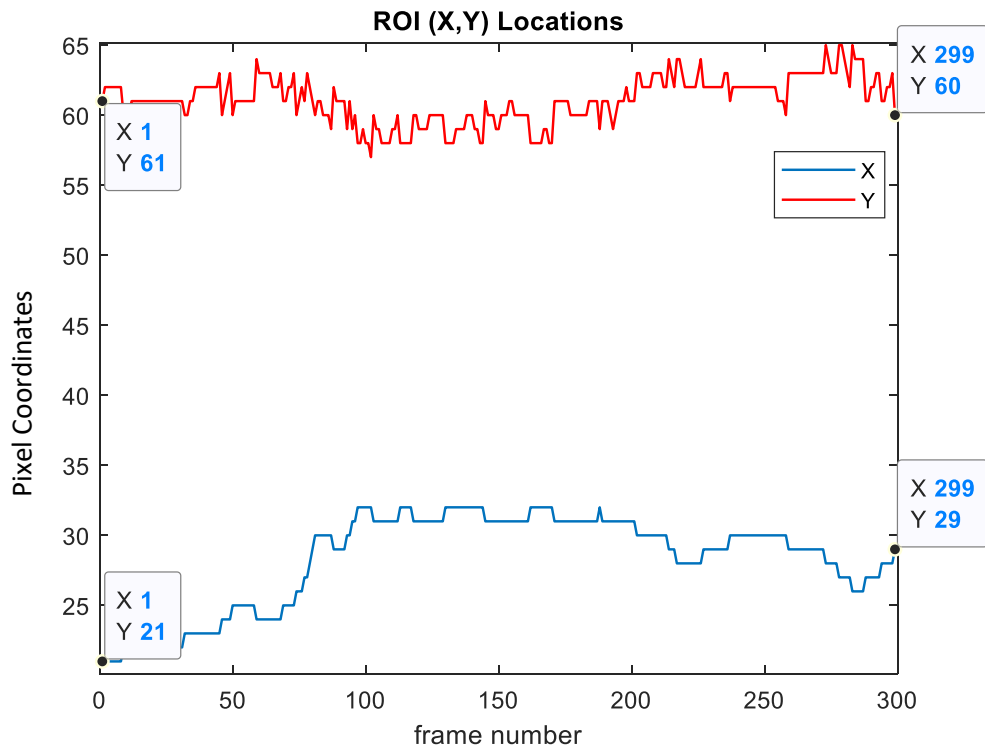


Figure 5-10 ROI (X, Y image pixel coordinates) tracked through the recorded frames. The starting coordinates were approximated in this Figure to (21, 61)

5.1.3.4 Temperature measurement

Once the ROI was detected in each image, the pixel values contained within the ROIs representing the temperatures were averaged to obtain a single value representing the temperature of the selected region. These values were then further averaged across all recorded images to obtain a better estimate of the temperature.

The above process was repeated for the front and back of the knees and ankles.

5.2 Results and discussion

The aim of this study was to investigate if high-resolution TI correlates with clinician musculoskeletal examination in the identification of changes in skin temperature. Eighty thermal images in total were analysed (twenty each from the front and back of knees and ankles).

To aid the analysis of the results, the patients were grouped into three categories based on the knees and ankles clinically identified to have active arthritis at the time of assessment.

- Category I: patients with only one knee/ankle with active arthritis

- Category II: patients with both knees/ankles with active arthritis
- Category III: patients with no knee/ankle with active arthritis

The knees and ankles were segmented with the segmentation process described in section 5.1.4.

Mean temperatures for the left and right knees and ankles were computed and compared against clinical assessment. The Percentage Temperature Difference (PTD) between the left and right knees and ankles were also obtained and compared between categories. The PTD was computed by taking the Absolute Temperature Difference (ATD) over the average of the left and right legs' temperatures as given in Equation 5-1, i.e. (Cole & Altman, 2017)

$$PTD = \frac{ATD}{(T_L + T_R)/2} \times 100 \quad 5-1$$

where T_L and T_R are the measured temperatures for the left and right joints' (knees or ankles) respectively.

5.2.1 Knee analysis

5.2.1.1 Category I – Patients with active arthritis in one knee only

Eight out of twenty patients were clinically diagnosed with active arthritis in one knee.

Table 5-1 present the mean temperature measurements and PTD values between the left and right joints of the front of the knees for category I patients.

Table 5-1 TI mean temperatures and temperature difference – Category I - Knees

Front knee – one knee with active arthritis							
Patient	Mean temperatures -TI		Thermal Imaging-Based (A) (Front knee)			Consultant's evaluation (Active arthritis) (B)	Correlation of methods (A) and (B)
	Left knee (°C)	Right knee (°C)	Warmer knee	ATD (°C)	PTD (%)		
1	33.67	32.89	Left	0.78	2.34	Left	Yes
3	30.18	31.17	Right	0.99	3.23	Right	Yes
5	32.17	31.97	Left	0.20	0.62	Right	No
6	30.46	30.90	Right	0.44	1.43	Right	Yes
9	29.61	30.60	Right	0.99	3.29	Left	No
10	30.20	30.45	Right	0.25	0.82	Right	Yes
11	32.61	28.78	Left	3.83	12.48	Left	Yes
12	31.43	31.16	Left	0.27	0.86	Left	Yes
Mean				0.97	3.14		

For the front of the knees, there was 75% (six out of eight) correlation between TI and clinical assessment with an average PTD of 3.14% (This PTD value will be compared will be compared with that from categories II and III in the following sections). TI results for patients 5 and 9 did not agree with clinical evaluation. These two cases are further analysed to explore the discrepancy in the thermal and clinical assessments.

5.2.1.1.1 Patient 5

The thermal images showing the left and right ROIs (in the box) are shown in Figure 5-11. TI reports the left knee to be warmer while clinical observation picks the right knee as the knee with active arthritis. From Figure 5-11, the darker the region, the higher the temperature as indicated on the colour bar, so the darker regions appear more on the left ROI than the right ROI. The patient, on clinical examination, was reported to have a warm, swollen and restricted right knee. They walked with a limp and had fixed flexion deformity on the right knee -this means they were unable to fully straighten or extend their right knee. This may lead to altered mobility and the patient leaning more on the left leg, causing more blood flow through the left leg, thereby resulting in the left knee having a higher temperature as measured by TI, for correlation purposes. Another factor to be considered is clinician's prior related knowledge of the patient's diagnosis (obtained through other examinations and assessments) and the visual

examination of the knees, which could lead them to decide the knee that is swollen and restricted to be the warmer knee.

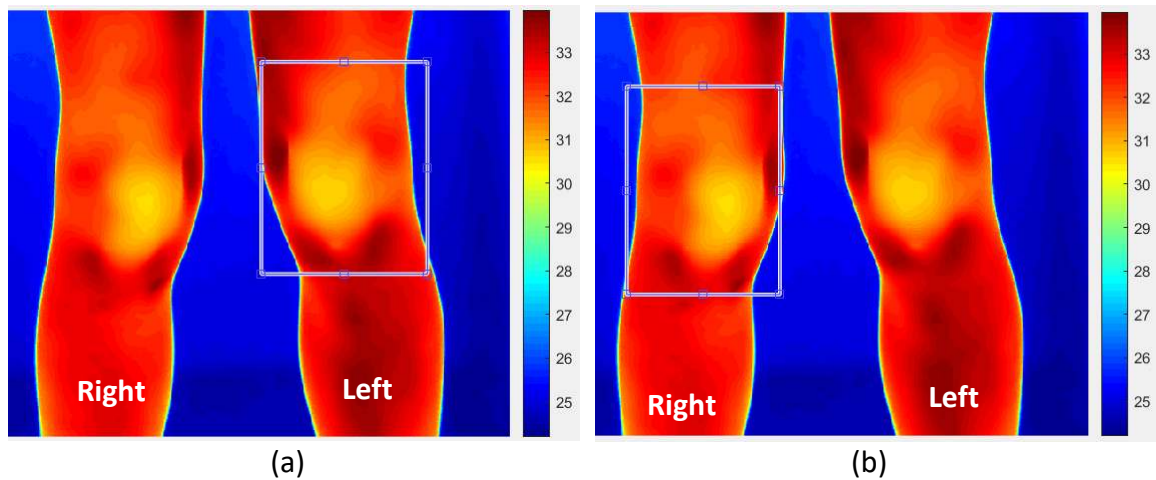


Figure 5-11 Patient 5 thermal images – (a) Left knee ROI (b) Right knee ROI

5.2.1.1.2 Patient 9

The situation is also similar for patient 9. On clinical examination, they were reported to have swollen left knee, established restriction on the left knee due to arthritic changes to left hip, with adaptive shortening of the overlying muscles causing fixed flexion deformity on the left knee. They also walked with 2 elbow crutches with reduced weight-bearing through the left leg. Warmth was not detected by the clinician for this patient.

On the thermal images (Figure 5-12), the fixed flexion deformity can be seen on the left leg as it looks slightly bent forward (the right leg appears as though it is behind the left leg). The darker regions which signify higher temperatures also appear more on the right leg than the left leg. So, although the left knee is clinically confirmed to have active arthritis, TI has indicated the right knee as being warmer due to the reduced weight bearing on the left knee.

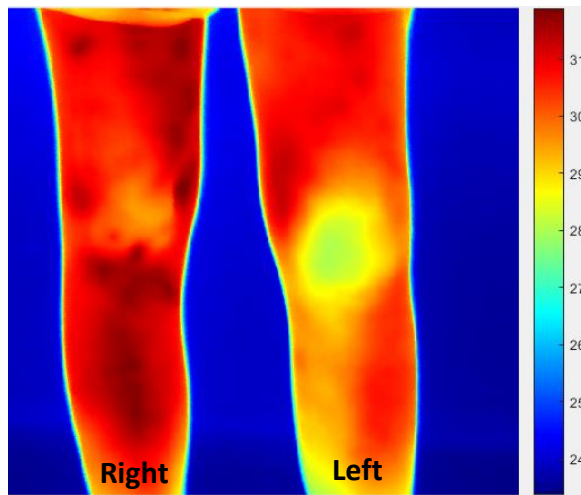


Figure 5-12 Patient 9 thermal image showing the right leg with darker regions (higher temperatures) than the left leg

Table 5-2 presents results for the back of the knees. Correlation between TI and consultant's evaluation is 50% while the other 50% did not agree including patients 5 and 9, whose front knee TI measurement did not also agree with the consultant's evaluation (same reasons apply for the front and back of knees for patients 5 and 9). Thermal images for the front and back of the knees of patients 1 and 12 are provided in Figure 5-13.

Table 5-2 Mean temperatures and PTD for back of knees

Back knee – one knee with active arthritis							
Patient	Mean temperatures -TI		Thermal Imaging-Based (A) (Back knee)			Consultant's evaluation (Active arthritis) (B)	Correlation of methods (A) and (B)
	Left knee (°C)	Right knee (°C)	Warmer knee	ATD (°C)	PTD (%)		
1	32.84	32.89	Right	0.05	0.15	Left	No
3	29.65	29.93	Right	0.27	0.92	Right	Yes
5	33.61	33.15	Left	0.46	1.37	Right	No
6	30.64	31.10	Right	0.46	1.48	Right	Yes
9	29.94	31.19	Right	1.25	4.09	Left	No
10	31.17	31.23	Right	0.06	0.18	Right	Yes
11	31.05	30.76	Left	0.29	0.94	Left	Yes
12	30.53	30.72	Right	0.19	0.60	Left	No
Mean				0.38	1.22		

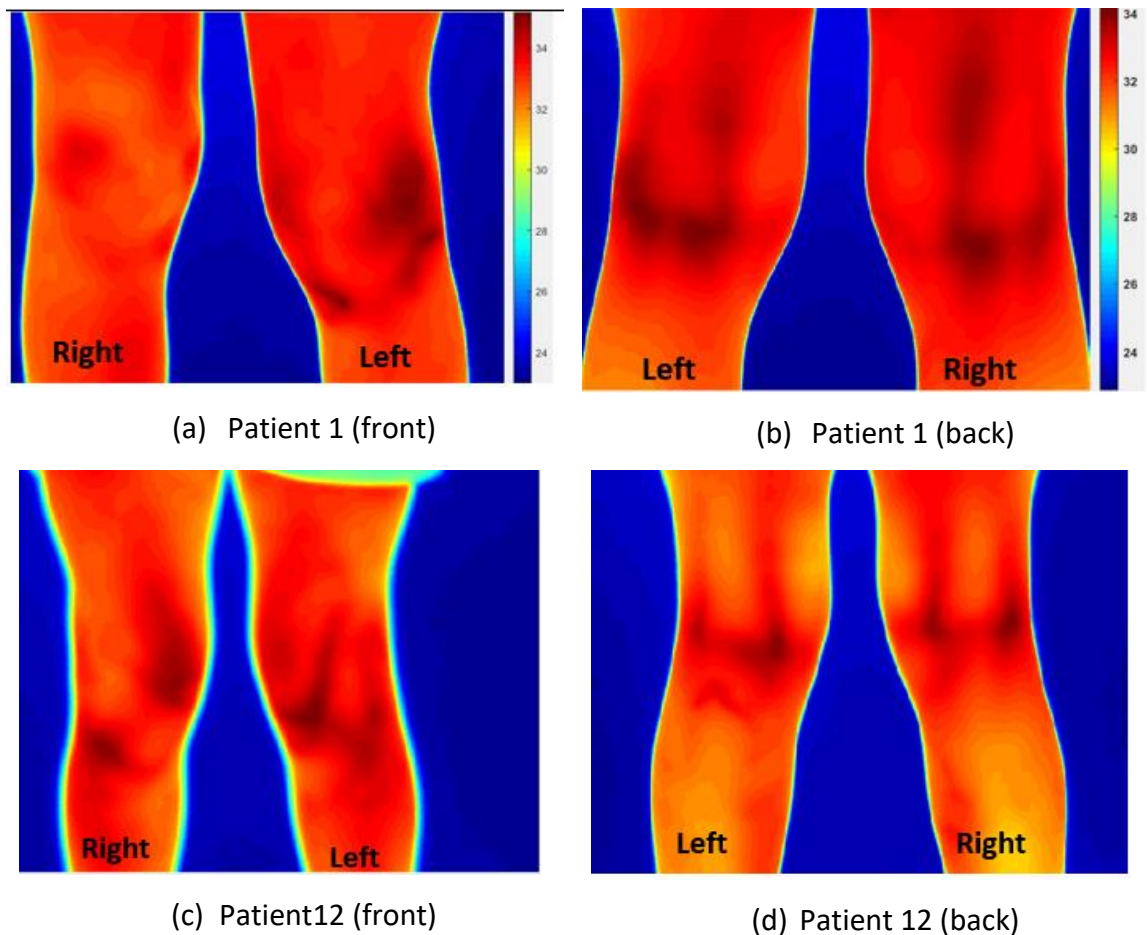


Figure 5-13 Thermal images for front and back of knees for patients' 1 and 12

For patients 1 and 12, the temperature difference between the left and right knees were more noticeable from the thermal images at the front than at the back (Figure 5-13). The mean PTD for front of the knees was higher at 3.14% than for back of knees at 1.22% indicating the temperature changes were more pronounced at the front than the back as well. These suggest that the front knees gave a better presentation of the situation. However, the results from the front and the back of knees (Tables 5-1 and 5-2) show a 75% correlation, indicating there is consistency in the results.

5.2.1.1.3 Patient 11

This patient presents a case where TI and consultant's evaluation did correlate. The thermal images for the front and back of the knees are shown in Figure 5-14. Clinical examination reported a warm, restricted and swollen left knee, and was diagnosed with active arthritis on the day of assessment. TI results also showed the left knee was warmer than the right by 12.48% at the front and 0.94% at the back.

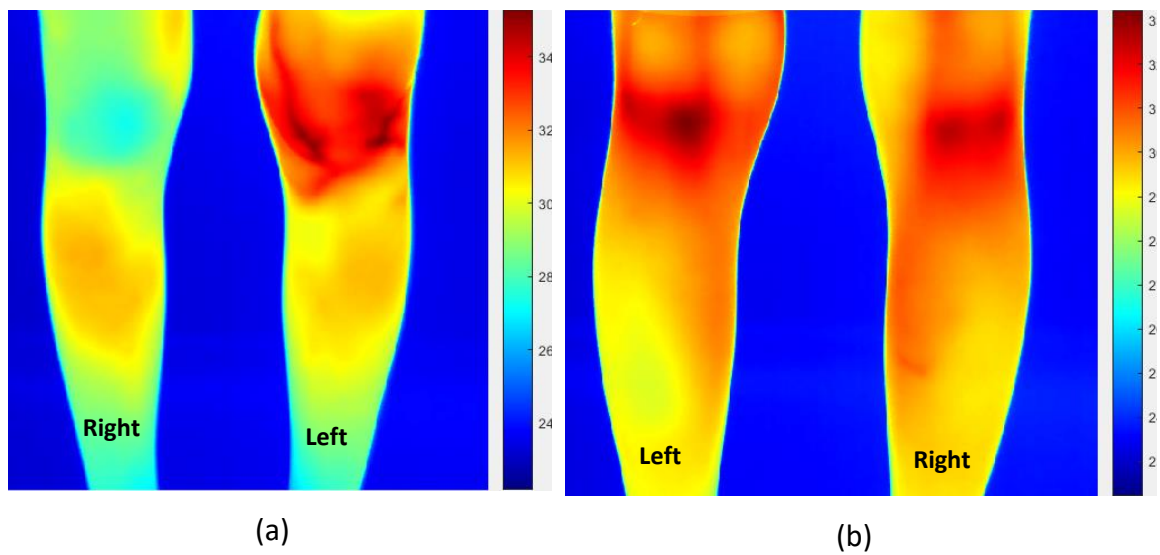


Figure 5-14 Patient 11 thermal images (a) Front knee (b) back knee

5.2.1.2 Category II – Patients with active arthritis in both knees

This category includes patients that had active arthritis in both knees according to clinical evaluation. Direct comparison between TI and consultant’s evaluation could not be carried out for this group as there was no record of normal skin temperature for each patient to be used as a baseline reference. However, to determine how skin temperature around the knee compared to other parts of the body, a section from the back of the left and right legs was segmented, averaged and used as a reference (to see if the knee temperatures are higher). Results are shown in Table 5-3.

Table 5-3 Front and back knee temperatures for when both knees are diagnosed with active arthritis

Active arthritis in both knees (Consultant's evaluation)									
Mean temperatures - TI									
Patient	Front of the knee				Back of the knee				Reference (°C)
	Left knee (°C)	Right knee (°C)	ATD (°C)	PTD (%)	Left knee (°C)	Right knee (°C)	ATD (°C)	PTD (%)	
2	28.34	28.47	0.13	0.46	29.11	29.21	0.11	0.36	28.33
7	32.23	33.14	0.91	2.78	31.79	31.80	0.01	0.03	29.21
8	30.16	30.81	0.65	2.12	30.96	30.95	0.01	0.04	29.35
14	31.56	31.33	0.23	0.72	31.49	31.50	0.01	0.03	30.03
15	33.17	32.82	0.35	1.05	32.68	32.73	0.06	0.17	31.35
16	32.68	32.90	0.23	0.69	32.72	32.16	0.57	1.74	31.61
17	30.90	31.16	0.26	0.84	30.90	30.71	0.19	0.60	29.42
19	32.56	32.81	0.25	0.77	32.42	32.36	0.05	0.16	30.89
Mean			0.37	1.18			0.12	0.39	

For all the patients in this category except patient 2 (front of the knees), the computed reference temperature, for both the front and back of the knees was lower than the knee temperatures (see Figures 5-15 and 5-16), giving an indication that the knees could have the active disease as evaluated by the consultant. For patient 2 (front of knees), the left and right knees and computed reference temperatures are close.

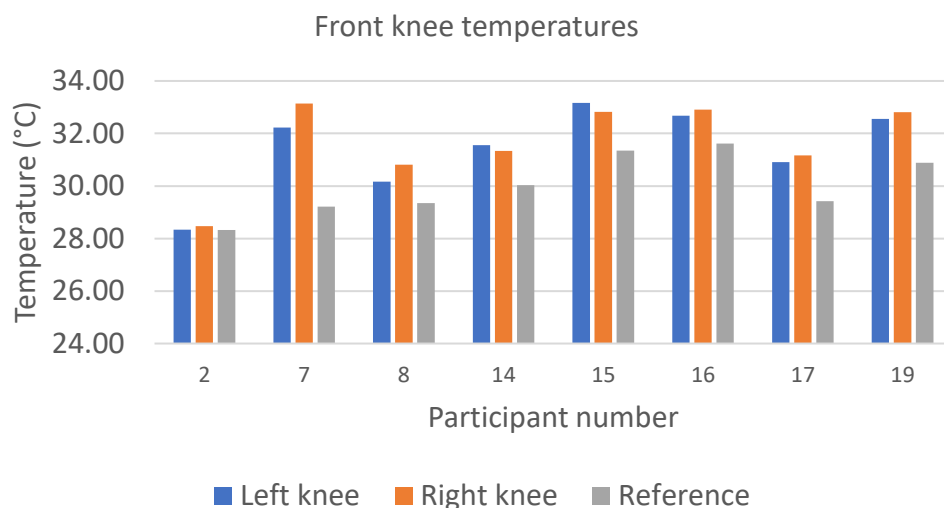


Figure 5-15 Chart showing reference temperature (grey bar) lower than the left and right knee temperatures for front of the knee

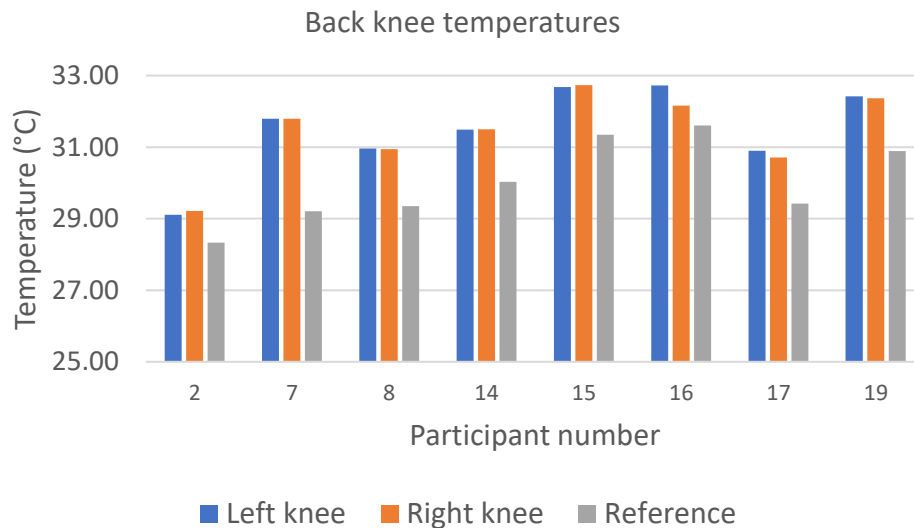


Figure 5-16 Chart showing reference temperature (grey bar) lower than the left and right knee temperatures for back of the knee

The PTD for categories I (one knee active) and II (both knees active) are summarised in Table 5-4. For the front knee, category I PTD was 2.7 times higher than the category II PTD and for the back knees, 3.1 times higher than the category II PTD.

Table 5-4 Average PTD for category I and II

Category	PTD (%)	
	Front knee	Back knee
I (one knee active)	3.14	1.22
II (both knees active)	1.18	0.39

Analysing the temperature difference was another way to investigate and compare the results with the clinician's assessment as this is independent of the computed reference temperatures. Theoretically, PTD for when one knee is active should be higher than that for when both knees are active. The result presented in Table 5-4 conforms to theory, further indicating that TI partially agrees with clinical assessment.

However, with no information regarding which knee was worse from the clinical examination or a measured reference temperature, there was no way to adequately correlate TI analysis with the consultant's evaluation. Results were not conclusive.

5.2.1.3 Category III – Patients with no active knee arthritis

Patients in this category did not have active arthritis in the knees at the time of the clinical assessment. It is expected then that the temperatures measured at the left and right knees to be approximately the same or with minimal difference. The PTD for the front and back of the knees is computed (Table 5-5) and compared with the PTD from category I.

Table 5-5 Front and back knee mean temperatures with no active arthritis

No active arthritis in the knees (Consultant's evaluation)								
Mean temperatures - TI								
Patient	Front knee				Back knee			
	Left knee (°C)	Right knee (°C)	ATD (°C)	PTD (%)	Left knee (°C)	Right knee (°C)	ATD (°C)	PTD (%)
4	31.90	31.87	0.03	0.09	32.39	32.06	0.32	1.01
13	30.38	30.28	0.10	0.33	32.41	31.70	0.71	2.21
18	32.40	32.18	0.23	0.70	31.25	31.51	0.26	0.83
20	31.61	31.76	0.15	0.48	31.07	31.45	0.38	1.23
Mean			0.13	0.40			0.42	1.32

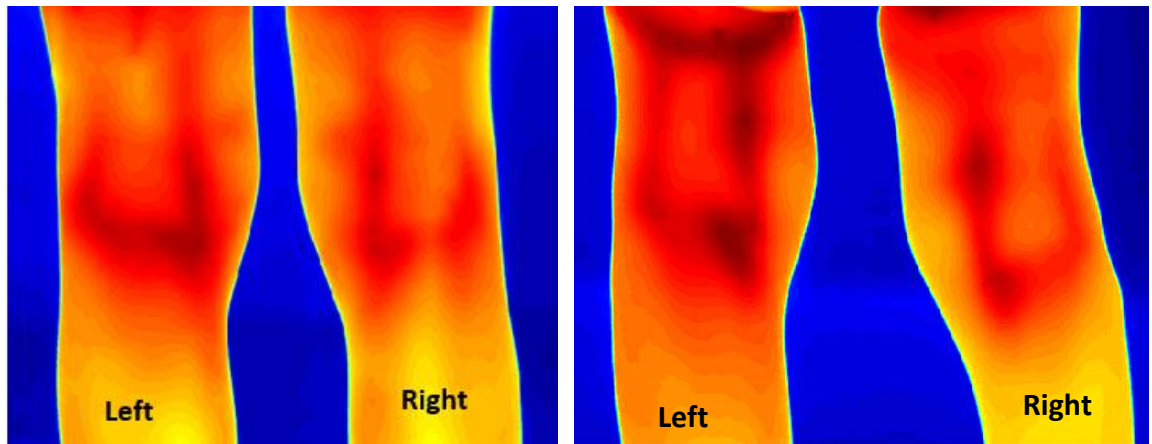
Table 5-6 shows the mean PTD for categories I and III patients for the front and back of the knees.

Table 5-6 Average PTD for category I and III

Category	PTD (%)	
	Front knee	Back knee
I (one active arthritic knee)	3.14	1.22
III (No active arthritic knee)	0.40	1.32

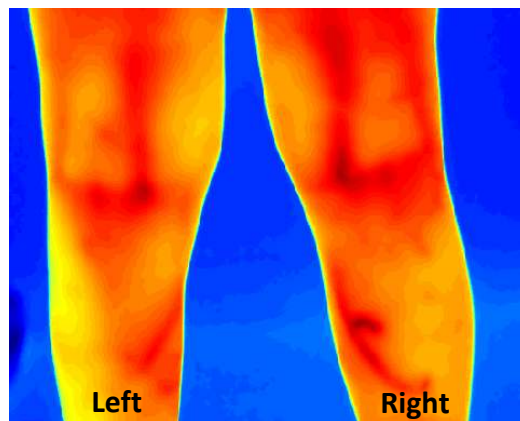
From Table 5-6, the PTD for the front of the knees is 7.85 times lower than that of category I, agreeing with theory. The back of the knees however, showed a slightly higher PTD than those of category I (1.08 times higher), suggesting there was a higher temperature change between the left and right knees at the back.

So, while the front of the knees did suggest both knees may be inactive as PTD is much lower than those of category I, the back of knees shows a slightly higher PTD, suggesting there may be some activity. There was, therefore, partial correlation between TI and consultant's evaluation. Same experiments on a larger data set, would give more details on the results. The thermal images for the back of the knees are provided in Figure 5-17 showing visually that there were significant temperature changes between both knees.



Patient 4

Patient 13



Patient 20

Figure 5-17 Thermal images showing back of knees for category III Patients

5.2.2 Ankle analysis

The results for the ankles are presented in this section.

5.2.2.1 Category I – Patients with active arthritis in one ankle

Patients in this group include 1, 2, 6, 7, 8, 9, 10, 13, and 16. The mean temperatures obtained for each patient for the front and back of ankles is shown in Tables 5-7 and 5-8. TI and clinical evaluation fully correlate for patients 6, 7, 8 and 10; partially correlate for patients 2, 13 and 16 (where the TI did not detect the same ankle as warmer for the front and the back) and no correlation for patients 1 and 9.

Table 5-7 Front ankle results for patients with one active ankle arthritis.

Front ankle – one ankle with active arthritis							
Patient	Mean temperatures -TI		Thermal Imaging-Based (A) (Front ankle)			Consultant's evaluation (Active arthritis) (B)	Correlation of methods (A) and (B)
	Left knee (°C)	Right knee (°C)	Warmer ankle	ATD (°C)	PTD (%)		
1	32.76	33.28	Right	0.52	1.58	Left	No
2	30.61	30.56	Left	0.05	0.15	Left	Yes
6	28.47	30.30	Right	1.82	6.20	Right	Yes
7	26.21	30.88	Right	4.67	16.37	Right	Yes
8	28.08	29.24	Right	1.16	4.04	Right	Yes
9	24.92	26.94	Right	2.01	7.77	Left	No
10	32.47	32.79	Right	0.32	0.97	Right	Yes
13	31.28	30.52	Left	0.76	2.46	Right	No
16	33.30	33.11	Left	0.19	0.57	Left	Yes
Mean				1.28	4.46		

Table 5-8 Back ankle results for patients with one active ankle arthritis

Back ankle – one ankle with active arthritis							
Patient	Mean temperatures -TI		Thermal Imaging-Based (A) (Back ankle)			Consultant's evaluation (Active arthritis) (B)	Correlation of methods (A) and (B)
	Left knee (°C)	Right knee (°C)	Warmer ankle	ATD (°C)	PTD (%)		
1	31.29	31.36	Right	0.07	0.22	Left	No
2	28.10	28.36	Right	0.27	0.95	Left	No
6	28.65	29.04	Right	0.39	1.36	Right	Yes
7	25.89	30.43	Right	4.54	16.12	Right	Yes
8	26.64	28.13	Right	1.49	5.45	Right	Yes
9	25.26	26.45	Right	1.19	4.59	Left	No
10	30.68	30.74	Right	0.05	0.18	Right	Yes
13	29.40	30.52	Right	1.12	3.74	Right	Yes
16	31.66	31.72	Right	0.06	0.21	Left	No
Mean				1.02	3.65		

The cases for some patients are explored further in the following sections

5.2.2.1.1 Patient 1

The TI and clinical report did not agree for this patient. Figure 5-18 provides the TI of the front and back of the ankles.

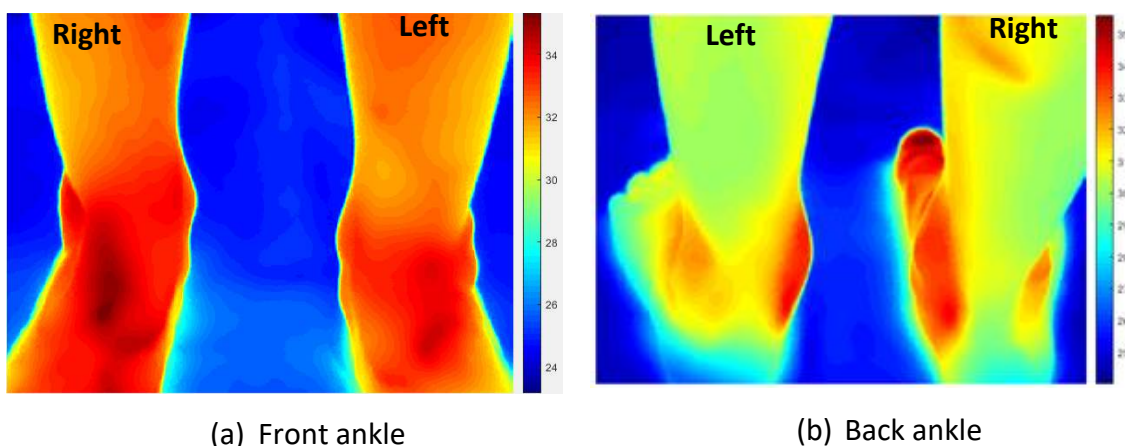


Figure 5-18 Thermal images for patient 1 showing the (a) front and (b) back of ankles
(The warmer regions are the darkest spots as indicated in the colour bar)

As seen from Figure 5-18, the right ankle showed warmer regions than the left ankle (the front more than the back). Clinical assessment reported the patient had a swollen left ankle thereby putting more weight on the right leg. Warmth was not detected on both ankles by the consultant. TI has detected the right ankle as the warmer joint and this could be due to the reduced weight bearing on the left leg, which causes more blood flow on the right leg.

5.2.2.1.2 Patient 9

Patient 9 TI data and clinical report did not also correlate. The thermal images are provided in Figure 5-19.

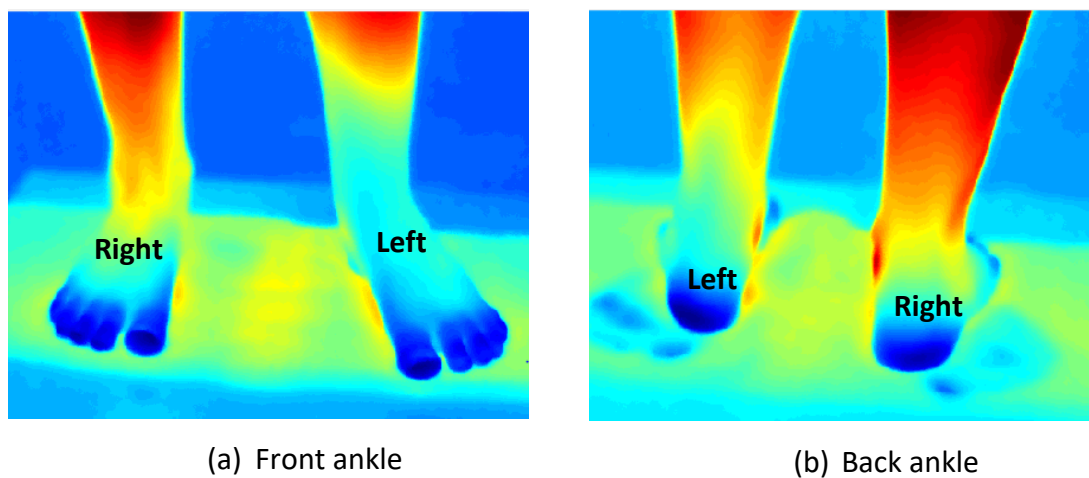
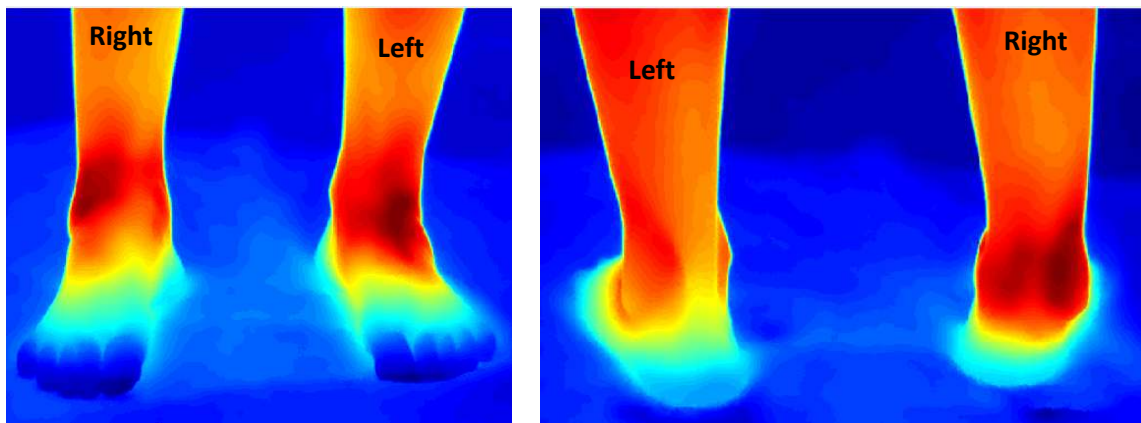


Figure 5-19: TI for patient 9 showing the front and back of ankles (The hotter regions are the darker regions)

The right ankle shows a higher temperature than the left for the front and back according to TI. Clinical report stated the left ankle was the joint with active arthritis; it also reported the patient had arthritic changes to their left hip, shortening of the overlying muscles causing flexion deformity on the left knee, walked with the aid of elbow crutches with reduced weight-bearing through the left leg as previously identified in the knees. The patient had more of their weight on the right limb, so more blood flows through the right than the left, and as discussed in the knee analysis, could be responsible for why both methods do not agree. The clinician did not also detect warmth at the ankles during their clinical assessment.

5.2.2.1.3 Patient 13

There was partial correlation in this case. Clinical report indicated the right ankle to be the affected joint. The patient had swollen, restricted right ankle, severe degenerative changes to the right ankle, walked with a significant limp and occasionally required a wheelchair. The clinicians did not record any joint warmth at the time of assessment. The TI results from the front of the ankles showed the left was warmer by 0.76°C and the back ankles showed the right ankle was warmer by 1.12°C . Thermal images are shown in Figure 5-20.



(a) Front ankle

(b) Back ankle

Figure 5-20: TI for Patient 13 showing the front and back of ankles (darker regions are warmest)

The thermal image of the front ankles clearly shows the left ankle was warmer. The image in Figure 5-20(a) gives an indication the left was leaned more into, as the right looks slightly jugged forward, and may have caused the left ankle to look warmer at the front.

5.2.2.1.4 Patient 7

This is a case where there was full correlation between TI and clinical report. TI images are shown in Figure 5-21.

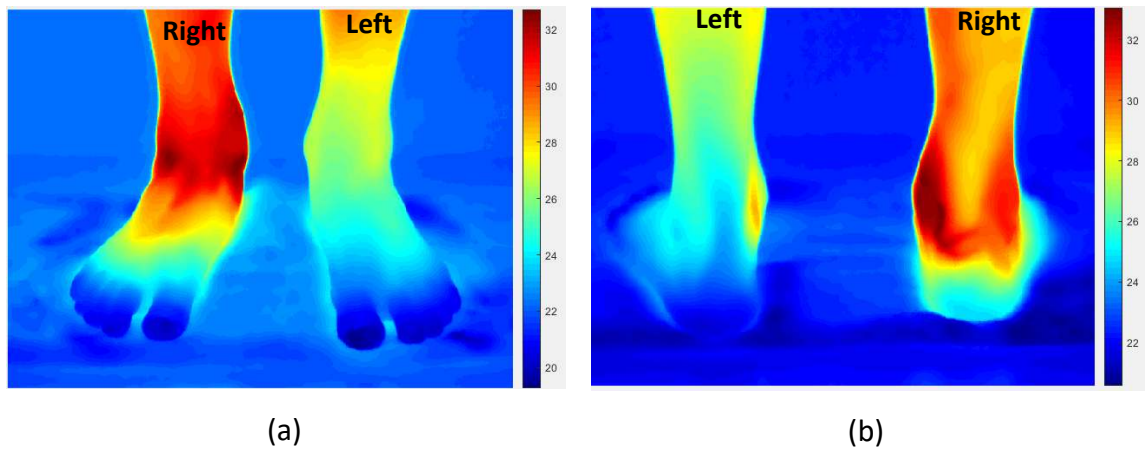


Figure 5-21: TI for patient 7 showing the front and back of ankles (darker regions are warmest)

Clinical report indicated the right ankle had active arthritis. TI also detected the same ankle as the warmer one as detailed in Tables 5-7 and 5-8.

5.2.2.2 Category II—Patients with active arthritis in both ankles

Four (4) of the patients had both ankles diagnosed with active arthritis on the day of assessment. An attempt to determine how the ankle temperatures compared against another section of the leg was performed to aid analysis. The results of the mean temperatures obtained for this group compared with the computed reference temperature (back of the legs) are shown in Table 5-9.

Table 5-9 Patients with active arthritis in both ankles

Active arthritis in both ankles (Consultant's evaluation)									
Mean temperatures - TI									
Patient	Front ankle				Back ankle				Reference (°C)
	Left ankle (°C)	Right ankle (°C)	ATD (°C)	PTD (%)	Left ankle (°C)	Right ankle (°C)	ATD (°C)	PTD (%)	
12	30.95	30.76	0.19	0.63	29.32	29.26	0.07	0.22	29.39
14	33.00	32.70	0.30	0.91	30.23	30.90	0.68	2.21	30.03
18	33.94	33.65	0.29	0.86	31.57	32.22	0.65	2.05	30.69
20	33.03	32.97	0.05	0.16	31.77	31.51	0.26	0.84	29.80
Mean			0.21	0.64			0.41	1.33	

Figures 5-22 and 5-23 compares the left, right and reference temperatures for the front and back of ankles respectively.

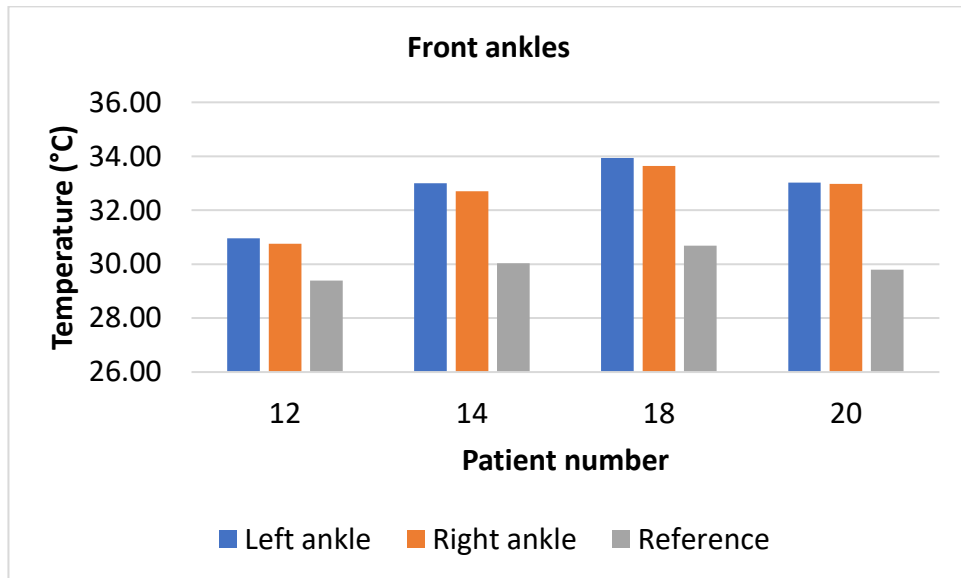


Figure 5-22 Comparing left ankle, right ankle and reference temperatures for front of ankles

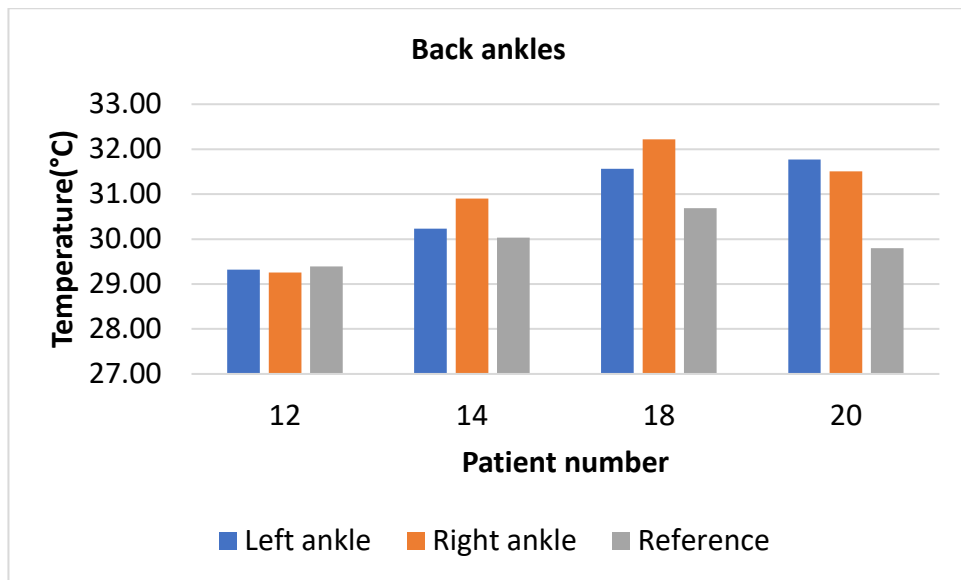


Figure 5-23 Comparing left ankle, right ankle and reference temperatures for back of ankles

From Figures 5-22 and 5-23, the computed reference temperature was lower than the right and left ankle temperatures for both the front and back ankles except for patient 12 whose computed reference temperature was slightly warmer than the left ankle at the back of the ankles. With most of the ankle temperatures higher than the reference (back leg section), could mean there was active arthritis in both ankles.

One of the challenges considered was the reference selection method. The region selected may not be a true representation of the patient's normal temperature as the selected sections could be affected by the arthritis as well or other external factors. However, with the reference temperatures being consistently lower than the ankle temperatures in 87.5% of the cases, does give strong indication the method could be accurate. A clinical measure of the normal skin temperature of the leg region would aid in making a more definite analysis.

The average PTD for the front and back of ankles was lower than that obtained for patients with only one ankle affected, as would be expected. This is shown in Table 5-10.

Table 5-10: Average PTD for Patients in categories I and II

Category	PTD (%)	
	Front knee	Back knee
I (one active arthritic ankle)	4.46	3.65
II (both active arthritic ankles)	0.64	1.33

The musculoskeletal examination did not record which ankle felt warmer (even though both were suspected), therefore proper correlation between TI and clinical examination was not possible. Further information regarding the skin temperature of the patients would aid for a more accurate comparison. Results were inconclusive

5.2.2.3 Category III - Patients with no active arthritis in the ankles

This group of patients did not have active arthritis in the ankles according to clinical reports. TI results obtained are shown in Table 5-11. The average PTDs were compared with those with only one ankle affected (Table 5-12).

Table 5-11 Patients with no active ankle arthritis

No active arthritis in the ankles (Consultant's evaluation)								
Mean temperatures - TI								
Patient	Front of the ankles				Back of the ankles			
	Left ankle (°C)	Right ankle (°C)	ATD (°C)	PTD (%)	Left ankle (°C)	Right ankle (°C)	ATD (°C)	PTD (%)
3	31.24	31.20	0.04	0.13	29.95	29.76	0.18	0.62
4	31.51	30.84	0.66	2.13	29.06	29.78	0.72	2.45
5	31.42	30.77	0.65	2.09	30.15	29.29	0.86	2.91
11	26.65	26.66	0.00	0.01	27.41	27.24	0.17	0.62
15	33.21	33.57	0.35	1.06	32.36	32.33	0.03	0.10
17	32.31	32.34	0.03	0.10	30.86	30.46	0.39	1.29
19	31.03	31.00	0.04	0.12	30.78	30.45	0.32	1.06
Mean			0.25	0.81			0.38	1.29

Table 5-12: Average PTD between patients in categories I and III

Category	PTD (%)	
	Front ankles	Back ankles
I (one active arthritic ankle)	4.46	3.65
III (no active arthritic ankle)	0.81	1.29

The PTDs for the front and back ankles are consistently lower for the patients with no active arthritic ankle than those with the one ankle affected.

5.3 Summary

The research methodology and results for the thermal imaging study were presented in this chapter. The thermal recording was performed in a room with consistent temperature (approximately 23.6°C) and humidity (33%). A 20-second thermal video (at 30 frames per second) of the front and back of the knees and ankles was collected after a 10-minute acclimatisation time using the FLIR T630sc thermal camera.

The regions of interest (ROIs) were then manually segmented after properly identifying the joints. A consistent method for locating the knee and ankle regions was adopted. To track the segmented ROI (template) through the recorded images, a template matching algorithm based on normalised cross correlation was implemented. The average of the pixel values (temperatures) contained within the ROIs was obtained for temperature measurement.

Patients were grouped into three from clinical evaluation of which knees/ankles had active arthritis at the time of the assessment – only one knee/ankle active, both knees/ankles active and no knee/ankle active (categories I to III respectively). Correlation between TI and clinical assessment was seen to be higher at the front of the joints with a 75% correlation at the front of knees and ankles for category I patients. Inconsistencies were observed in some patients, which may be due to the increased reliance on the side with no active arthritis, leading to a higher physical activity and a temperature increase that exceeds that produced by the arthritis. Clinician’s prior knowledge of the patients and their diagnosis may also influence which joint they detect as warmer.

For categories II and III patients, the Percentage Temperature Difference (PTD) was observed to be consistently lower than those of category I patients, agreeing with theory.

These findings confirm the ability of TI to assist clinicians in determining joints' temperature and therefore gives good indication that TI may potentially be an effective tool to aid clinical diagnosis of JIA.

In the next chapter, the results obtained from the visual imaging study are presented and discussed.

Chapter 6

6 Visual imaging (VI) and its Correlation with Thermal Imaging to Assist with Clinical JIA diagnosis

Clinicians look for skin colour changes at the joints of patients suspected of JIA as the changes provide further evidence of the condition. This colour evaluation is subjective and as sometimes the changes are subtle, their detection can be challenging. An automated quantitative way of analysing colour of the joints can make the assessment more accurate and consistent.

A method of analysing joint colour in JIA patients was developed and evaluated on 20 JIA patients. The visual image analysis on the patient's knee (front and back) and ankle (front and back) were obtained. These were investigated to explore whether JIA had altered the skin colour of the joint suspected of JIA. The FLIR T630sc camera used for the thermal recording contains a visual camera which was used to take single visual colour images from the front and back of the knees and ankles for each patient.

The images taken were compared to a reference image (a section under just under the knee) based on their colour features using the Euclidean distance metric method. The image that was more different from the reference image, in terms of colour, was more likely the active arthritic joint. The results obtained were correlated to the consultant's evaluation as well as the thermal imaging results from Chapter 5.

6.1 Methodology

6.1.1 Data collection

Single visual images of the front and back of knees and ankles of the twenty patients with active arthritis on one or both knees and ankles were taken in standing position, using the FLIR T630sc camera. The acquired images were in JPEG format with a resolution of 2592 x 1944 pixels. The visual images were taken immediately after acquiring the thermal images, ensuring the knees and ankles were not touched.

6.1.2 Data processing

The steps involved in processing the images are explained in the following subsections.

6.1.2.1 Identification and segmentation of the regions of interest (ROI)

The ROI identification process used for selecting the knees and ankles in the thermal images discussed in chapter 5 (Section 5.1.3) was also implemented here for identifying the areas to be segmented. The selected regions for the knees and ankles in a patient were roughly the same size as illustrated in the knee example in Figure 6-1. The areas selected under the knees were cropped and used for reference. Figure 6-2 shows the cropped ROIs.

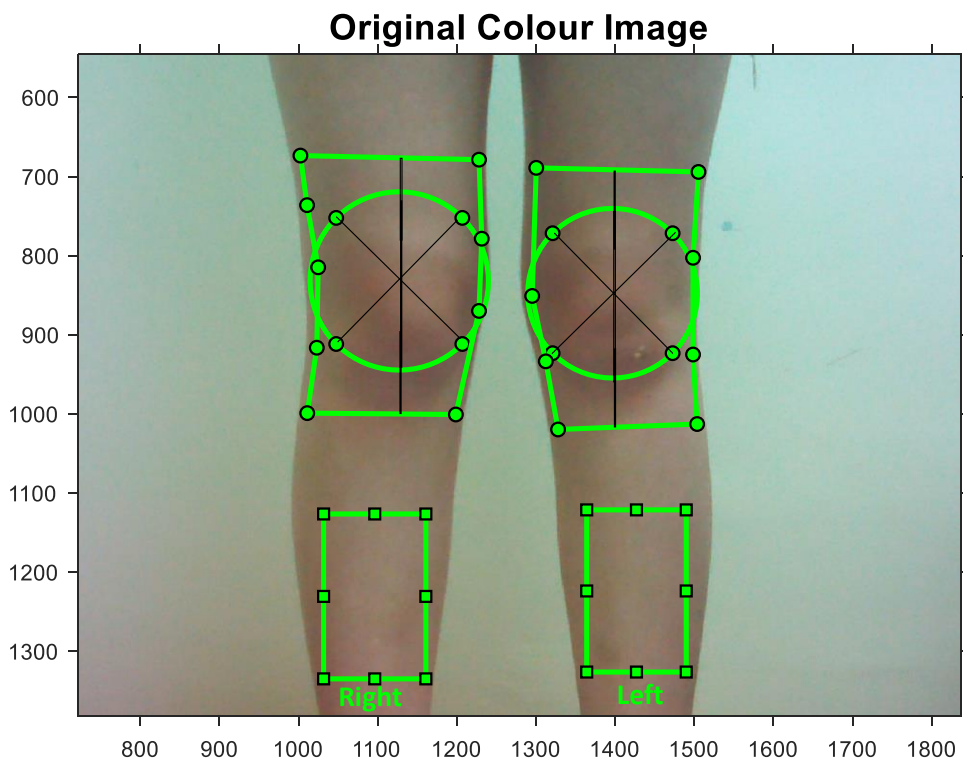


Figure 6-1 The cropped knee region and areas under them used to obtain the reference are shown.

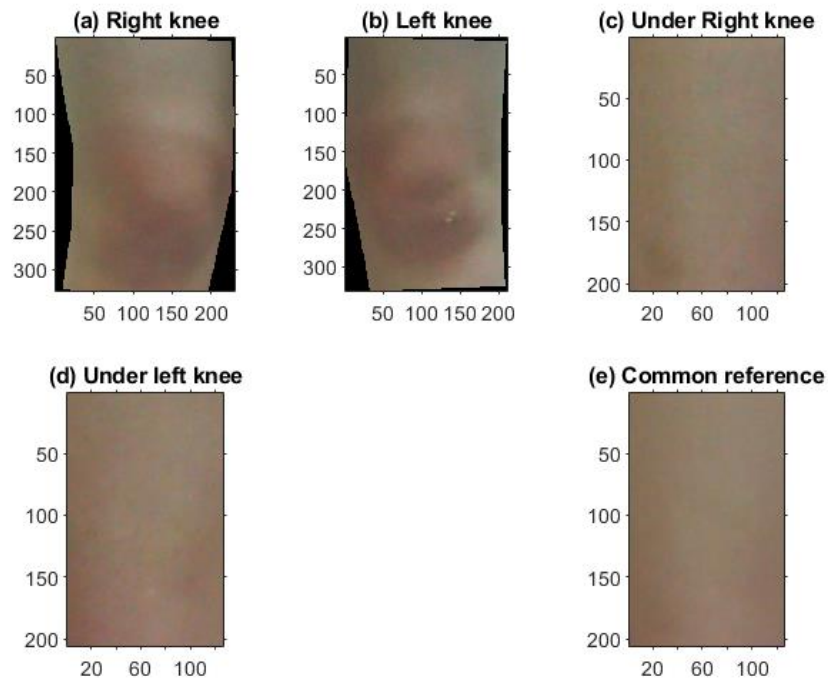


Figure 6-2 Sample of knee segmented regions after cropping showing the black background of the cropped ROIs in (a) and (b)

6.1.2.2 Reference image consideration

Comparing the left and right joints to a reference was considered rather than comparing the joints directly because even two healthy joints would not be of the same colour when quantified. So, the idea to compare to a reference image was to determine, which was more different to that reference section taken from the same patient.

There were two options to compare the colours of the knees/ankles for the patients:

1. Comparison of the colour of each knee/ankle with a reference region taken from under the same knee (i.e. comparing left knee/ankle with reference taken from under left knee and right knee/ankle with reference taken from under right knee). In this approach, the possible colour offset of a leg would not affect the comparisons but the issue with this approach is that the two knees are using different references (Results are presented in Table 6-1).
2. Comparison of the colours of the knees/ankles with the average of the reference regions taken under both knees. In this approach, a common reference is used for both knees/ankles and the difficulty referred to in

approach A is overcome and thus chosen for the analysis of the visual images (see Table 6-2).

Figure 6-1 shows the reference regions under the knees manually cropped by displaying the visual image on the screen. The sizes of the two references were the same and they were averaged to obtain a common reference.

6.1.2.3 Similarity metric

The Euclidean distance metric was used to determine the similarity between the images using the histograms as a colour feature. The histograms, which hold the colour information of the images, (knees, ankles and reference), were obtained and the similarity index was computed by calculating the Euclidean distance between their histograms. The smaller the distance, the higher the similarity between the images. The Euclidean distance (*eDistance*) for n pixels between the colour distributions of the test image, A and the reference image, B is given in Equation 6-1.

$$eDistance = \sqrt{\sum_{i=1}^n (A_i - B_i)^2} \quad 6-1$$

6.1.2.4 Comparing the colours of the ROIs and Reference

In order to compare the colours of the knees/ankles with the common reference, the colour histograms of the knee/ankle regions and that of the common reference were obtained in the red, green and blue channels. The pixel values histogram bin number covered the full range for each channel, i.e. 0 to 255. Bin 0 was excluded as it represented the black background of the cropped region (the cropped regions for the knee/ankle appeared on a square frame with areas not covered by the selected region appeared as black – see Figures 6-2(a) and (b)). The Euclidean distance of the histograms of each knee/ankle and that of the reference for each channel were then determined. The mean distance was then computed by averaging the distances obtained from the red, green and blue channels of the colour images. The knee/ankle image with a larger distance was considered the joint with more changes in colour as compared to the other knee/ankle.

6.1.2.5 Operation of the algorithm

Eighty visual images in total were processed (twenty each from the front and back of the knees and ankles). The acquired images were subsequently processed offline in MATLAB[®]. Each visual image was loaded and displayed on a computer screen and the knees, ankles, and reference were identified and cropped. The histograms for the images were computed and the similarity between the joints and reference was determined by finding the Euclidean distance between their histograms (colour distributions). The image less similar to the reference was considered to be the joint with more colour changes, and for the purpose of this study, assumed to be due to the active arthritis.

6.1.2.6 Testing the algorithm

The images to be compared in this study had no obvious differences in colour as can be seen in Figures 6-1 and 6-2. Therefore, some sample coloured pictures were initially used to test the working of the algorithm.

Figures 6-3 show some sample images tested.




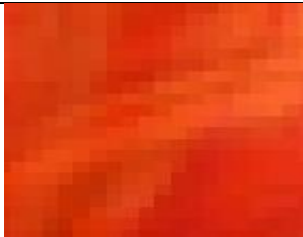


	Reference image	Test image 1	Test image 2
(a)		 Distance = 1412	 Distance = 1960
(b)		 Distance = 53	 Distance = 64

Figure 6-3 Sample images used to test similarity algorithm (Keen, 2005)

In order to illustrate the effectiveness of colour assessments, the images shown in Figure 6-3 were used. The figure shows two sets of images, (a) and (b) and the

similarity algorithm was tested to see if the images that more are more similar in colour would have a smaller distance. The reference images were used to compare with the test images 1 and 2.

Following the algorithm procedures, for the set of images in (a), the histogram (which stores the colour information) of all three images were obtained and the Euclidean distances between the histograms of the reference image and the test image 1 was 1412 and between those of the reference and test image 2, was 1960. The test image 1 had a smaller distance to the reference than the test image 2.

For the second set of images in (b), the Euclidean distances between the histograms of the reference image and test images 1 and 2, were also computed and compared. The test 1 image was also seen to have a smaller distance to the reference than the test 2 image at 53 and 64 respectively.

This was a test of image similarity, and it can be concluded from the test, that the images in test 1 were more like their reference images than those in test 2, as would be expected from perceived similarity (see Figure 6-3). The algorithm was, therefore, able to detect the more similar pictures in these samples.

6.2 Results and discussion

Visual imaging (VI) results were compared with TI to determine if the joint with more colour changes in comparison to the reference was the warmer joint and compared with the consultant's evaluation to determine if it was also the joint clinically assessed with active arthritis (correlation analysis with consultants' assessment was only possible for patients with one active arthritic knee/ankle).

6.2.1 Analysis of the front of the knees (Correlation with TI and consultant's evaluation)

The front of the knees was processed using the reference image methods 1 and 2 described in section 6.1.2.2 to determine which correlated higher with the consultant's report and TI. The percentage distance difference (PDD) between the left and right knees was computed to determine how they differed.

Tables 6-1 and 6-2 present the VI results obtained using the two reference image types and the correlation with TI and clinical assessment.

Table 6-1 Correlation between VI using 'under same knee' reference, consultant's evaluation and TI results

Front of the Knee						
Subject	VI – Distance measures		Consultant's evaluation- active arthritic knee (A)	TI's warmer knee (B)	Correlation	
	'Under same knee' reference (1)				A	B
	PDD between left and right knee (%)	Knee with higher distance				
1	4.73	Right	Left	Left	No	No
2	7.99	Right	Both	Right	-	Yes
3	18.76	Right	Right	Right	Yes	Yes
4	11.71	Right	None	Left	-	No
5	21.76	Left	Right	Left	No	Yes
6	5.17	Left	Right	Right	No	No
7	12.42	Left	Both	Right	-	No
8	11.72	Right	Both	Right	-	Yes
9	18.08	Left	Left	Right	Yes	No
10	10.08	Right	Right	Right	Yes	Yes
11	11.70	Right	Left	Left	No	No
12	7.81	Left	Left	Left	Yes	Yes
13	5.16	Left	None	Left	-	Yes
14	14.94	Left	Both	Left	-	Yes
15	1.61	Right	Both	Left	-	No
16	3.38	Right	Both	Right	-	Yes
17	27.34	Right	Both	Right	-	Yes
18	0.07	Right	None	Left	-	No
19	8.68	Right	Both	Left	-	No
20	3.94	Right	None	Right	-	Yes

Table 6-2 Correlation between VI using common reference, consultant's evaluation and TI results

Front of the Knee						
Subject	VI – Distance measures		Consultant's evaluation- active arthritic knee (A)	TI's warmer knee (B)	Correlation	
	Common reference (2)				A	B
	PDD between Left and Right knee (%)	Knee with Higher Distance				
1	2.82	Left	Left	Left	Yes	Yes
2	8.57	Right	Both	Right	-	Yes
3	17.46	Right	Right	Right	Yes	Yes
4	1.24	Right	None	Left	-	No
5	11.74	Left	Right	Left	No	Yes
6	3.08	Left	Right	Right	No	No
7	2.77	Right	Both	Right	-	Yes
8	10.91	Right	Both	Right	-	Yes
9	5.32	Left	Left	Right	Yes	No
10	5.99	Right	Right	Right	Yes	Yes
11	10.96	Right	Left	Left	No	No
12	2.10	Left	Left	Left	Yes	Yes
13	2.04	Left	None	Left	-	Yes
14	6.50	Left	Both	Left	-	Yes
15	7.72	Left	Both	Left	-	Yes
16	5.03	Right	Both	Right	-	Yes
17	22.98	Right	Both	Right	-	Yes
18	0.10	Left	None	Left	-	Yes
19	13.64	Left	Both	Left	-	Yes
20	3.16	Right	None	Right	-	Yes

Table 6-1 shows a 50% correlation between VI and consultants' evaluation and 55% correlation between VI and TI. Table 6-2, on the other hand, shows a 62.5% correlation between VI and consultants' evaluation and an 80% correlation between VI and TI. The results show that the common reference method correlated slightly higher than the 'under same knee' reference. The common reference method, which used a more unified reference image, was therefore chosen for the analysis of the visual images.

6.2.2 Results for the back of the knees (Correlation with consultants' evaluation and TI)

The results for the back of the knees are shown in Table 6-3.

Table 6-3 Back of the knee correlation between VI, consultants' evaluation and TI

Back of the Knee						
Subject	VI – Distance measures		Consultant's evaluation- active arthritic knee (A)	TI's warmer knee (B)	Correlation	
	Common reference				A	B
	PDD between left and right knee (%)	Knee with higher distance				
1	6.82	Right	Left	Left	No	No
2	3.76	Left	Both	Right	-	No
3	1.63	Left	Right	Right	No	No
4	2.21	Right	None	Left	-	No
5	1.90	Left	Right	Left	No	Yes
6	9.50	Left	Right	Right	No	No
7	0.72	Right	Both	Right	-	Yes
8	6.40	Left	Both	Right	-	No
9	3.65	Right	Left	Right	No	Yes
10	1.27	Left	Right	Right	No	No
11	2.38	Left	Left	Left	Yes	Yes
12	9.85	Right	Left	Left	No	No
13	10.01	Right	None	Left	-	No
14	12.97	Right	Both	Left	-	No
15	10.03	Left	Both	Left	-	Yes
16	0.72	Right	Both	Right	-	Yes
17	3.06	Right	Both	Right	-	Yes
18	16.99	Left	None	Left	-	Yes
19	0.37	Left	Both	Left	-	Yes
20	4.53	Left	None	Right	-	No

As can be seen from Table 6-3, VI did not show a high correlation with clinical assessment and TI at 12.5% and 45% respectively. This finding shows that the colours of the front and back of the knees were not closely related since a higher correlation was obtained at the front of the knees.

6.2.3 Results for the front of the ankles (Correlation with consultants' evaluation and TI)

Table 6-4 presents the results obtained from the front of the ankles.

Table 6-4 Correlation between VI, consultant's evaluation and TI results for front of the ankle

Front of the ankle						
Subject	VI – Distance measures		Consultant's evaluation- active arthritic ankle (A)	TI's warmer ankle (B)	Correlation	
	Common reference				A	B
	PDD between left and right ankle (%)	Ankle with higher distance				
1	0.56	Right	Left	Right	No	Yes
2	3.26	Left	Left	Left	Yes	Yes
3	9.28	Left	None	Left	-	Yes
4	2.44	Right	None	Left	-	No
5	1.50	Left	None	Left	-	Yes
6	2.44	Left	Right	Right	No	No
7	3.70	Right	Right	Right	Yes	Yes
8	4.76	Right	Right	Right	Yes	Yes
9	4.17	Right	Left	Right	No	Yes
10	8.12	Left	Right	Right	No	No
11	13.78	Right	None	Right	-	Yes
12	3.43	Right	Both	Left	-	No
13	4.10	Right	Right	Left	Yes	No
14	3.13	Right	Both	Left	-	No
15	0.30	Left	None	Right	-	No
16	0.55	Left	Left	Left	Yes	Yes
17	10.17	Left	None	Right	-	No
18	0.84	Right	Both	Left	-	No
19	1.92	Left	None	Left	-	Yes
20	5.56	Left	Both	Left	-	Yes

From Table 6-4, VI shows a 62.5% correlation with the consultant's evaluation and a 55% correlation with TI.

6.2.4 Results for the back of the ankles (Correlation with consultants' evaluation and TI)

The results from analysing the back of the ankles is presented in Table 6-5

Table 6-5 Correlation between VI, consultant's evaluation and TI results for back of the ankle

Back of the ankle						
Subject	VI – Distance measures		Consultant's evaluation- active arthritic ankle (A)	TI's warmer ankle (B)	Correlation	
	Common reference				A	B
	PDD between left and right ankle (%)	Ankle with higher distance				
1	5.72	Right	Left	Right	No	Yes
2	14.17	Right	Left	Right	No	Yes
3	15.98	Right	None	Left	-	No
4	14.41	Right	None	Right	-	Yes
5	2.56	Left	None	Left	-	Yes
6	3.74	Right	Right	Right	Yes	Yes
7	2.50	Right	Right	Right	Yes	Yes
8	14.16	Left	Right	Right	No	No
9	3.49	Right	Left	Right	No	Yes
10	9.76	Right	Right	Right	Yes	Yes
11	12.47	Left	None	Left	-	Yes
12	5.35	Left	Both	Left	-	Yes
13	16.97	Left	Right	Right	No	No
14	5.40	Left	Both	Right	-	No
15	2.68	Right	None	Left	-	No
16	3.02	Right	Left	Right	No	Yes
17	16.72	Right	None	Left	-	No
18	4.27	Left	Both	Right	-	No
19	5.56	Right	None	Left	-	No
20	6.53	Right	Both	Left	-	No

From Table 6-5, VI shows a 37.5% correlation with clinical evaluation and a 55% correlation with TI.

6.2.5 Summary of the correlation results

Table 6-6 Correlation results (Techniques compared separately)

Joint	VI correlation with (%)	
	Consultants evaluation of joint with active arthritis	TI detected warmer joints
Front of knees	62.5	80
Back of knees	12.5	45
Front of ankles	62.5	55
Back of ankles	37.5	55

The above average correlation of VI with TI at the front of knees, front and back of ankles does suggest the joint detected to be warmer by TI also had greater changes in their colours (see Table 6-6).

The results obtained for the front of the knees indicated the highest correlation and so this area was more sensitive to the colour changes. In most patients, the knee with the greater Euclidean distance was also the active arthritic knee and the warmer knee when comparing the techniques separately. A 62.5% correlation with clinical assessment and 80% correlation with TI, confirm that in some patient, JIA may alter the skin colour of the affected joint, and so the technique may potentially aid in JIA diagnosis.

The combined correlation between VI, TI and the consultant's evaluation was also explored. Results are summarised in Table 6-7. There was a 50% correlation at the front of the knees which identified the knees with a higher Euclidean distance as the TI detected warmer knee as well as consultants' assessed JIA active knee. For the rest of the joints, VI did not show a high correlation with the other techniques combined.

Table 6-7 Combined correlation between VI, consultants' evaluation and TI

Joint	Combined VI correlation with Consultants' evaluation of joint with active arthritis and TI detected warmer joints (%)
Front of knees	50.0
Back of knees	12.5
Front of ankles	33.3
Back of ankles	33.3

The findings from this correlation analysis indicate that the three techniques (VI, TI and consultants' evaluation) do not necessarily have a direct relationship. In comparison with clinical assessment and TI, it is possible for the knee with active arthritis to not have more changes in colour, and for the warmer knee to also not have more changes in colour respectively. But in some patients, JIA may cause some skin colour changes.

A further consideration was the selected reference region could also be affected by arthritis and so not a true representation of the patients' normal skin colour. A normative study would provide information that could assist in further analysis.

However, with the correlation seen in Table 6-1 and the combined correlation at the front of the knees, the VI technique may potentially assist clinicians in diagnosing JIA.

6.3 Summary

The correlation analysis between Visual Imaging (VI), Thermal imaging (TI) and the consultants' evaluation were presented and discussed in this chapter.

Single visual images of the front and back of the knees and ankles of twenty patients with active arthritis on one or both knees and ankles were collected using the FLIR T630sc camera. A new and consistent method to identify the ROIs from the image was developed, and these (ROIs) were segmented for further processing. A section between the knees and ankles from both legs was selected, averaged and used as a reference image for comparing the left and right joints to see which differed more from the reference image. The Euclidean distance metric was used to determine the similarity between the images using the histograms as a colour feature.

Comparing the techniques separately (VI with consultant's evaluation and VI with TI), results showed higher correlations at the front of the knees and ankles, and so these areas may have been more sensitive to the colour changes. VI correlations of 62.5% and 80% with the consultant's evaluation and TI results respectively were observed at the front of the knees; and 62.5% and 55% at the front of the ankles. Combined correlation between VI, TI and consultants' evaluation of 50% was also observed at the front of the knees. This was the region with the highest correlation as compared to the other joints.

These findings indicate that though it is possible for JIA to alter the skin colour of a patient (as seen with the combined correlation of 50%), it is not always the case. It is not always necessary that JIA would affect the skin colour of a patient. These techniques do not directly relate. However, with the correlation results, the VI technique may potentially assist in JIA diagnosis.

The next chapter presents and discusses the results obtained using accelerometers to measure the joint range of movement restriction, one of the symptoms of JIA.

Chapter 7

7 Accelerometry to Aid Assessment of Joint Movement in JIA

In this chapter, accelerometry techniques are developed and are compared with the gold standard clinician assessment using validated pGALS (Paediatric Gait, Arms, Legs and Spine) musculoskeletal examination tool in the identification of inflamed knee joints in children and young people (CYP) with Juvenile idiopathic arthritis (JIA). Joint restriction at the joints is one of the characteristic symptoms of JIA, hence, the ability to accurately quantify the joints range of motion (ROM) may aid in the early detection of joint inflammation. It may also aid and provide objectivity to movement analysis and may be a useful tool for monitoring progress during treatment.

The use of accelerometers to measure human knee movement patterns such as the movement angle, acceleration, velocity, displacement to detect altered movement in inflamed knee joints was explored. A suitable signal processing method was designed for evaluating human movement. Accelerometry data were recorded to determine knee movement patterns in walking and lying down positions.

7.1 Methodology

7.1.1 Materials

ADXL335 tri-axial accelerometers with dimensions 4 mm x 4 mm x 1.45 mm were used for the measurements. The ADXL335 (Figure 7-1) measures acceleration forces with a full- scale range of ± 3 g (Analog Devices, 2009). It measures static acceleration in tilt sensing applications as well as dynamic acceleration from motion, shock or vibration. The output signals are analogue voltages that are proportional to acceleration (Analog Devices, 2009).



Figure 7-1 ADXL335 accelerometer

These sensors were connected to the Arduino Mega 2560 microcontroller board (Figure 7-2), which was in turn connected to a computer with a USB connection. The microcontroller board digitised the analogue x, y and z voltage outputs from the accelerometers for display, storage and processing by the computer. The recording sample rate was approximately 212 samples/second.

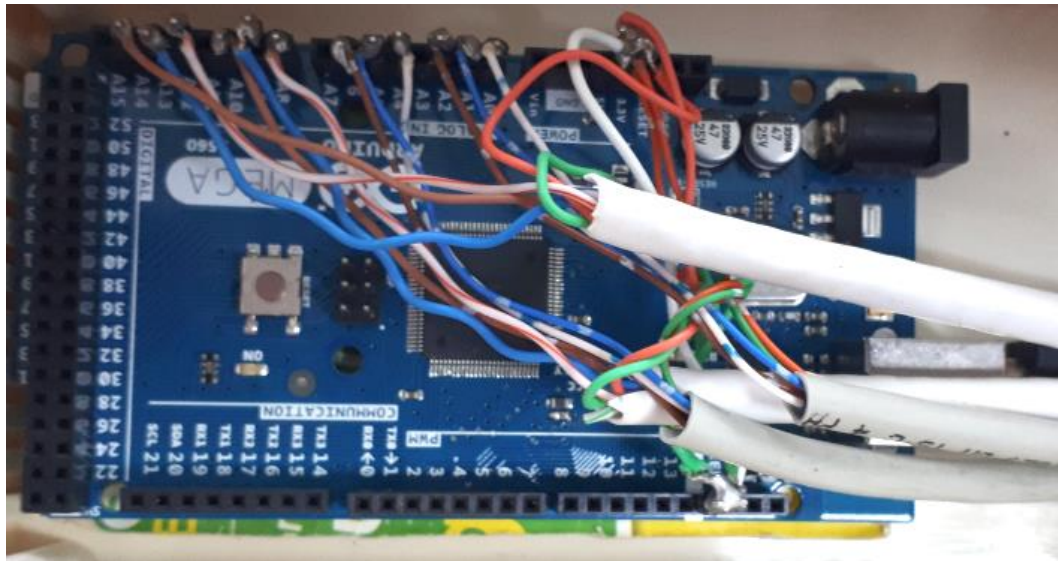


Figure 7-2 Arduino MEGA 2560 hooked up with accelerometer connections

7.1.2 Experimental setup in the University Laboratory

In order to have a better understanding of the device's operation prior to its application to patients, a series of laboratory experiments were performed.

7.1.2.1 Angle measurements of a static platform

This investigation involved recording data using the Arduino microcontroller (Arduino mega 2560) board-accelerometer setup connected to a computer. Four tri-axial accelerometers connected to the Arduino board were attached at four points on a flat plastic board that was initially flat at an angle 0° and then tilted using a pull-up mechanism to different angles up to about 22° . The aim of the experiment was to determine the separate tilt angles from the four accelerometers placed at different locations on the board.

A protractor was also attached to this set-up to allow actual inclination angle to be obtained. To reduce measurement errors, the experiment was performed twice, and

the average of the data recorded at each angle was then used for processing. Figure 7-3 shows the experimental set-up.

The recorded accelerometer data was processed using MATLAB[®] codes to estimate the angle of tilt. The mean and offset of the data at 0° were determined, and then subsequent readings at non-zero angles were corrected for this offset. The tilt angles were calculated from each accelerometer data obtained at the different angles using Equation 7-1. The estimated accelerometer angles were compared with the actual angles read from the protractor. Only a narrow range of angles (from 0° to 22°) were considered for this experiment as the aim was just to estimate the angle of tilt from recorded data and to see if the results correlates with the protractor measurements.



Figure 7-3 Experimental setup using four accelerometers for estimating tilt angles

$$\text{tilt angle} = \text{arctangent} \left(\frac{a_x}{\sqrt{a_y^2 + a_z^2}} \right) \quad (7-1)$$

Where a_x , a_y and a_z are the measures for the accelerometer in the x , y , and z axes respectively.

7.1.2.2 Angle measurements of a hinge joint

A hinge joint was also built to model the knee in a simple manner as shown in Figure 7-4. It allows the movement to be precisely controlled and the angle to be measured using a goniometer (protractor).

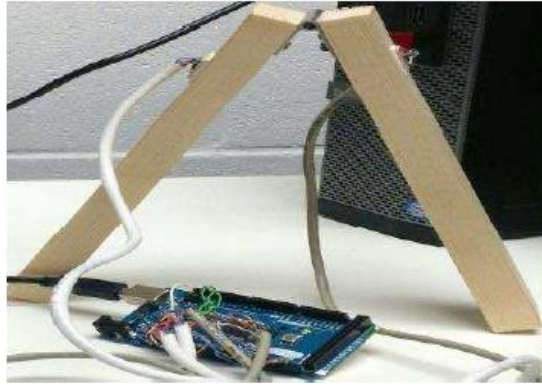


Figure 7-4 Model of hinge joint showing attached accelerometer sensors

The model consisted of two wooden bars of the same dimension jointed by a hinge. Two accelerometer sensors were attached to the bars using double-sided adhesives. This provided a very simple model of a situation that accelerometers are attached to the left and right human thighs and shanks (just above and below the knee joint) in order to obtain the relevant movement angles. The wooden bars were then moved in different scenarios to obtain the angle at the joint, which were confirmed with a flexible goniometer (see Figure 7-5).

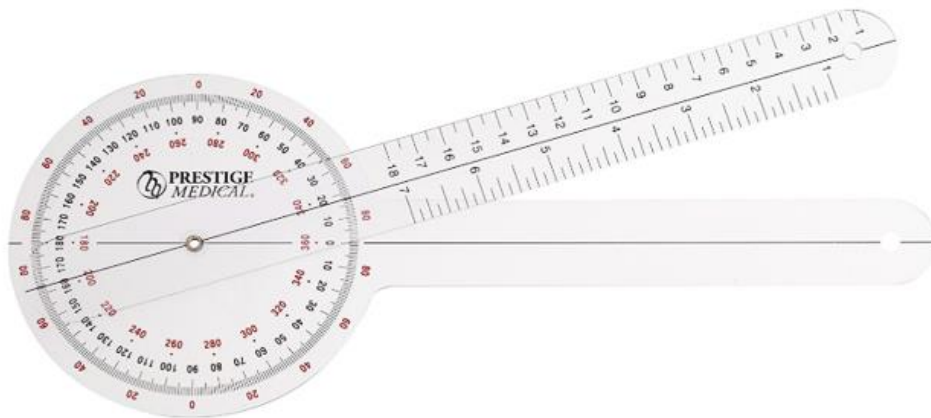


Figure 7-5 Flexible goniometer

7.1.2.3 Angle measurements from an adult subject

To make the device wearable, the accelerometers were housed in a small casing and the microcontroller was housed in a box (top was transparent) and put in a waist pouch, to avoid contact with the participants. A photo of the device is shown in Figures 7-6 and 7-7

Further experiments were performed with the sensors attached to both right and left thighs and shanks (a sensor just above and a sensor just below each knee, see Figure 7-8) of a healthy adult subject as he performed the following movements;

- Sitting on a chair, the subject moved his lower legs up and down freely and simultaneously to their full extension and flexion.
- Lying on a table on his back fully stretched one of his legs to touch the table and then bent it fully toward his chest, repeating 30 times. This was repeated for each leg.
- Walked normally the length of long corridor (length about 10 m).

The movements' angles, angular accelerations, angular velocities and total angular displacement were calculated from the accelerometer readings that were recorded.



Figure 7-6 Photo of the accelerometers and microcontroller housed in suitable casings



Figure 7-7 Photo of the microcontroller housed in a waist pouch



Figure 7-8 Accelerometers strapped to the thighs and shanks of an adult subject

7.1.3 Set up at the hospital

At the hospital, participants attended a 30-minute session. Four accelerometers, two for each leg, were placed just above and just below each knee joint using specially designed adjustable elastic. Participants were asked to perform the following movements: (see Figure 7-7 for a photo of the device)

- Lying on their backs on a bed, and bent a leg, attempting to their best ability to bring the heel to buttocks (flexion) and straighten the leg (extension), repeating the motion 10 times (see Figure 7-9). This was repeated for each leg.

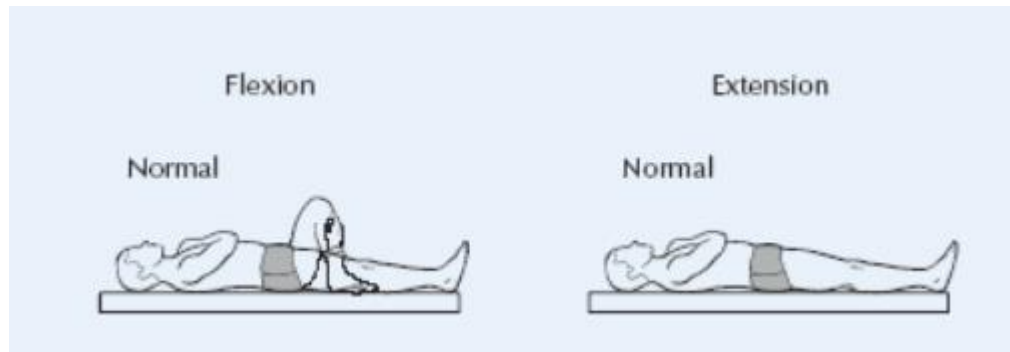


Figure 7-9 Flexion and Extension (Global Alliance for Musculoskeletal Health, 2015)

- Walking normally in a straight line the length of 10 meters.

7.1.4 Participants

Four children and young people (CYP) aged 8-16 years with diagnosis of JIA and current active arthritis of one knee and without suspected active arthritis of other lower limb joints (e.g. Hips, ankles), including the contra-lateral knee joint, were recruited. Recruiting a larger number of patients within the study's time period proved difficult as the patients had to fully conform to the NHS approved ethics.

Participants were recruited from routine steroid joint injection clinics and routine outpatient clinics. Each participant had both knee joints studied. Movement data from the inflamed knee joint was compared with that obtained from the contra-lateral non-inflamed knee joint, which acted as a control for the purpose of the study.

7.1.5 Clinical Evaluation

Musculoskeletal examination was undertaken on each study participant by an experienced consultant paediatric rheumatologist according to a standardized examination tool: Paediatric Gait, Arms, Legs, Spine (pGALS) which is a validated musculoskeletal examination screening tool, to determine the presence of active knee arthritis (see Chapter 4).

7.1.6 Measurements

The digitised accelerometer readings were collected from all the four accelerometer sensors simultaneously. Accelerometers 1 and 2 were attached to the right thigh and shank and accelerometers 3 and 4 were attached to the left thigh and shank of the

participants. Figure 7-10 presents a schematic diagram of the knee showing accelerometer positions and the relative angle of the knee joint, α .

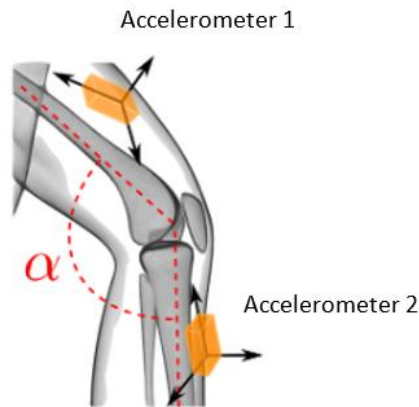


Figure 7-10 Typical knee showing accelerometer positions and knee angle, α (Seel, Raisch, & Schauer, 2014)

Accelerometer outputs from the more sensitive axes, y and z axes were used (the assumption was that the knee moved in one plane up and down without deviating horizontally to the left and right thus the x -axis of the accelerometer that represented horizontal movements was not used). To obtain the knee joint angles, the angles of inclination made by the thighs, β_{thigh} , and shanks, φ_{shank} , were first computed with Equations 7-2 and 7-3 respectively. The relative knee joint angle for the lying down, α_{lying} , and walking $\alpha_{walking}$ scenarios was computed with Equations 7-4(a) and (b) respectively.

$$\beta_{thigh} = \arctangent2 (ay_1, az_1) \quad (7-2)$$

$$\varphi_{shank} = \arctangent2 (ay_2, az_2) \quad (7-3)$$

$$\alpha_{lying} = 180 - (\beta_{thigh} + \varphi_{shank}) \quad (7-4a)$$

$$\alpha_{walking} = 360 - (\beta_{thigh} + \varphi_{shank}) \quad (7-4b)$$

where ay_1 and az_1 are the acceleration measures for the y and z axes of the accelerometer attached to the thigh, ay_2 and az_2 are the acceleration measures for the y and z axes of the accelerometer attached to the shank. Similar calculations were also performed for accelerometers 3 and 4 attached to the left knee to obtain the angle of the left knee joint.

Once the joint angles (α) were determined, the angular velocity (v), angular acceleration (a) and total angular displacement (d) were determined for both legs using Equations 7-5 to 7-7 respectively.

$$v(t) = \frac{d(\alpha)}{dt} \quad (7-5)$$

$$a(t) = \frac{d(v)}{dt} \quad (7-6)$$

$$d(t) = \int_{t=0}^{t=T} v(t) \quad (7-7)$$

where T is the signal recording's duration.

The velocity indicates the rate of change of speed of the leg as it is swung. The acceleration measures changes in the velocity of the swing; and the displacement shows the total movement made by each leg. These results were compared for both right and left legs to determine movement pattern differences.

7.1.7 Operation of the algorithm

Using MATLAB[®], the digitised accelerometer data collected from the thighs and shanks for both lying down and walking scenarios were loaded into the computer system as an array of 8 columns, representing the y and z axes of each accelerometer, i.e. $y_1, z_1, y_2, z_2, y_3, z_3, y_4, \text{ and } z_4$. The accelerometer's output, A , was converted to acceleration force values expressed in g using Equation 7-8.

$$A(g) = (A - zero_g) * \left(\frac{\text{reference_voltage}}{1024 * \text{sensitivity}} \right) \quad (7-8)$$

where $zero_g$ (zero voltage: 1.65V) and sensitivity (330mV/g) are specified in the accelerometer's datasheet, the analogue-digital-converter (ADC) resolution value is 1024 and the reference voltage is that from the microcontroller (Arduino mega 2560 board: 3.3V). Equation 7-8 is specific to the type of accelerometer used in this study.

The left and right thighs and shanks angles were computed using Equations 7-2 and 7-3. A sample of the resultant accelerometer signal obtained from one of the legs in the lying down position is provided in Figure 7-11 showing the characteristic high frequency noise components hence embedded (usually during movement initiation or sudden change in the movement's direction) in an accelerometry signal.

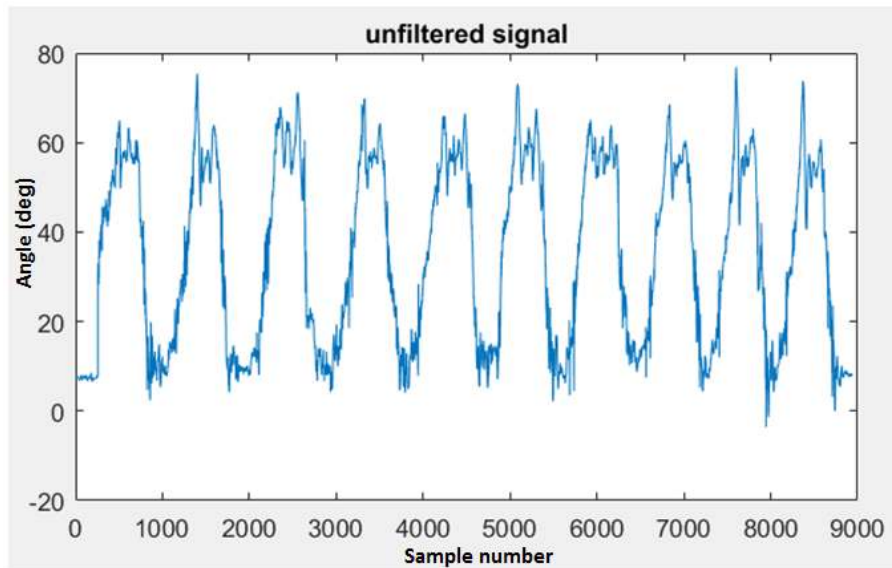


Figure 7-11: Sample accelerometer signal from characterised with noise

A Butterworth low pass filter of the 3rd order with a suitable cut off frequency, f_c , in the range of 0.5Hz to 3Hz determined by finding the frequency component of the signal in the frequency spectrum, was then applied to denoise the signal. Sample of the denoised signal is shown in Figure 7-12.

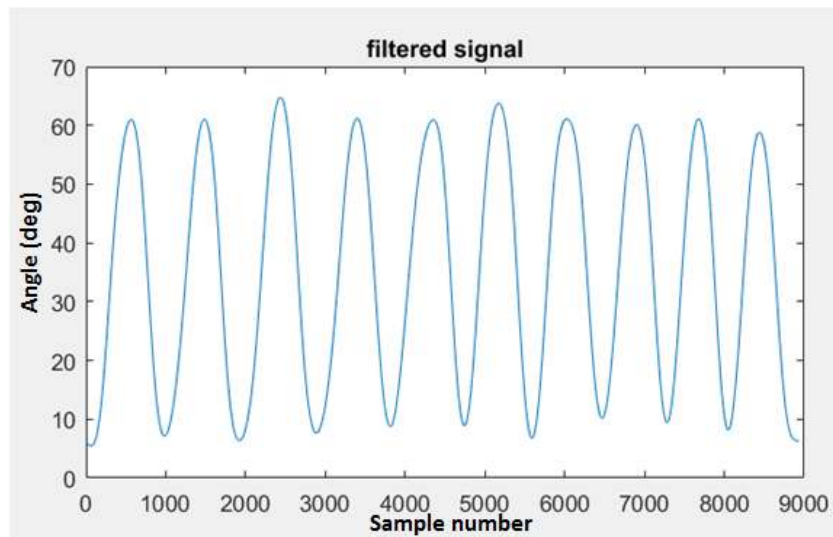


Figure 7-12 Sample accelerometer filtered signal

The relative knee angle, angular velocity, angular acceleration and total angular displacement is then obtained afterwards.

7.2 Results and discussion

7.2.1 Static platform experiment

Table 7-1 presents the results of the accelerometer (Acc1, Acc2, Acc3, and Acc4) and protractor measurements. The absolute errors (E_{Acc1} , E_{Acc2} , E_{Acc3} , and E_{Acc4}) between the accelerometer and protractor readings are also shown.

Table 7-1 Accelerometer and protractor measurements and the associated absolute errors

Protractor readings (degrees)	Acc1	Acc2	Acc3	Acc4	E_{Acc1}	E_{Acc2}	E_{Acc3}	E_{Acc4}
1	1.15	1.13	1.01	0.89	0.15	0.13	0.01	0.11
2	2.19	2.22	2.00	1.83	0.19	0.22	0.00	0.17
3	3.12	2.90	2.99	2.86	0.12	0.10	0.01	0.14
4	4.58	4.45	4.44	4.24	0.58	0.45	0.44	0.24
5	5.58	5.39	5.43	5.28	0.58	0.39	0.43	0.28
6	6.57	6.33	6.40	6.28	0.57	0.33	0.40	0.28
7	7.74	7.52	7.59	7.46	0.74	0.52	0.59	0.46
8	8.65	8.29	8.40	8.23	0.65	0.29	0.40	0.23
9	9.70	9.33	9.53	9.31	0.70	0.33	0.53	0.31
10	10.97	10.57	10.71	10.56	0.97	0.57	0.71	0.56
11	11.98	11.53	11.71	11.50	0.98	0.53	0.71	0.50
12	12.56	12.21	12.82	12.65	0.56	0.21	0.82	0.65
13	13.26	12.79	13.65	13.39	0.26	0.21	0.65	0.39
14	14.20	13.61	14.07	14.42	0.20	0.39	0.07	0.42
15	15.46	14.83	15.26	15.03	0.46	0.17	0.26	0.03
16	16.29	15.81	16.15	15.85	0.29	0.19	0.15	0.15
17	17.29	16.55	17.05	16.85	0.29	0.45	0.05	0.15
18	18.19	17.65	18.15	17.91	0.19	0.35	0.15	0.09
19	19.28	18.59	18.97	18.80	0.28	0.41	0.03	0.20
20	20.63	20.08	20.61	20.27	0.63	0.08	0.61	0.27
21	21.74	20.89	21.40	21.03	0.74	0.11	0.40	0.03
22	22.51	21.72	22.33	22.06	0.51	0.28	0.33	0.06
Average error					0.48	0.30	0.35	0.26
Standard deviation (error)					0.26	0.15	0.26	0.17

The average error from the accelerometers was less than 0.5° , which was within an acceptable range given the application in this study. Figure 7-13 shows the angles

estimated by the accelerometers closely tracked the actual angles measured with the protractor.

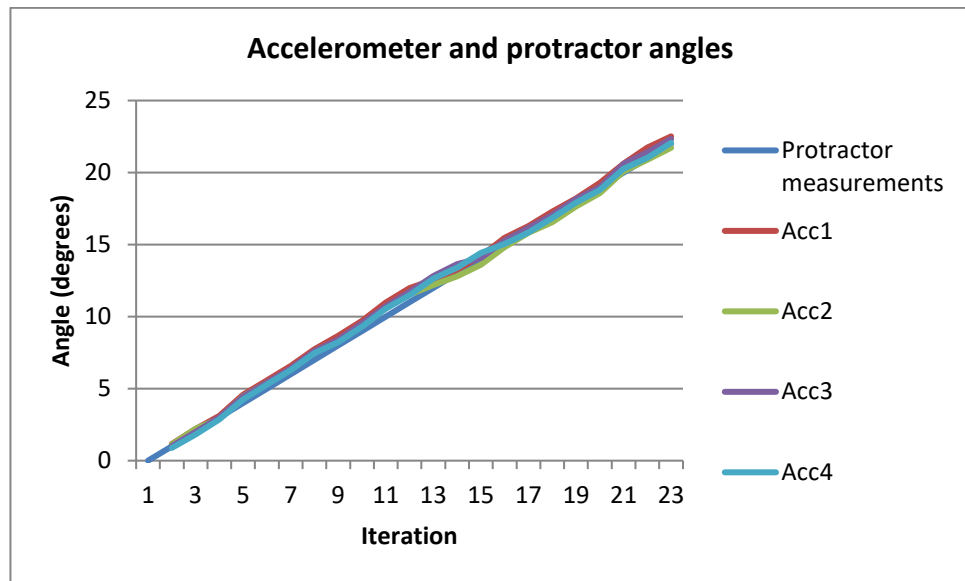


Figure 7-13 Accelerometer and protractor measurements

7.2.2 Knee model experiment

For validating the joint angles measured by the two accelerometers attached to the hinge joint, a flexible goniometer was used (shown in Figure 7-5). Table 7-2 presents the estimated joint angles as measured by the accelerometers. Figure 7-14 shows the result of the estimated angles measured by the accelerometers. The offset of the data at 0° was determined, and then subsequent non-zero angles were corrected for this offset. The hinge joint was moved approximately between 30° and 90° (these were not very exact as the joint was in motion) in 8 iterations and confirmed with a goniometer (simulating flexion and extension movements in the lying down position). The estimated accelerometer measurements were able to closely track the angles measured by the goniometer.

Table 7-2 Estimated goniometer and accelerometer angles

Iterations	30° region (°)	90° region (°)
1	29.69	90.95
2	27.99	92.99
3	28.98	91.73
4	28.23	90.42
5	28.61	90.99
6	28.32	90.81
7	28.90	90.51
8	28.00	90.33

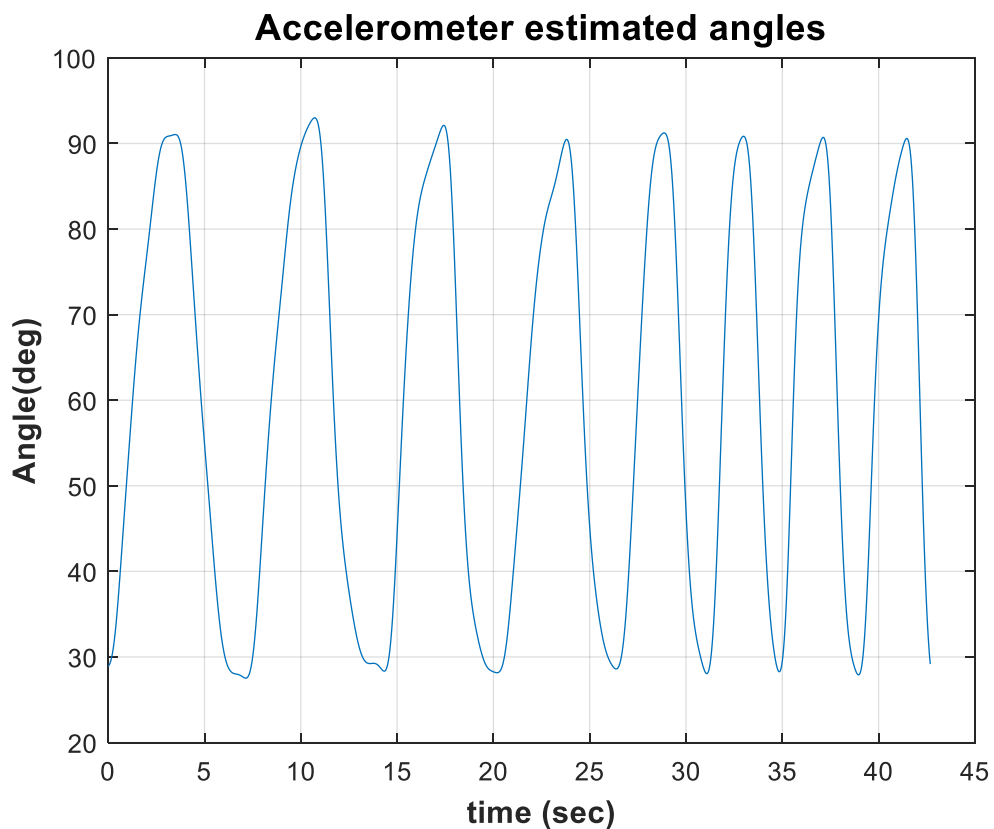


Figure 7-14 Accelerometer estimated angles from the hinge joint experiment

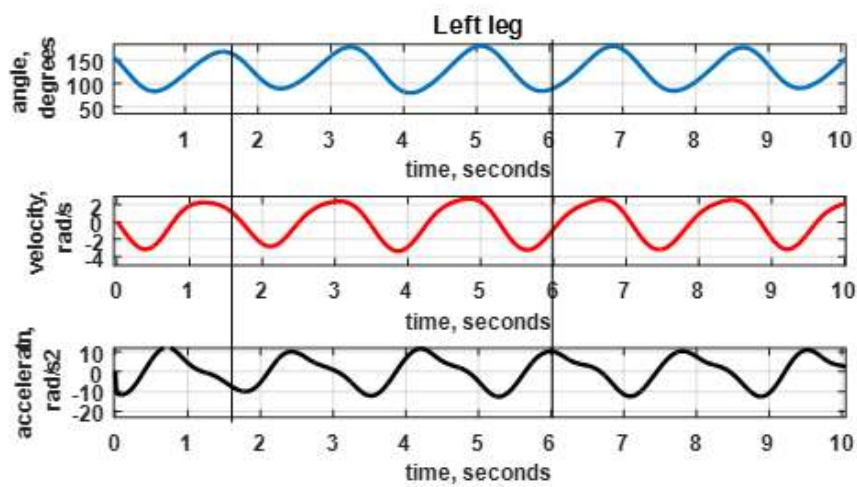
7.2.3 Experiment performed on healthy adult knees

To further test the technique, experiments were performed on the healthy adult knees in three scenarios to determine if accelerometers can be used to describe movement patterns.

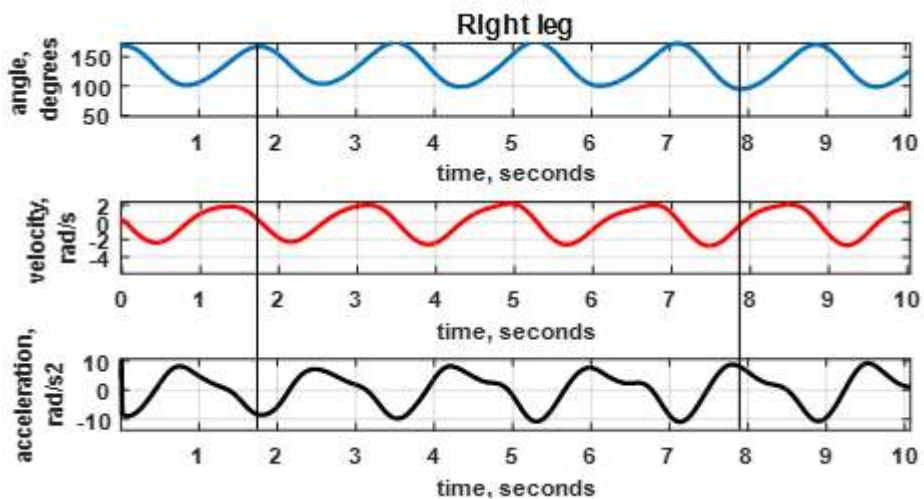
(a) Sitting scenario

Movement information (angle of movement, angular velocity, angular acceleration and angular displacement) obtained when the subject sat on a chair and swung their legs

are presented in this section. To look at the signals in more detail, Figures 7-15 (a) and (b) show zoomed in sections, indicating the relationship between the angles, velocities and accelerations respectively (see the vertical black line running through the graphs) for the left and right legs. The figures show that when the angle peaks (at state of rest at maximum extension of the leg), the velocity tends to zero indicating no movement and velocity peaks when rate of change of movement is highest. Acceleration peaks when rate of change of velocity is highest. Both right and left legs show similar movement patterns.



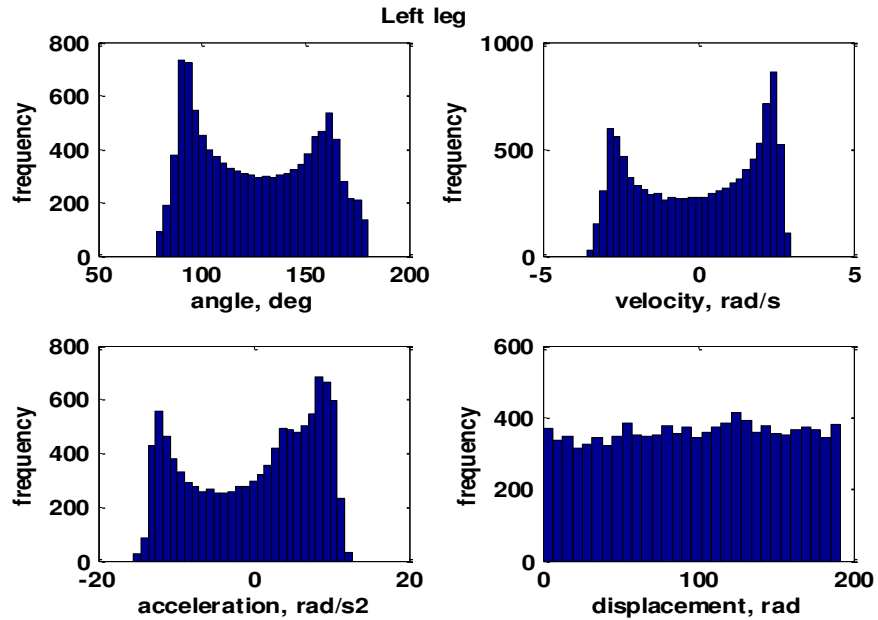
(a)



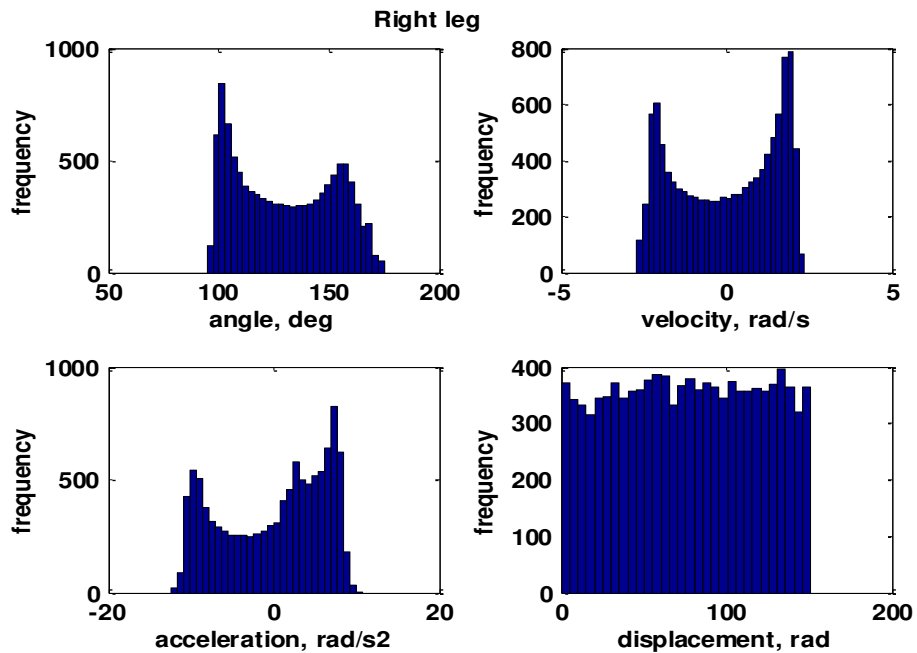
(b)

Figure 7-15 Measurements from (a) left leg (b) right leg showing relationship between the movement data (Snippets)

The plots results comparing the differences in the patterns of movements for the left and right legs are provided in Figures 7-16(a) and (b). The results indicate that even though the subject had been healthy, differences in the movements of left and right leg exist.



(a)



(b)

Figure 7-16 Histograms of data for (a) left and (b) right legs (Nwaizu, Saatchi, & Burke, 2016)

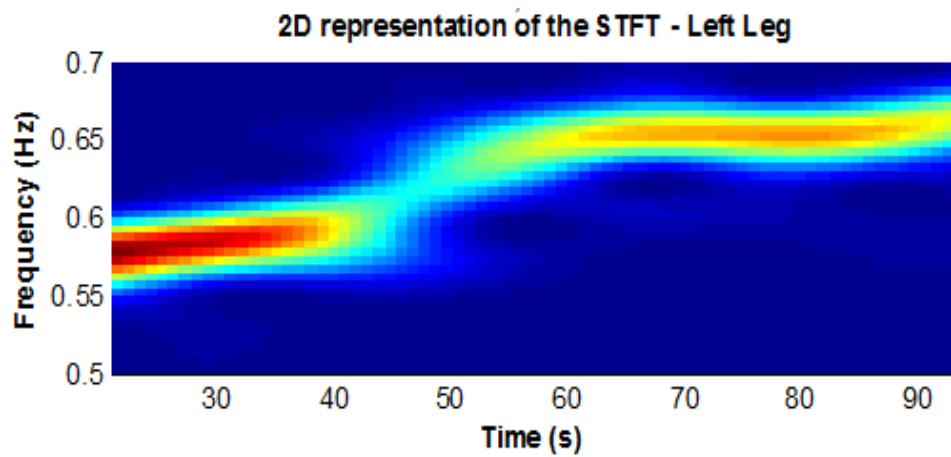
The movement information is summarised in Table 7-3 detailing the range of motion (ROM), angular velocity, angular acceleration and angular displacement information measured from both legs.

The left leg covered a wider range of movement, by approximately 21.91° than the right leg, and had a higher total angular displacement with a difference of 41 radians. The maximum velocity and acceleration for the left leg in the positive direction were also higher than the right leg by 0.63 *rad/s* and 1.83 *rad/s*² respectively

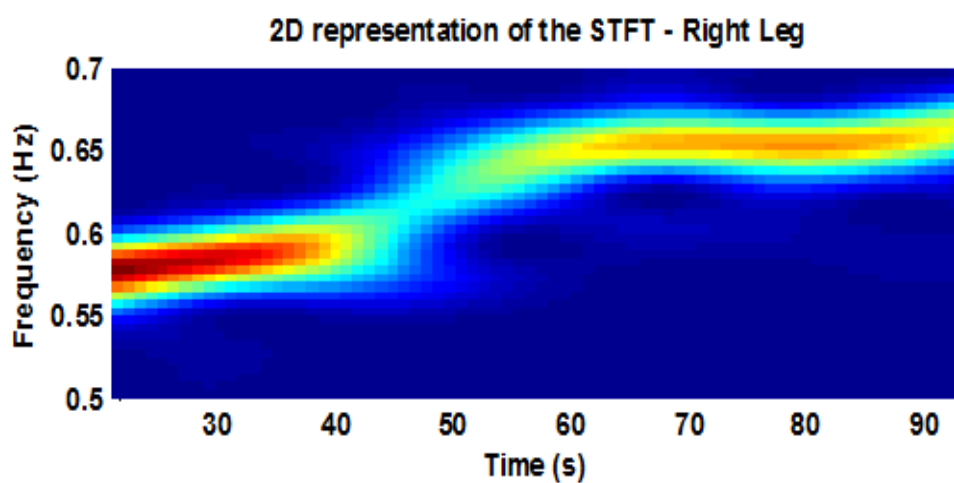
Table 7-3 Movement information from the left and right legs

Leg	Knee ROM (degrees)	Angular velocity – forward swing (rad/s)	Angular acceleration – forward swing (rad/s²)	Total angular displacement (rad)
Left	102.14	2.98	12.62	191.60
Right	80.23	2.35	10.79	150.77

The frequency of movement was further analysed by obtaining the frequency spectrogram (also known as short-time Fourier transform) of the knee angles, computed by finding fast Fourier transform (FFT) of the signal, to see the time-frequency relationship of the leg swing and the extent of the movements over time. These are shown in Figures 7-17(a) and (b) for the left and right legs respectively. The plots show that at the start of the movement, up to the 40 seconds mark, the legs moved slower (0.55Hz) but the range of movement, indicated by the magnitude (bright red colour) was higher. Thereafter, the legs moved relatively faster (about 0.65Hz) but covered a lower range of movement (again, this is indicated by the magnitude of the plot).



(a)



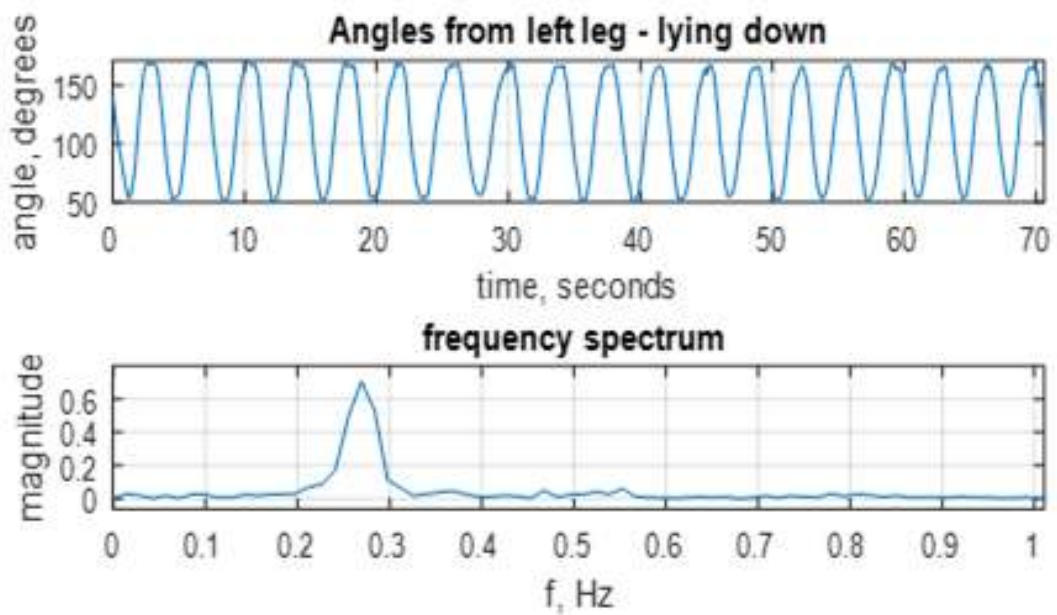
(b)

Figure 7-17 STFT of movement angles for the (a) left and (b) right legs. Higher amplitudes are shown in bright red up to 40 seconds and the yellow colour thereafter shows reduced relative amplitude (Nwaizu, Saatchi, & Burke, 2016)

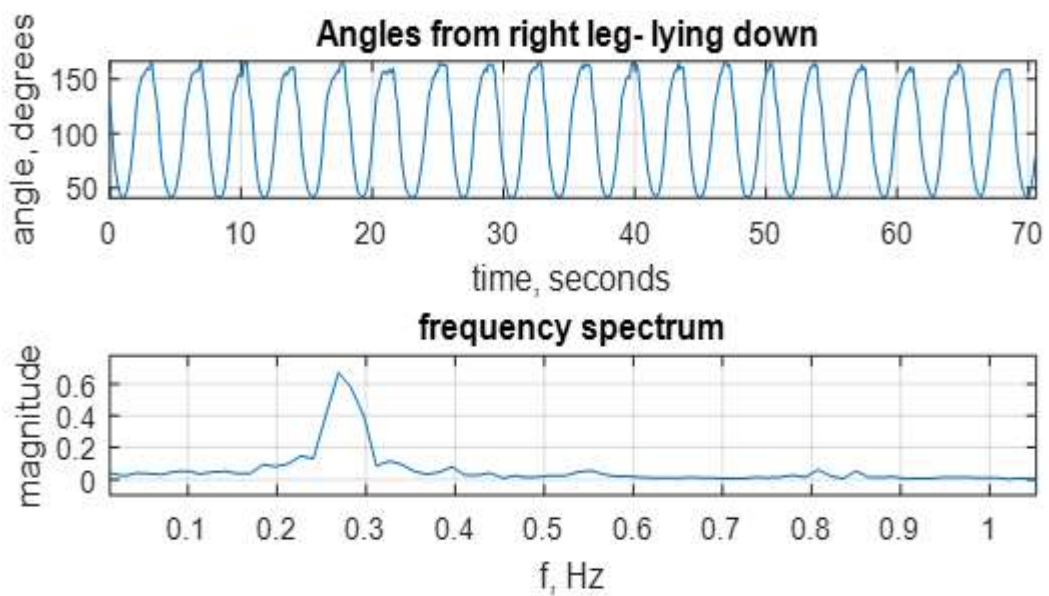
These results show that the subject moved the left leg faster and to a slightly wider range than the right leg in this experiment. The frequency analysis was also able to indicate how and when each leg moved and to what extent, further confirming the accelerometry system's ability to describe distinct movement patterns.

(b) Lying down scenario

The results obtained when the subject laid down is provided in this section. Figures 7-18 (a) and (b) show the angles measured, movement frequency for the left and right legs while the subject laid on his back and moved his legs in turn from fully stretched on the ground to fully bent close to the chest.



(a)



(b)

Figure 7-18 Angle measurement for (a) left leg (b) right leg, subject laid on his back

The related data are summarised in Table 7-4. The left leg was able to cover a range of 119° ($52.9^\circ : 167.9^\circ$) and the right leg covered a similar range of 119.2° ($43.9^\circ : 163.1^\circ$), which indicates that both legs were able to flex and extend in the same manner. The frequency of the movement for both legs was 0.26Hz , thus taking 3.8 seconds to complete a movement cycle. The spectrograms provided in Figure 7-19 confirm both legs movement frequency being in the 0.26Hz range.

Table 7-4 Legs' movement's range and frequency for laid down position

Leg	Knee ROM (°)	Movement frequency (Hz)
Left	52.9 - 167.9	0.26
Right	43.9 - 163.1	0.26

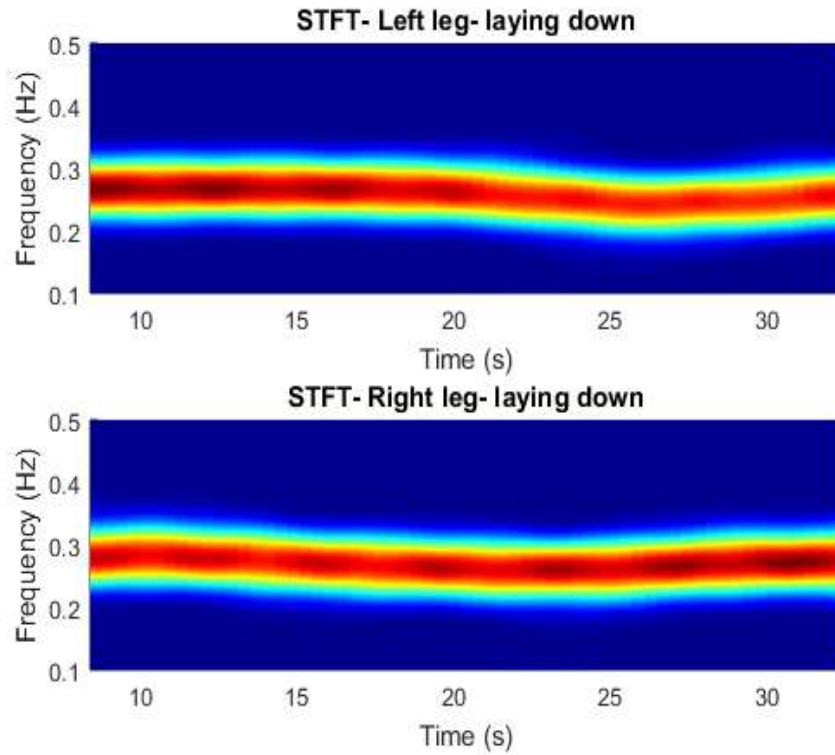
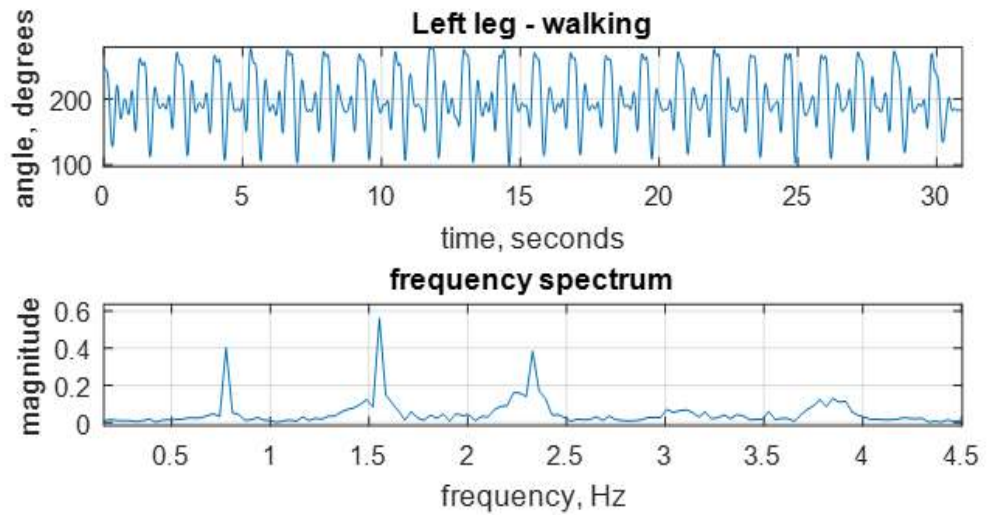


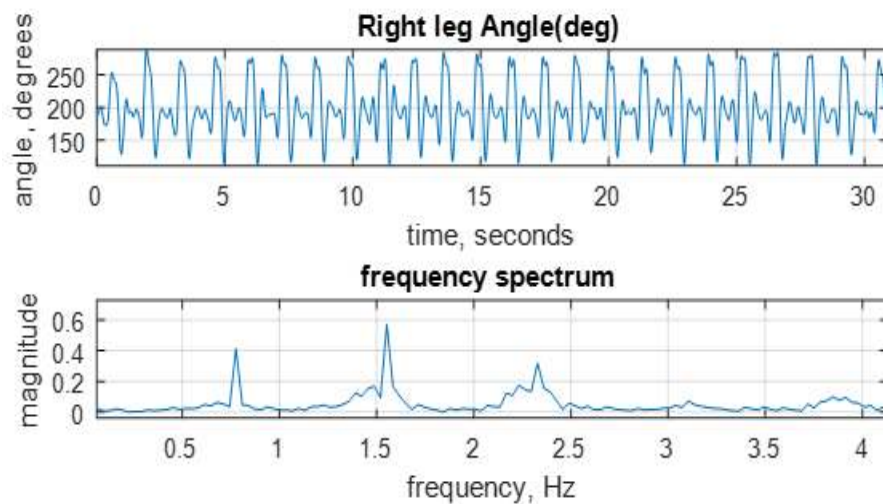
Figure 7-19 Short-time Fourier transform of legs' angular movement, subject laid on his back

(c) Walking scenario

In the walking scenario (results shown in Figure 7-20), the angular range of movement was just slightly higher for the left leg than the right leg by a 10° margin. The related data is provided in Table 7-5. The largest peaks present in the magnitude frequency spectrum of the angular movement were at 0.77 Hz, 1.55 Hz and 2.33 Hz with the dominant frequency at 1.55Hz, and this is clearly shown in Figure 7-21.



(a)



(b)

Figure 7-20 Angle measurements from the (a) left and (b) right legs, subject walking

Table 7-5 Legs' movement range and frequency while walking

Legs	Knee Movement Range(degree)	Frequency (Hz) associated with the three largest peaks in the magnitude spectrum
Left leg	101.7 - 274.5	0.77, 1.55, 2.33
Right leg	115.2 - 284.1	0.77, 1.55, 2.33

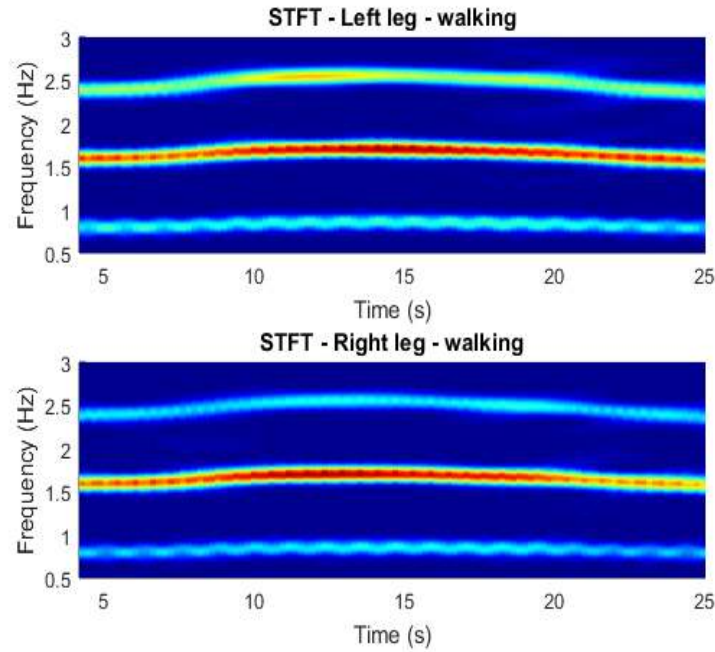


Figure 7-21 Short-time Fourier transform of the legs' angular rotation signal, subject walking

The results from these movement scenarios confirmed that accelerometers have the potential to be a useful tool in clinics to aid the analysis of human movement patterns in the detection or diagnosis of arthritis.

7.2.4 Analysis of data collected from CYP with active JIA on one knee

Data collected from lying down and walking scenarios of CYP with active JIA on one knee on the day of clinical assessment is presented in this section. The healthy knee (i.e. the knee without active JIA) acted as a reference for comparison for the participants. The results describe the movement pattern for each participant and a comparison is made between accelerometer results and clinical observation. The analysis of accelerometry data was performed without the knowledge of clinical diagnosis to avoid bias.

Four participants were recruited. Recruitment of a larger number of patients with the study's time frame proved difficult and there were strict ethics requirements related to inclusion criteria for the patients. The results are presented and discussed accordingly.

In the lying down position shown, the movement goes from full extension (tending towards 180°) to full flexion (heel to bottom- tending towards 0°). In the walking position, forward swing tends towards 270°, backward swing tends towards 0° and heel strike about the 180° angle (shown in the oval section - see sample of walking data shown in Figure 7-22).

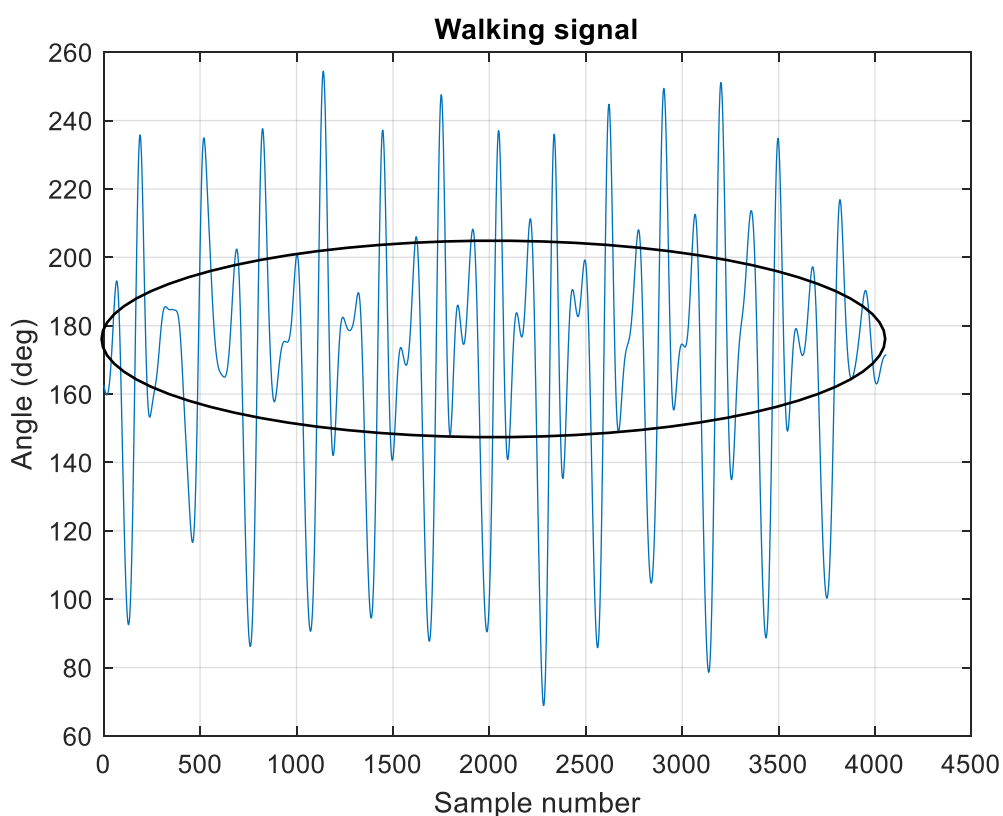


Figure 7-22 Sample walking signal showing forward swing, backward swing and heel strike region in the oval section

7.2.4.1 Patient 1

The results for patient 1 are summarised in Table 7-6 for both lying down and walking and compared with clinical observation

Table 7-6 Patient 1 movement information and clinical assessment

Position	Parameter	Left knee	Right knee	Accelerometry finding	Clinical observation
Lying down	Angle (°) (ROM)	42: 163 (121)	58: 155 (97)	Right knee suspected	Warm, swollen & restricted Right knee
	Frequency spectrum (Hz) (Amplitude)	0.27 (0.79)	0.26 (0.69)		
	Angular velocity (rad/s)	-1.8: 2.0	-1.5: 1.6		
	Angular acceleration (rad/s ²)	-4.0: 3.3	-3.2: 2.9		
	Total angular displacement(rad)	39.2	32.8		
	Time (s)	36	37		
Walking	Angle (°) (ROM)	80: 239 (159)	99: 234 (135)	Right knee suspected	Warm, swollen & restricted Right knee
	Frequency spectrum (Hz) (Amplitude)	0.8, 1.6, 2.3 (0.22, 0.44, 0.17)	0.8, 1.6, 2.4 (0.44, 0.30, 0.07)		
	Angular velocity (rad/s)	-11.7: 16.1	-9.3: 8.7		
	Angular acceleration (rad/s ²)	-132: 133	-67: 85		
	Total angular displacement(rad)	83.36	54.64		
	Time (s)	16	16		

The knee ROM and movement frequency for lying down position are shown in Figures 7-23 and 7-24 respectively for both legs.

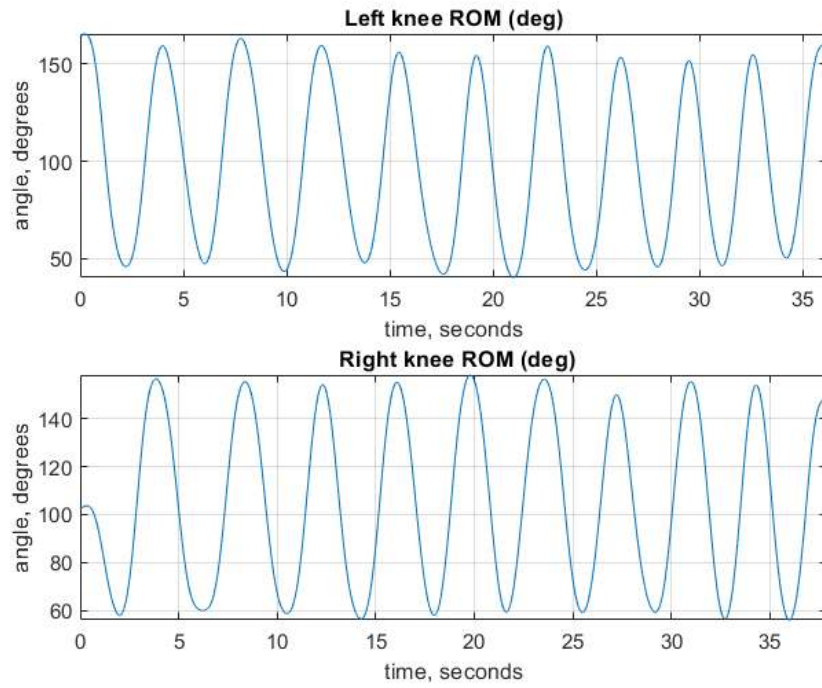


Figure 7-23 Lying down ROM

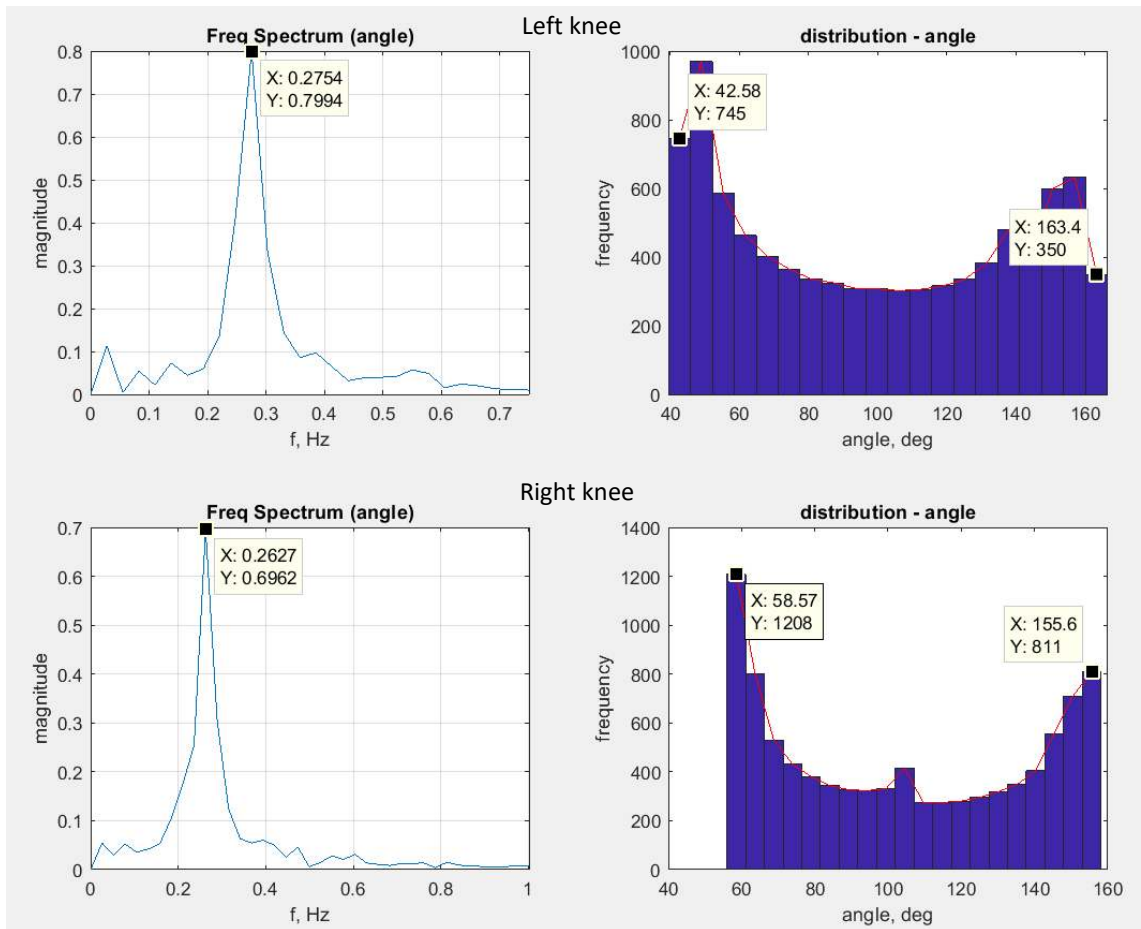


Figure 7-24 Movement frequency and data distribution for both legs

Similarly, the walking information is shown in Figures 7-25 and 7-26.

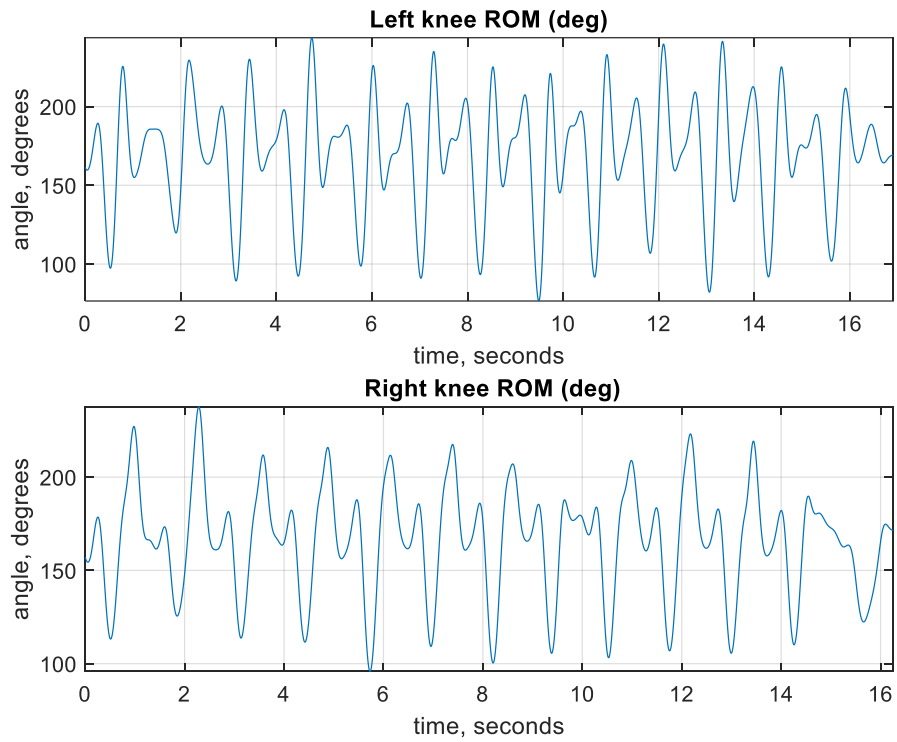


Figure 7-25 Walking ROM

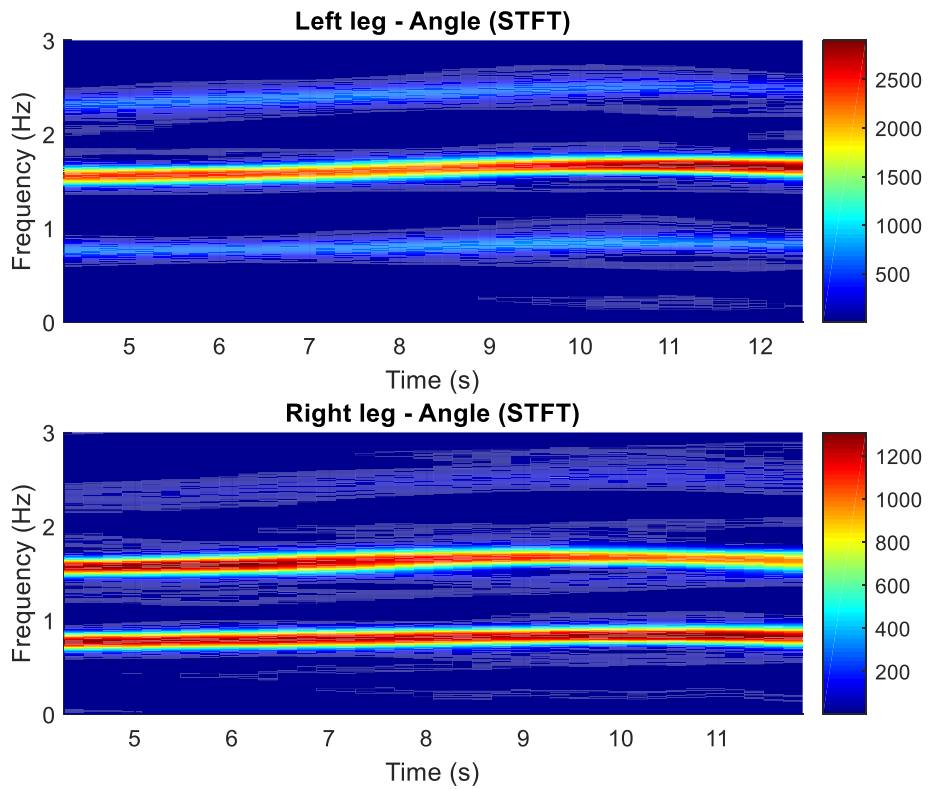


Figure 7-26 Frequency components of the walking signal

The spectrograms shown in Figure 7-26 indicate the frequency components of the walking signal over the recording time. Three components are well highlighted at 0.8Hz, 1.6Hz and 2.3Hz for both legs.

The accelerometer readings indicate that the participant was able to move the left leg more swiftly and to a wider angle covering a wider ROM. The main frequency components for both legs were approximately same, suggesting that the legs were able to make a cycle of movement in about the same time but to a lower extent for the right leg. Total angular displacement was also higher in the left leg. The right leg was therefore suspected to have active arthritis on the day of the clinical examination. The patient has been clinically diagnosed with Oligoarticular JIA. Clinical assessment on the day observed the right knee to be warm, swollen and restricted with fixed flexion deformity (FFD) - inability to fully extend the knee. Accelerometer findings and clinical reports therefore agree for this participant.

7.2.4.2 Patient 2

Movement information for patient 2 is provided in Table 7-7.

Table 7-7 Patient 2 movement information and clinical assessment

Position	Parameter	Left knee	Right knee	Accelerometry finding	Clinical observation
Lying down	Angle (°) (ROM)	61: 162 (101)	44: 166 (122)	Left knee suspected	Warm, swollen and restricted Left knee
	Frequency spectrum (Hz) (Amplitude)	0.46 (0.41)	0.50 (0.76)		
	Angular velocity (rad/s)	-1.9: 1.9	-2.6: 2.6		
	Angular acceleration (rad/s ²)	-5.1: 5.1	-7.8: 7.7		
	Total angular displacement(rad)	26.7	30.9		
	Time (s)	23.8	19.8		
walking	Angle (°) (ROM)	99: 218 (119)	63: 226 (163)	Left knee suspected	Warm, swollen and restricted Left knee
	Frequency spectrum (Hz) (Amplitude)	0.8, 1.6, 2.5 (0.26, 0.35, 0.23)	0.8, 1.6, 2.5 (0.42, 0.62, 0.24)		
	Angular velocity (rad/s)	-11: 13	-13: 18		
	Angular acceleration (rad/s ²)	-101: 115	-135: 150		
	Total angular displacement(rad)	54.04	65.70		
	Time (s)	12.16	12.07		

For patient 2, the accelerometer findings show the left knee as the restrictive knee on the day of data collection. The ROM, angular velocity and angular acceleration recorded lower numbers in comparison to the right knee. The patient had previous diagnosis of Oligoarticular JIA and was clinically assessed to have warm, swollen and restricted left knee with fixed flexion deformity. The accelerometer and clinical findings correlate.

7.2.4.3 Patient 3

The movement information for patient 3 is provided in Table 7-8.

Table 7-8 Patient 3 movement information and clinical assessment

Position	Parameter	Left knee	Right knee	Accelerometry finding	Clinical observation
Lying down	Angle (°) (ROM)	57: 168 (111)	67: 143 (76)	Right knee suspected	Swollen right knee
	Frequency spectrum (Hz) (Amplitude)	0.31 (0.57)	0.24 (0.32)		
	Angular velocity (rad/s)	-1.7: 1.7	-1.0: 1.0		
	Angular acceleration (rad/s ²)	-2.8: 2.9	-1.6: 1.6		
	Total angular displacement(rad)	28.89	21.49		
	Time (s)	31.79	40.51		
walking	Angle (°) (ROM)	69:212 (143)	102: 217 (115)	Right knee suspected	Swollen right knee
	Frequency spectrum (Hz)	0.62, 1.28, 1.90 (0.20, 0.31, 0.20)	0.62, 1.28, 1.90 (0.24, 0.25, 0.13)		
	Angular velocity (rad/s)	-8.1: 9.3	-5.7: 7.5		
	Angular acceleration (rad/s ²)	-82.1: 92.7	-61.5: 69.3		
	Total angular displacement(rad)	65.8	50.5		
	Time (s)	28.83	28.83		

Patient 3 had a previous diagnosis of Polyarticular JIA and was assessed with a swollen right knee on day assessment indicating the presence of active arthritis. The accelerometry findings also point to the right knee as the suspected knee (results shown in Table 7-8). Both findings correlate.

7.2.4.4 Patient 4

The results obtained for patient 4 are presented in Table 7-9.

Table 7-9 Patient 4 movement information and clinical assessment

Position	Parameter	Left knee	Right knee	Accelerometry finding	Clinical observation
Lying down	Angle (°) (ROM)	35: 165 (130)	34: 158 (124)	Right knee covered slightly less ROM	Swollen and restricted (fixed flexion deformity) right knee
	Frequency spectrum (Hz) (Amplitude)	0.27 (0.59)	0.36 (0.58)		
	Angular velocity (rad/s)	-1.82: 1.83	-1.76: 1.76	Both legs had approximately the same angular velocity and acceleration	
	Angular acceleration (rad/s ²)	-3.7: 3.7	-4.1: 4.0		
	Total angular displacement(rad)	36.76	25.53		
	Time (s)	33.29	24.87	Task was completed slightly quicker on the right leg	
Walking	Angle (°) (ROM)	107:185 (78)	95:184 (89)	Left knee had lower ROM, angular velocity and angular acceleration	
	Frequency spectrum (Hz)	0.9, 1.9	0.9, 1.9		
	Angular velocity (rad/s)	-7.2: 6.3	- 7.6: 8.2		
	Angular acceleration (rad/s ²)	-64.9: 77.2	-72.1:86.6		
	Total angular displacement(rad)	26.72	28.74		
	Time (s)	11.03	11.03		

For the lying down position, the accelerometer findings suggested the right knee covered slightly less ROM but was moved swifter than the left leg; other parameters were approximately the same. The walking data suggested that the left knee moved with a slightly lower ROM, angular velocity and acceleration. Further analysis on the frequency spectrum of the walking signal (see spectrogram in Figure 7-27) highlighted the two frequency components, 0.9Hz and 1.9Hz, present in this walking signal. It also

shows the 0.9Hz component, being the more dominant one for both left and right legs, however, the amplitude is higher for the right leg than the left leg (indicated by deeper colour as shown on colour bar). This would suggest that the right leg had higher magnitude of movements than the left leg.

Patient 4 had a diagnosis of Oligoarticular JIA. Clinical assessment on the day of data collection, reported the right knee to be swollen and restricted with fixed flexion deformity. Clinical reports also stated that the patient has previously had swelling, warmth and fixed flexion deformities on both knees and this may have been identified by the accelerometer data, as the lying down results were approximately same for both legs. Accelerometer findings pointed more towards the left leg and so did not correlate with clinical assessment for patient 4.

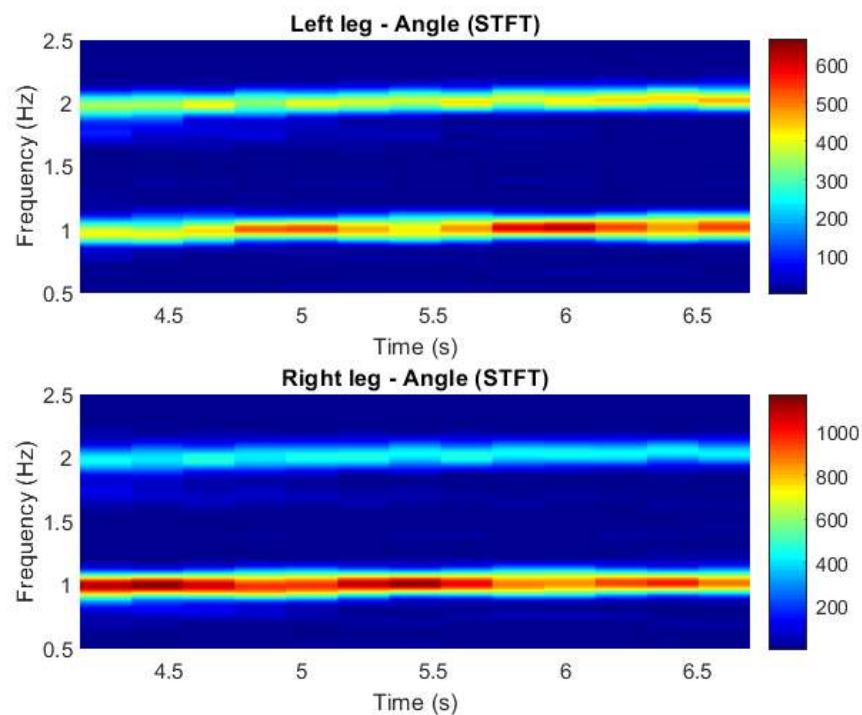


Figure 7-27 STFT showing the dominant 0.9Hz frequency component

The correlation results are summarised in Table 7-10. The results show that accelerometers can potentially in the future assist clinicians make a diagnosis of JIA.

Table 7-10 Correlation between accelerometer and clinical findings

Patient	Suspected knee joint		Correlation between A and B
	Accelerometer finding (A)	Clinical observation (B)	
1	Right knee	Right knee	Yes
2	Left knee	Left knee	Yes
3	Right knee	Right knee	Yes
4	Left knee	Right knee	No

7.3 Summary

The use of accelerometers to describe movement data from the knee joints was investigated. Laboratory experiments were initially performed to test the effectiveness of the accelerometer to measure movement data of a hinge joint and used a flexible goniometer for measuring the actual angles being recorded, and results showed the accelerometer was able to track the goniometer readings.

Further work was then carried out to measure the knee ROM on an adult human subject with the sensors attached to both the left and right thighs and shanks in three scenarios: sitting and swinging the knee freely, lying down and flexing the knee from heel to bottom, and walking. The angle of knee movement, velocity, acceleration and displacement were computed from the recorded data. The experimental results further indicated the accelerometer's ability to measure movement data.

A pilot study which involved recording accelerometer movement data from patients with active JIA on only one knee was then carried out in two scenarios: flexing and extending their legs in the laid down position; and walking a 10-meter length. Correlation was performed between accelerometry and clinical examination. Of the 4 subjects that participated, 75% of the cases correlated.

The results obtained from this study gave a good indication that accelerometry may potentially be an effective tool to aid clinical JIA diagnosis.

In the next chapter, the overall conclusion of the study is presented, and some further works are outlined.

Chapter 8

8 Conclusions and Further work

8.1 Conclusions

An investigation to correlate thermal, visual imaging and accelerometry measurements with the clinical musculoskeletal examinations in Children and Young People (CYP) suspected of Juvenile Idiopathic Arthritis (JIA) was carried out. The aim was to evaluate these techniques to assist clinicians in their diagnosis of the condition.

To achieve this aim, the following objectives were met:

- Segmented the ROIs from the thermal and visual images using the MATLAB® ROI-based processing method.
- Accurately tracked the ROIs through the recorded thermal video using a template matching algorithm based on the normalised cross correlation method.
- Computed the average temperature of the thermal imaging (TI) ROIs
- Quantified the skin colour changes of the Visual imaging (VI) ROIs using the histogram method and found similarity between knee/ankle joints and a reference image using the Euclidean distance metric.
- Designed an accelerometry system that used 4 accelerometers hooked up to an Arduino mega 2560 microcontroller. The sensors were attached just above and below the knees of the patients as knee movement data was collected in lying down and walking scenarios.
- The collected accelerometry data was processed to describe knee movement information such as range of movement, velocity, acceleration and displacement.
- The developed techniques were evaluated on patients in the hospital and the results obtained were compared with the consultant's assessment.

The following contributions to knowledge were made. This study for the first time brought together thermal and visual imaging and accelerometry developments to assist with clinical JIA diagnosis. To identify the ROIs to be segmented, this study also devised a new and consistent method using the curvatures of the knees and ankles as a point of reference, thereby introducing a less subjective way of manually segmenting the ROIs. In the VI study, the colour changes on the knees and ankles were not visually noticeable, so to compare the ROIs (knees or ankles), a reference image method was adapted, such that the left and right knees/ ankles were compared to a common reference and the side more different to the reference was considered to have more colour change and therefore the affected side. In the accelerometry study, a 4-sensor method, 2 for each leg, placed just above and below the knees to measure the joint angle in two movement scenarios: lying down and walking; was adapted. The developed techniques were evaluated on 22 patients from the hospital and the findings were correlated against the consultant's evaluation.

8.1.1 Thermal/Visual Imaging developments

Twenty patients participated in this study in thermal and visual measurements. The front and back of the knees and ankles of each patient were recorded and analysed. A new method to identify the region of interest centred on the knee or ankle was devised. To aid the analysis of the results, the patients were grouped into three categories:

- Category I – patients with one active knee or ankle arthritis
- Category II – patients with active arthritis in both knees or ankles
- Category III – Patients with no active knee or ankle arthritis

8.1.1.1 Thermal Imaging (TI)

For category I patients, the correlation between TI and clinical assessment was 75% and 67% for the front of the knees and ankles respectively; 50% and 33% for the back of the knees and ankles respectively. These results indicate that the front of the joints had a more pronounced sign of thermal and visual changes related to active arthritis. It was observed that in most patients that there were not agreements, the patients had more distinct arthritic symptoms. The clinician's prior knowledge of the patients'

diagnosis could have also affected the clinical assessment of the joint temperature by being more biased toward detecting the arthritic knee as warmer.

For category II patients, direct correlation of the affected arthritic knee or ankle and healthy knee or ankle was not practical. Therefore, a region that both sides could be compared was selected by identifying a reference region. This region was obtained by averaging a section mid-way between the knee and the ankle. The reference temperatures were observed to be lower than the knee or ankle temperatures for both the front and the back in most patients except in a patient at the back of the ankles. The Percentage Temperature Difference (PTD) was also seen to be lower than those for category I. A consideration was the computed reference temperature may not be the true normal skin temperature of the patient, however, because the result was consistent, in almost all the patients, it gives a good indication, that there were active arthritis in both knees and ankles.

For Category III, the TI results could also not be correlated directly with the clinical report as there was no measure of normal skin temperature for the subjects to use for comparison, however, the PTD of the joints in this category was 7.85 times lower than those in Category I, as would be expected for cases with no arthritis.

These findings, therefore, indicate that TI can potentially be an effective tool to aid in JIA diagnosis.

8.1.1.2 Visual imaging (VI)

The Euclidean distance between the colour distributions of the selected reference image and the left and right knees and ankles were computed to determine which knee or ankle had a larger distance (the analysis was performed for both the front and back of the knees and ankles). The joint with the larger distance between the left and the right side was the joint with more colour changes. The VI results were compared with TI and consultants' evaluation.

Higher correlations to the consultant's evaluation and TI were observed at the front of the knees and ankles with the highest being at the front of the knees, indicating this region was more sensitive to colour changes. Separate correlations of 62.5% and 80% with the consultant's and TI results respectively were observed at the front of knees; and 62.5% and 55% observed at the front of the ankles. A combined correlation

between VI, TI and consultant's results showed a 50% correlation at the front of the knees and a 33.3% correlation at the front of the ankles. These results confirmed that an active arthritic joint does not necessarily have skin colour changes, however, in some patients, JIA may have altered the skin colour of the affected joint, and so the technique may potentially aid in JIA diagnosis.

8.1.2 Accelerometry

Due to constraints during the study only 4 patients undertook the accelerometry tests. Accelerometry developments to describe movements at the knee joint with only one active knee arthritis were explored. A 75% correlation was observed with clinical assessment, indicating the accelerometry system was able to differentiate the affected knee from the healthy knee. The discrepancy was found in the patient that had previous active arthritis on the knee that was not clinically diagnosed on the day of assessment. Hence, the system may have also identified some symptoms of activity from the undiagnosed knee. However, the results gave a good indication that accelerometry may be able to describe movement data that can assist clinicians in diagnosing JIA.

So, to a very large extent, the results from the three techniques correlated with the standard clinical musculoskeletal examination. The thermal and visual imaging methods were non-contact, less invasive and quick methods that were easy for the children to cope with. The accelerometry method as well, though a contact method of monitoring, was also easy to carry out and participants coped equally well with the data recording session.

8.2 Further work

This study established a proof of concept demonstrating the value of TI, VI and accelerometry as part of diagnosing arthritis. Future work could be to acquire a larger data of patients with only one active arthritic joint so that a more informed pattern could be determined from the results. A larger data set will give more details that will aid analysis.

There would also be a need to obtain a healthy data set i.e. from persons with no JIA to better understand what a range of normal temperature/skin colour could be as one

of the challenges in this study was in the selection of the reference sections for the thermal/visual imaging techniques.

Automatic segmentation of the knees and ankles could also be explored in order to remove any secondary errors that could be introduced by manually segmenting the regions of interest (ROIs).

For the accelerometry study, addition of gyroscope to denoise the accelerometer signal could be further explored. Findings from the work done in this study show it may improve the accelerometer data and may potentially be able to detect the clinically diagnosed joint without picking the redundant activities from a previously active joint.

Joints affected by arthritis can become swollen. It will be valuable to be able to automatically quantify the extent that the joint is swollen as this can provide objective information.

This study was on children. In future it will be useful to extend it to adults with arthritis.

References

- Albarbar, A., & Teay, S. H. (2017). MEMS accelerometers: Testing and practical approach for smart sensing and machinery diagnostics. *Advanced mechatronics and MEMS devices II* (pp 19-40) Springer, Cham. Retrieved from https://link.springer.com/chapter/10.1007/978-3-319-32180-6_2#citeas
- Alkali, A. H., Saatchi, R., Elphick, H., & Burke, D. (2017). Thermal image processing for real-time non-contact respiration rate monitoring. *IET Circuits, Devices & Systems*, 11(2), 142-148. doi:[10.1049/iet-cds.2016.0143](https://doi.org/10.1049/iet-cds.2016.0143)
- Andrejasic, M. (2008). *MEMS accelerometers* Retrieved from http://mafija.fmf.uni-lj.si/seminar/files/2007_2008/MEMS_accelerometers-koncna.pdf
- Armbrust, W., Bos, G. J., Geertzen, J. H., Sauer, P. J., Dijkstra, P. U., & Lelieveld, O. T. (2017). Measuring physical activity in juvenile idiopathic arthritis: Activity diary versus accelerometer. *The Journal of Rheumatology*, 44(8), 1249-1256. doi:[10.3899/jrheum.160671](https://doi.org/10.3899/jrheum.160671)
- Arthritis Care. (2016). Understanding arthritis. Retrieved from https://www.arthritiscare.org.uk/assets/000/001/429/Understanding_FINAL_100516_web_original.pdf?1463670233
- Arthritis Foundation. (2013). Juvenile arthritis. Retrieved from <http://www.kidsgetarthritisoo.org/pdfs/educational-rights-tool-kit/JA-general.pdf>
- Arthritis Research, UK. (2018). What treatments are there for JIA? Retrieved from <https://www.arthritisresearchuk.org/arthritis-information/conditions/juvenile-idiopathic-arthritis/treatments.aspx>
- Baerveldt, A., & Klang, R. (1997). A low-cost and low-weight attitude estimation system for an autonomous helicopter. Paper presented at the *Proceedings of IEEE International Conference on Intelligent Engineering Systems*, 391-395. doi:[10.1109/INES.1997.632450](https://doi.org/10.1109/INES.1997.632450)

Bailey, K. (2014). Juvenile idiopathic arthritis. Retrieved from <https://www.jia.org.uk/what-is-jia->

Bakhshi, S., Mahoor, M. H., & Davidson, B. S. (2011). Development of a body joint angle measurement system using IMU sensors. Paper presented at the *2011 Annual International Conference of the IEEE Engineering in Medicine and Biology Society*, 6923-6926. doi:10.1109/IEMBS.2011.6091743

Bennett, C. L., Odom, C., & Ben-Asher, M. (2013). Knee angle estimation based on imu data and artificial neural networks. Paper presented at the *2013 29th Southern Biomedical Engineering Conference (SBEC)*, 111-112. doi: [10.1109/SBEC.2013.64](https://doi.org/10.1109/SBEC.2013.64)

Borojevic, N., Kolaric, D., Grazio, S., Grubisic, F., Antonini, S., & Nola, I. A. (2011). Thermography hand temperature distribution in rheumatoid arthritis and osteoarthritis. *Periodicum Biologorum*, *113*(4), 445-448.

Bhargava, R., Hahn, G., Hirsch, W., Kim, M., Mentzel, H., Olsen, O. E., . . . Vazquez, E. (2013). Contrast-enhanced magnetic resonance imaging in pediatric patients: Review and recommendations for current practice. *Magnetic Resonance Insights*, *6*, 95-111. doi:10.4137/MRI.S12561

Borchers, A. T., Selmi, C., Cheema, G., Keen, C. L., Shoenfeld, Y., & Gershwin, M. E. (2006). Juvenile idiopathic arthritis. *Autoimmunity Reviews*, *5*(4), 279-298. doi://doi.org/10.1016/j.autrev.2005.09.011

Boros, C., & Whitehead, B. (2010). Juvenile idiopathic arthritis. *Australian Family Physician*, *39*(9), 630 -636. Retrieved from https://www.racgp.org.au/download/documents/AFP/2010/September/201009b_0ros.pdf

Brenner, M., Braun, C., Oster, M., & Gulko, P. S. (2006). Thermal signature analysis as a novel method for evaluating inflammatory arthritis activity. *Annals of the Rheumatic Diseases*, *65*(3), 306-311. doi:10.1136/ard.2004.035246

Butterfield, A., & Szymanski, J. (2018). Filter. In A. J. Butterfield, & J. Szymanski (Eds.), *A dictionary of electronics and electrical engineering* () Oxford University Press. Retrieved

from

<http://www.oxfordreference.com.hallam.idm.oclc.org/view/10.1093/acref/9780198725725.001.0001/acref-9780198725725-e-1736>

Chang, H. J., Burke, A. E., & Glass, R. M. (2010). Juvenile idiopathic arthritis. *JAMA*, 303(13) doi:10.1001/jama.303.13.1328

Chen, K., & Bassett, D. (2005). The technology of accelerometry-based activity monitors: Current and future. *Medicine & Science in Sports & Exercise*, 37(11), S490 - S500.

Chen, S., Zhang, D., Wu, J., & Zhang, B. (2016). Facial color feature extraction for disease diagnosis using non-base colors. Paper presented at the 2016 2nd IEEE International Conference on Computer and Communications (ICCC), 808-813. doi:[10.1109/CompComm.2016.7924815](https://doi.org/10.1109/CompComm.2016.7924815)

Chen, Y., Chen, W., & Ni, H. (2016). Image segmentation in thermal images. Paper presented at the 2016 IEEE International Conference on Industrial Technology (ICIT), 1507-1512. doi:10.1109/ICIT.2016.7474983

Clifford, M., & Gomez, L. (2005). Measuring tilt with low-g accelerometers. *AN3107, Application Note, NXP*, Retrieved from <https://www.nxp.com/docs/en/application-note/AN3107.pdf>

Cole, T. J., & Altman, D. G. (2017). Statistics notes: What is a percentage difference? *Bmj*, 358, j3663. doi:<https://doi-org.hallam.idm.oclc.org/10.1136/bmj.j3663>

Colton, S. (2007). The balance filter. Retrieved from http://d1.amobbs.com/bbs_upload782111/files_44/ourdev_665531S2JZG6.pdf

Dadafshar, M. (2014). Accelerometer and gyroscopes sensors: Operation, sensing, and applications. Retrieved from <https://pdfserv.maximintegrated.com/en/an/AN5830.pdf>

Davis Instruments. (2012). Thermal imaging technical resource. Retrieved from <https://pim-resources.coleparmer.com/data-sheet/thermalimagingtechresource.pdf>

De Salis, A. F., Saatchi, R., & Dimitri, P. (2018). Evaluation of high resolution thermal imaging to determine the effect of vertebral fractures on associated skin surface temperature in children with osteogenesis imperfecta. *Medical & Biological Engineering & Computing*, 1-11. doi:<https://doi.org/10.1007/s11517-018-1806-3>

Djurić-Jovičić, M. D., Jovičić, N. S., & Popović, D. B. (2011). Kinematics of gait: New method for angle estimation based on accelerometers. *Sensors*, 11(11), 10571-10585. [10.3390/s111110571](https://doi.org/10.3390/s111110571)

Dong, W., Chen, I., Lim, K. Y., & Goh, Y. K. (2007). Measuring uniaxial joint angles with a minimal accelerometer configuration. Paper presented at the *Proceedings of the 1st International Convention on Rehabilitation Engineering & Assistive Technology: In Conjunction with 1st Tan Tock Seng Hospital Neurorehabilitation Meeting*, 88-91.

Duarte, A., Carrao, L., Espanha, M., Viana, T., Freitas, D., Bartolo, P., . . . Almeida, H. A. (2014). Segmentation algorithms for thermal images. *Procedia Technology*, 16, 1560-1569. doi:<https://doi.org/10.1016/j.protcy.2014.10.178>

Ellis, K., Godbole, S., Marshall, S., Lanckriet, G., Staudenmayer, J., & Kerr, J. (2014). Identifying active travel behaviors in challenging environments using GPS, accelerometers, and machine learning algorithms. *Frontiers in Public Health*, 2, 36. doi:10.3389/fpubh.2014.00036

Ellis, J. A., Munro, J. E., & Ponsonby, A. (2009). Possible environmental determinants of juvenile idiopathic arthritis. *Rheumatology*, 49(3), 411-425. doi:10.1093/rheumatology/kep383

Esfandyari, J., De Nuccio, R. & Xu, G. (2011). Solutions for MEMS sensor fusion. Retrieved from http://uk.mouser.com/applications/sensor_solutions_mems/

Fairfield Independent Hospital. (2019). MRI scan. Retrieved from <https://www.fairfield.org.uk/tests/private-mri-scan/>

Fisher, C. J. (2010). Using an accelerometer for inclination sensing. AN-1057, Application note, Analog devices Retrieved

from <https://www.analog.com/media/en/technical-documentation/application-notes/AN-1057.pdf>

FLIR. (2016). FLIR T630sc; Retrieved from http://www.flirmedia.com/MMC/THG/Brochures/RND_060/RND_060_US.pdf

FLIR. (2019). FLIR T630sc portable thermal imaging camera | FLIR systems. Retrieved from <https://www.flir.com/products/t630sc/>

FLIR Systems. (2015). Cooled vs uncooled thermal imaging. Retrieved from http://www.flirmedia.com/MMC/THG/Brochures/RND_038/RND_038_US.pdf

Foerster, F., Smeja, M., & Fahrenberg, J. (1999). Detection of posture and motion by accelerometry: A validation study in ambulatory monitoring. *Computers in Human Behavior*, 15(5), 571-583. [https://doi.org/10.1016/S0747-5632\(99\)00037-0](https://doi.org/10.1016/S0747-5632(99)00037-0)

Foster, H. E., Kay, L. J., Friswell, M., Coady, D., & Myers, A. (2006). Musculoskeletal screening examination (pGALS) for school-age children based on the adult GALS screen. *Arthritis Care & Research*, 55(5), 709-716. doi:<https://doi.org.hallam.idm.oclc.org/10.1002/art.22230>

Foster, H. E., Eltringham, M. S., Kay, L. J., Friswell, M., Abinun, M., & Myers, A. (2007). Delay in access to appropriate care for children presenting with musculoskeletal symptoms and ultimately diagnosed with juvenile idiopathic arthritis. *Arthritis and Rheumatism*, 57(6), 921-927. doi:10.1002/art.22882

Foster, H. E., & Jandial, S. (2008). pGALS—A screening examination of the musculoskeletal system in school-aged children. *Reports on the Rheumatic Diseases (Series 5), Hands On*, 15 Retrieved from <https://www.rch.org.au/uploadedFiles/Main/Content/MedEd/fracp/pGALS%20.pdf>

Foster, H. E., & Jandial, S. (2013). pGALS—paediatric gait arms legs and spine: A simple examination of the musculoskeletal system. *Pediatric Rheumatology*, 11(1), 44. doi: [10.1186/1546-0096-11-44](https://doi.org/10.1186/1546-0096-11-44)

Fraden, J. (2004). *Handbook of modern sensors physics, designs, and applications* (3rd ed.). New York: AIP.

Frize, M., Adea, C., Payeur, P., Di Primio, G., Karsh, J., & Ogungbemile, A. (2011). Detection of rheumatoid arthritis using infrared imaging. Paper presented at the *Medical Imaging 2011: Image Processing*, , 7962 79620M. doi:<https://doi.org/10.1117/12.874552>

Giancane, G., Consolaro, A., Lanni, S., Davi, S., Schiappapietra, B., & Ravelli, A. (2016). Juvenile idiopathic arthritis: Diagnosis and treatment. *Rheumatology and Therapy*, 3(2), 187-207. doi:<https://doi.org/10.1007/s40744-016-0040-4>

Global Alliance for Musculoskeletal Health. (2015). The knee. Retrieved from <https://bjdonline.org/the-knee/>

Griffin, A. (2009, September 16). *Template matching in matlab using normxcorr2. (normalised cross correlation)*. [Video file] Retrieved from <https://www.youtube.com/watch?v=Q-OzmDen4HU&t=2s>

Hamill, J., Knutzen, K. M., & Derrick, T. R. (2014). *Biomechanical basis of human movement* (4th ed.). Philadelphia, PA: Lippincott Williams & Wilkins.

Hanania, J., Stenhouse, K. & Donev, J. (2017). Energy education - stefan-boltzmann law. Retrieved from https://energyeducation.ca/encyclopedia/Stefan-Boltzmann_law

Hawley, D., Offiah, A. C., Hawley, S. J., & Burke, D. (2015). PP10. Evaluation of skin temperature using liquid crystal and infrared thermometers in children attending specialist paediatric rheumatology clinics. *Rheumatology*, 54(suppl_2), ii9. <https://doi.org/10.1093/rheumatology/keu503>

Hemke, R., Maas, M., van Veenendaal, M., Dolman, K. M., van Rossum, M. A., van den Berg, J Merlijn, & Kuijpers, T. W. (2014). Contrast-enhanced MRI compared with the physical examination in the evaluation of disease activity in juvenile idiopathic arthritis. *European Radiology*, 24(2), 327-334. <https://doi.org/10.1007/s00330-013-3036-2>

Hendelman, D., Miller, K., Baggett, C., Debold, E., & Freedson, P. (2000). Validity of accelerometry for the assessment of moderate intensity physical activity in the field. *Medicine and Science in Sports and Exercise*, 32(9 Suppl), 442.

Hernandez-Hernandez, M. V., & Diaz-Gonzalez, F. (2017). Role of physical activity in the management and assessment of rheumatoid arthritis patients. *Reumatología Clínica*, 13(4), 214-220. doi:10.1016/j.reuma.2016.04.003

Hernandez-Hernandez, V., Ferraz-Amaro, I., & Diaz-Gonzalez, F. (2014). Influence of disease activity on the physical activity of rheumatoid arthritis patients. *Rheumatology*, 53(4), 722-731. doi:10.1093/rheumatology/ket422

Hickman, D., & Riley, T. (2010). Thermal imager technical guidance document. Retrieved from <https://www.cpni.gov.uk/system/files/documents/cf/1e/Thermal-Imager-technical-guidance.pdf>

Higgins, W. T. (1975). A comparison of complementary and kalman filtering. *IEEE Transactions on Aerospace and Electronic Systems*, 11(3), 321-325. doi: [10.1109/TAES.1975.308081](https://doi.org/10.1109/TAES.1975.308081)

Hobby Electronics. (2018). Triple axis accelerometer breakout - ADXL335. Retrieved from <http://www.hobbytronics.co.uk/adxl335>

Ilowite, N. T., Walco, G. A., & Pochaczewsky, R. (1992). Assessment of pain in patients with juvenile rheumatoid arthritis: Relation between pain intensity and degree of joint inflammation. *Annals of the Rheumatic Diseases*, 51(3), 343-346. doi:10.1136/ard.51.3.343

Ingle, V., & Proakis, J. (2012). *Digital signal processing using MATLAB* (Third ed.). United States of America: Global Engineering: Christopher M. Shortt.

Jin, C., Yang, Y., Xue, Z., Liu, K., & Liu, J. (2013). Automated analysis method for screening knee osteoarthritis using medical infrared thermography. *Journal of Medical and Biological Engineering*, 33(5), 471-477. doi: 10.5405/jmbe.1054

Kainuma, M., Furusyo, N., Urita, Y., Nagata, M., Ihara, T., Oji, T., . . . Hayashi, J. (2015). The association between objective tongue color and endoscopic findings: Results from

the kyushu and okinawa population study (KOPS). *BMC Complementary and Alternative Medicine*, 15(1), 372. <https://doi.org/10.1186/s12906-015-0904-0>

Kamen, G., Patten, C., Du, C. D., & Sison, S. (1998). An accelerometry-based system for the assessment of balance and postural sway. *Gerontology*, 44(1), 40-45. doi:10.1159/000021981

Karantonis, D. M., Narayanan, M. R., Mathie, M., Lovell, N. H., & Celler, B. G. (2006). Implementation of a real-time human movement classifier using a triaxial accelerometer for ambulatory monitoring. *IEEE Transactions on Information Technology in Biomedicine*, 10(1), 156-167. doi: [10.1109/TITB.2005.856864](https://doi.org/10.1109/TITB.2005.856864)

Kavanagh, J. J., & Menz, H. B. (2008). Accelerometry: A technique for quantifying movement patterns during walking. *Gait & Posture*, 28(1), 1-15. doi:10.1016/j.gaitpost.2007.10.010

Keen, N. (2005). *Color moments*. School of Informatics, University of Edinburgh: Retrieved from http://homepages.inf.ed.ac.uk/rbf/CVonline/LOCAL_COPIES/AV0405/KEEN/av_as2_nkeen.pdf

Kim, B., Lee, S., Cho, D., & Oh, S. (2008). A proposal of heart diseases diagnosis method using analysis of face color. Paper presented at the *2008 International Conference on Advanced Language Processing and Web Information Technology*, 220-225. doi:<https://doi.org/10.1109/ALPIT.2008.27>

Kodituwakku, S. R., & Selvarajah, S. (2004). Comparison of color features for image retrieval. *Indian Journal of Computer Science and Engineering*, 1(3), 207-211. Retrieved from <http://citeseerx.ist.psu.edu/viewdoc/download?doi=10.1.1.301.8601&rep=rep1&type=pdf>

Kurata, S., Makikawa, M., Kobayashi, H., Takahashi, A., & Tokue, R. (1998). Joint motion monitoring by accelerometers set at both near sides around the joint. Paper presented at the *Proceedings of the 20th Annual International Conference of the IEEE Engineering in Medicine and Biology Society*, 4 1936-1939. doi:10.1109/IEMBS.1998.746978

Land Instruments International. (2004). *A basic guide to thermography* Retrieved from http://www.lirkorea.com/Landinstruments.net%20Website/infrared/downloads/pdf/thermography_guide.pdf

Lasanen, R., Piippo-Savolainen, E., Remes-Pakarinen, T., Kroger, L., Heikkila, A., Julkunen, P., . . . Toyras, J. (2015). Thermal imaging in screening of joint inflammation and rheumatoid arthritis in children. *Physiological Measurement*, *36*(2), 273 -282. <https://doi.org/10.1088/0967-3334/36/2/273>

Lee, J., Song, J., Hootman, J. M., Semanik, P. A., Chang, R. W., Sharma, L., . . . Dunlop, D. D. (2013). Obesity and other modifiable factors for physical inactivity measured by accelerometer in adults with knee osteoarthritis. *Arthritis Care & Research*, *65*(1), 53-61. doi:10.1002/acr.21754

Lerkvaleekul, B., Jaovisidha, S., Sungkarat, W., Chitrapazt, N., Fuangfa, P., Ruangchaijatuporn, T., & Vilaiyuk, S. (2017). The comparisons between thermography and ultrasonography with physical examination for wrist joint assessment in juvenile idiopathic arthritis. *Physiological Measurement*, *38*(5), 691-700. <https://doi.org/10.1088/1361-6579/aa63d8>

Lewis, J. P. (1995). Fast template matching. Paper presented at the *Vision Interface*, 95 120-123. Retrieved from http://scribblethink.org/Work/nvisionInterface/vi95_lewis.pdf

Li, B., Huang, Q., Lu, Y., Chen, S., Liang, R., & Wang, Z. (2008). A method of classifying tongue colors for traditional chinese medicine diagnosis based on the CIELAB color space. Paper presented at the *International Conference on Medical Biometrics*, 153-159. doi: https://doi.org/10.1007/978-3-540-77413-6_20

Liu, B., & Wang, T. (2006). *Inspection of face and body for diagnosis of diseases* Foreign Languages Press.

Liu, M., & Guo, Z. (2008). Hepatitis diagnosis using facial color image. Paper presented at the *International Conference on Medical Biometrics*, 160-167. doi:https://doi.org/10.1007/978-3-540-77413-6_21

Lloyd, J. M. (2013). *Thermal imaging systems*. Springer Science & Business Media.

London Knee Specialists. (2019). Anatomy of the knee - knee conditions. Retrieved from <https://www.londonkneespecialists.co.uk/services/anatomy-of-the-knee/>

Luinge, H. J., & Veltink, P. H. (2004). Inclination measurement of human movement using a 3-D accelerometer with autocalibration. *IEEE Transactions on Neural Systems and Rehabilitation Engineering*, 12(1), 112-121. doi: [10.1109/TNSRE.2003.822759](https://doi.org/10.1109/TNSRE.2003.822759)

Lyons, G. M., Culhane, K. M., Hilton, D., Grace, P. A., & Lyons, D. (2005). A description of an accelerometer-based mobility monitoring technique. *Medical Engineering and Physics*, 27(6), 497-504. doi:[10.1016/j.medengphy.2004.11.006](https://doi.org/10.1016/j.medengphy.2004.11.006)

Mahata, S., Saha, S. K., Kar, R., & Mandal, D. (2018). Optimal design of fractional order low pass butterworth filter with accurate magnitude response. *Digital Signal Processing*, 72, 96-114. doi:[//doi-org.hallam.idm.oclc.org/10.1016/j.dsp.2017.10.001](https://doi-org.hallam.idm.oclc.org/10.1016/j.dsp.2017.10.001)

Mali, S. N., & Tejaswini, M. L. (2014). Color histogram features for image retrieval systems. *International Journal of Innovative Research in Science, Engineering and Technology (an ISO 3297: 2007 Certified Organization)*, 3(4) Retrieved from <http://www.rroij.com/peer-reviewed/color-histogram-features-for-image-retrievalsystems-46853.html>

Martinez-Mendez, R., Sekine, M., & Tamura, T. (2012). Postural sway parameters using a triaxial accelerometer: Comparing elderly and young healthy adults. *Computer Methods in Biomechanics and Biomedical Engineering*, 15(9), 899-910. doi: [10.1080/10255842.2011.565753](https://doi.org/10.1080/10255842.2011.565753)

Mathworks. (2018). 1-D wavelet decomposition. Retrieved from https://uk.mathworks.com/help/wavelet/ref/wavedec.html?searchHighlight=decomposition%20tree&s_tid=doc_srchtile

MathWorks. (2019a). *Image processing toolbox documentation* (R2019a ed.) Retrieved from https://uk.mathworks.com/help/images/index.html?s_cid=doc_ftr

MathWorks. (2019b). Wavelet packets. Retrieved from <https://uk.mathworks.com/help/wavelet/ug/wavelet-packets.html>

McDaniel, G. W., & Robinson, D. Z. (1962). Thermal imaging by means of the evaporograph. *Applied Optics*, 1(3), 311-324. doi:10.1364/AO.1.000311

McMahon, A., & Tattersall, R. (2011). Diagnosing juvenile idiopathic arthritis. *Paediatrics and Child Health*, 21(12), 552-557. doi:<https://doi-org.hallam.idm.oclc.org/10.1016/j.paed.2011.07.005>

Miller, E., Uleryk, E., & Doria, A. S. (2009). Evidence-based outcomes of studies addressing diagnostic accuracy of MRI of juvenile idiopathic arthritis. *American Journal of Roentgenology*, 192(5), 1209-1218. doi:10.2214/AJR.08.2304

Miller, G. (2012). Biomedical transport processes. *Introduction to biomedical engineering (third edition)* (pp. 937-993) Elsevier. Retrieved from <https://www.sciencedirect.com/topics/pharmacology-toxicology-and-pharmaceutical-science/thermal-radiation>

Mohiyuddin, N., Dhage, P., & Warhade, K. K. (2014). Rheumatoid arthritis detection using thermal imaging and fuzzy-c-means algorithm. *International Journal of Computer & Mathematical Sciences*, 3(8), 46-55. Retrieved from <https://pdfs.semanticscholar.org/d775/ad919f943482361aba76f4be7c8073271814.pdf>

Mojsilovic, A., Hu, H., & Soljanin, E. (2002). Extraction of perceptually important colors and similarity measurement for image matching, retrieval and analysis. *IEEE Transactions on Image Processing*, 11(11), 1238-1248. doi:10.1109/TIP.2002.804260

Munsayac, F. E. T., Alonzo, L. M. B., Lindo, D. E. G., Baldovino, R. G., & Bugtai, N. T. (2017). Implementation of a normalized cross-correlation coefficient-based template matching algorithm in number system conversion. Paper presented at the *2017 IEEE 9th International Conference on Humanoid, Nanotechnology, Information Technology, Communication and Control, Environment and Management (HNICEM)*, 1-4. doi:[10.1109/HNICEM.2017.8269520](https://doi.org/10.1109/HNICEM.2017.8269520)

Narwade, J., & Kumar, B. (2016). Local and global color histogram feature for color content-based image retrieval system. Paper presented at the *Proceedings of the*

- International Congress on Information and Communication Technology*, 293-300.
doi:10.1007/978-981-10-0767-5_32
- Naz, R., Ahmad, M., & Karandikar, M. (2015). Arthritis prediction by thermal image processing & neural network. *IOSR Journal of VLSI and Signal Processing (IOSR-JVSP)*, 5(4), 28-34. doi:10.9790/4200-05422834
- NHS. (2015a). Ultrasound scan. Retrieved from <https://www.nhs.uk/conditions/ultrasound-scan/>
- NHS. (2015b). X-ray. Retrieved from <https://www.nhs.uk/conditions/X-ray/>
- NHS. (2016a). Diagnosis, Rheumatoid arthritis. Retrieved from <https://www.nhs.uk/conditions/rheumatoid-arthritis/diagnosis/>
- NHS. (2016b). Symptoms, rheumatoid arthritis. Retrieved from <https://www.nhs.uk/conditions/rheumatoid-arthritis/symptoms/>
- [NHS. \(2017\). Arthritis. Retrieved from https://www.nhs.uk/conditions/arthritis/](https://www.nhs.uk/conditions/arthritis/)
- NHS. (2018). MRI scan. Retrieved from <https://www.nhs.uk/conditions/mri-scan/>
- Norgaard, M., Twilt, M., Andersen, L. B., & Herlin, T. (2016). Accelerometry-based monitoring of daily physical activity in children with juvenile idiopathic arthritis. *Scandinavian Journal of Rheumatology*, 45(3), 179-187. doi:10.3109/03009742.2015.1057862
- Norgaard, M., Lomholt, J. J., Thastum, M., Herlin, M., Twilt, M., & Herlin, T. (2017). Accelerometer-assessed daily physical activity in relation to pain cognition in juvenile idiopathic arthritis. *Scandinavian Journal of Rheumatology*, 46(1), 22-26. doi:10.3109/03009742.2016.1160146
- Nwaizu, H., Saatchi, R., & Burke, D. (2016). Accelerometer based human joints' range of movement measurement. Paper presented at the *2016 10th International Symposium on Communication Systems, Networks and Digital Signal Processing (CSNDSP)*, 1-6. <https://doi.org/10.1109/CSNDSP.2016.7573970>

Nwaizu, H., Saatchi, R., & Burke, D. (2017). Inertial measurement techniques for human joints' movement analysis. *AAATE 2017: Advancing Assistive Technology and eAccessibility for People with Disabilities and the Aging Population*, 242(Studies in Health Technology and Informatics), 717-724. doi:10.3233/978-1-61499-798-6-717

O'Dell, W. (2005). Template matching. Retrieved from <https://imagej.nih.gov/ij/plugins/template-matching.html>

OrthoInfo. (2019). Talus fractures - OrthoInfo - AAOS. Retrieved from <https://www.orthoinfo.org/en/diseases--conditions/talus-fractures/>

Ostergaard, M., Edmonds, J., McQueen, F., Peterfy, C., Lassere, M., Ejbjerg, B., . . . Conaghan, P. (2005). An introduction to the EULAR–OMERACT rheumatoid arthritis MRI reference image atlas. *Annals of the Rheumatic Diseases*, 64(suppl 1), i3-i7. <http://dx.doi.org/10.1136/ard.2004.031773>

Owen, R., Ramlakhan, S., Saatchi, R., & Burke, D. (2018). Development of a high-resolution infrared thermographic imaging method as a diagnostic tool for acute undifferentiated limp in young children. *Medical & Biological Engineering & Computing*, 56(6), 1115-1125. <https://doi-org.hallam.idm.oclc.org/10.1007/s11517-017-1749-0>

Pan, J., Hu, B., & Zhang, J. Q. (2006). An efficient object tracking algorithm with adaptive prediction of initial searching point. Paper presented at the *Pacific-Rim Symposium on Image and Video Technology*, 1113-1122. https://doi.org/10.1007/11949534_112

Parker, M. (2010). *Digital signal processing everything you need to know to get started*. Burlington, MA; Amsterdam; London: Newnes/Elsevier; Newnes.

Perveen, N., Kumar, D., & Bhardwaj, I. (2013). An overview on template matching methodologies and its applications. *International Journal of Research in Computer and Communication Technology*, 2(10), 988-995. Retrieved from <https://pdfs.semanticscholar.org/93cf/4a44197e600d4014e234ea6cd3599b962ba4.pdf>

Pincus, T., & Sokka, T. (2009). Laboratory tests to assess patients with rheumatoid arthritis: Advantages and limitations. *Rheumatic Disease Clinics*, 35(4), 731-734. doi:10.1016/j.rdc.2009.10.007

Prakken, B., Albani, S., & Martini, A. (2011). Juvenile idiopathic arthritis. *The Lancet*, 377(9783), 2138-2149. doi://doi.org/10.1016/S0140-6736(11)60244-4

Prioreschi, A., Hodkinson, B., Avidon, I., Tikly, M., & McVeigh, J. A. (2013). The clinical utility of accelerometry in patients with rheumatoid arthritis. *Rheumatology (Oxford, England)*, 52(9), 1721-1727. doi:10.1093/rheumatology/ket216

Qiao, Y., Wei, Z., & Zhao, Y. (2017). Thermal infrared pedestrian image segmentation using level set method. *Sensors*, 17(8), 1811. doi:<https://doi.org/10.3390/s17081811>

Ramos, P. C., Ceccarelli, F., & Jousse-Joulin, S. (2012). Role of ultrasound in the assessment of juvenile idiopathic arthritis. *Rheumatology*, 51(suppl_7), vii10-vii12. doi:<https://doi.org/10.1093/rheumatology/kes333>

Ravelli, A., & Martini, A. (2007). Juvenile idiopathic arthritis. *The Lancet*, 369(9563), 767-778. doi://doi.org/10.1016/S0140-6736(07)60363-8

Reddy, N. P., Rothschild, B. M., Mandal, M., Gupta, V., & Suryanarayanan, S. (1995). Noninvasive acceleration measurements to characterize knee arthritis and chondromalacia. *Annals of Biomedical Engineering*, 23(1), 78-84. doi:10.1007/BF02368303

Reddy, N. P., Rothschild, B. M., Verrall, E., & Joshi, A. (2001). Noninvasive measurement of acceleration at the knee joint in patients with rheumatoid arthritis and spondyloarthritis of the knee. *Annals of Biomedical Engineering*, 29(12), 1106-1111. doi:10.1114/1.1424916

Reddy, K. R., Priya, K. H., & Neelima, N. (2015). Object detection and tracking--A survey. Paper presented at the 2015 International Conference on Computational Intelligence and Communication Networks (CICN), 418-421. doi:10.1109/CICN.2015.317

Ring, E.F.J (1990). Quantitative thermal imaging. *Clinical Physics and Physiological Measurement*, 11(4A), 87-95. <https://doi.org/10.1088/0143-0815/11/4a/310>

Ring, E. F. J. (2004). The historical development of thermal imaging in medicine. *Rheumatology*, 43(6), 800-802. doi:10.1093/rheumatology/keg009

Ring, E. (2006). The historical development of thermometry and thermal imaging in medicine. *Journal of Medical Engineering & Technology*, 30(4), 192-198. doi:10.1080/03091900600711332

Ring, E. F. J. (2007). The historical development of temperature measurement in medicine. *Infrared Physics and Technology*, 49(3), 297-301. doi:10.1016/j.infrared.2006.06.029

Ring, F. (2010). Thermal imaging today and its relevance to diabetes. *Journal of Diabetes Science and Technology*, 4(4), 857-862. doi:10.1177/193229681000400414

Salisbury, R. S., Parr, G., De Silva, M., Hazleman, B. L., & Page-Thomas, D. P. (1983). Heat distribution over normal and abnormal joints: Thermal pattern and quantification. *Annals of the Rheumatic Diseases*, 42(5), 494-499. doi:10.1136/ard.42.5.494

Sanchez, B. M., Lesch, M., Brammer, D., Bove, S. E., Thiel, M., & Kilgore, K. S. (2008). Use of a portable thermal imaging unit as a rapid, quantitative method of evaluating inflammation and experimental arthritis. *Journal of Pharmacological and Toxicological Methods*, 57(3), 169-175. doi:10.1016/j.vascn.2008.01.003

Sasiadek, J. Z. (2002). Sensor fusion. *Annual Reviews in Control*, 26(2), 203-228. [https://doi.org/10.1016/S1367-5788\(02\)00045-7](https://doi.org/10.1016/S1367-5788(02)00045-7)

Seel, T., Raisch, J., & Schauer, T. (2014). IMU-based joint angle measurement for gait analysis. *Sensors (Basel, Switzerland)*, 14(4), 6891-6909. doi:10.3390/s140406891

Semanik, P., Song, J., Chang, R. W., Manheim, L., Ainsworth, B., & Dunlop, D. (2010). Assessing physical activity in persons with rheumatoid arthritis using accelerometry. *Medicine and Science in Sports and Exercise*, 42(8), 1493-1501. doi:10.1249/MSS.0b013e3181cfc9da

Sha, Y., Jhuo, Y., Chen, K., & Wang, S. (2013). Thermal radiation material for electronic devices applications. Paper presented at the *2013 8th International Microsystems, Packaging, Assembly and Circuits Technology Conference (IMPACT)*, 74-77. doi:10.1109/IMPACT.2013.6706676

Shen, X. W., Yao, M. L., Jia, W. M., & Yuan, D. (2012). Adaptive complementary filter using fuzzy logic and simultaneous perturbation stochastic approximation algorithm. *Measurement*, 45(5), 1257-1265. doi:10.1016/j.measurement.2012.01.011

Sheybani, E. F., Khanna, G., White, A. J., & Demertzis, J. L. (2013). Imaging of juvenile idiopathic arthritis: A multimodality approach. *Radiographics : A Review Publication of the Radiological Society of North America, Inc*, 33(5), 1253-1273. doi:10.1148/rg.335125178

Snehalatha, U., Anburajan, M., Sowmiya, V., Venkatraman, B., & Menaka, M. (2015). Automated hand thermal image segmentation and feature extraction in the evaluation of rheumatoid arthritis. *Proceedings of the Institution of Mechanical Engineers, Part H: Journal of Engineering in Medicine*, 229(4), 319-331. <https://doi-org.hallam.idm.oclc.org/10.1177%2F0954411915580809>

Snehalatha, U., Rajalakshmi, T., Gopikrishnan, M., & Gupta, N. (2017). Computer-based automated analysis of X-ray and thermal imaging of knee region in evaluation of rheumatoid arthritis. *Proceedings of the Institution of Mechanical Engineers, Part H: Journal of Engineering in Medicine*, 231(12), 1178-1187. <https://doi.org/10.1177/0954411917737329>

Spalding, S. J., Kwoh, C. K., Boudreau, R., Enama, J., Lunich, J., Huber, D., . . . Hirsch, R. (2008). Three-dimensional and thermal surface imaging produces reliable measures of joint shape and temperature: A potential tool for quantifying arthritis. *Arthritis Research & Therapy*, 10(1), R10. doi:<https://doi.org/10.1186/ar2360>

Stanford Health Care. (2019a). Magnetic resonance imaging - MRI. Retrieved from <https://stanfordhealthcare.org/medical-tests/m/mri.html>

Stanford Health Care. (2019b). Risks of magnetic resonance imaging (MRI). Retrieved from <https://stanfordhealthcare.org/medical-tests/m/mri/risk-factors.html>

Suma, A. B., Snehalatha, U., & Rajalakshmi, T. (2016). Automated thermal image segmentation of knee rheumatoid arthritis. Paper presented at the *2016 International Conference on Communication and Signal Processing (ICCSP)*, 535-539. <https://doi.org/10.1109/ICCSP.2016.7754195>

Syed, N. (2016). Infrared thermography [powerpoint slides]. Retrieved from <https://www.slideshare.net/shuttary/infrared-thermography-57831050>

Taieb, C., Bruel, P., & Auges, M. (2014). Knee arthritis: A confirmed burden. *Osteoarthritis and Cartilage*, 22, S224-S225. doi:<https://doi.org/10.1016/j.joca.2014.02.434>

Tan, L., & Jiang, J. (2013). *Digital signal processing* doi:10.1016/C2011-0-05250-X

Thompson, M. (Ed.). (2014). *Intuitive analog circuit design* (2nd ed.) Retrieved from <https://www-sciencedirect-com.hallam.idm.oclc.org/topics/engineering/magnitude-response>

Tseng, S. P., Wen-Lung, L., Chih-Yang, S., Jia-Wei, H., & Chin-Sheng, C. (2011). Motion and attitude estimation using inertial measurements with complementary filter. Paper presented at the *2011 8th Asian Control Conference (ASCC)*, 863-868.

Tyson, J. (2001). How night vision works. Retrieved from <https://electronics.howstuffworks.com/gadgets/high-tech-gadgets/nightvision.htm>

Varju, G., Pieper, C. F., Renner, J. B., & Kraus, V. B. (2004). Assessment of hand osteoarthritis: Correlation between thermographic and radiographic methods. *Rheumatology*, 43(7), 915-919. <https://doi.org/10.1093/rheumatology/keh204>

Veltink, P. H., Bussmann, H. B., Koelma, F., Franken, H. M., Martens, W. L., & van Lummel, R. C. (1993). The feasibility of posture and movement detection by accelerometry. Paper presented at the *Proceedings of the 15th Annual International Conference of the IEEE Engineering in Medicine and Biology Society*. 1230-1231. doi:10.1109/IEMBS.1993.979109

Versus Arthritis. (2018a). Rheumatoid arthritis (RA). Retrieved from <https://www.versusarthritis.org/about-arthritis/conditions/rheumatoid-arthritis/>

Versus Arthritis. (2018b). The inflammatory arthritis pathway. Retrieved from </about-arthritis/treatments/the-inflammatory-arthritis-pathway/>

Vollmer, M., & Möllmann, K. (2010). Fundamentals of infrared thermal imaging. *Infrared Thermal Imaging: Fundamentals, Research and Applications*, 1-72.

Wallace, C. A., Giannini, E. H., Spalding, S. J., Hashkes, P. J., O'neil, K. M., Zeff, A. S., . . . Schanberg, L. E. (2012). Trial of early aggressive therapy in polyarticular juvenile idiopathic arthritis. *Arthritis & Rheumatism*, 64(6), 2012-2021. doi:10.1002/art.34343

Wang, L., Zhang, Y., & Feng, J. (2005). On the euclidean distance of images. *IEEE Transactions on Pattern Analysis and Machine Intelligence*, 27(8), 1334-1339. doi:10.1109/TPAMI.2005.165

Wang, X., Zhang, B., Guo, Z., & Zhang, D. (2013). Facial image medical analysis system using quantitative chromatic feature. *Expert Systems with Applications*, 40(9), 3738-3746. doi://doi.org/10.1016/j.eswa.2012.12.079

Willemsen, A. T. M., Van Alste, J. A., & Boom, H. (1990). Real-time gait assessment utilizing a new way of accelerometry. *Journal of Biomechanics*, 23(8), 859-863.

Williams, T. L. (2009). *Thermal imaging cameras characteristics and performance*. Boca Raton: CRC Press.

Williston, K. (2009). *Digital signal processing*. Burlington, MA : Oxford: Newnes.

Woodford, C. (2018). Accelerometers. Retrieved from <https://www.explainthatstuff.com/accelerometers.html>

Woods, A. (2004). Arthritis. *Nursing*, 34(8), 54-55. Retrieved from <http://web.a.ebscohost.com/hallam.idm.oclc.org/ehost/pdfviewer/pdfviewer?vid=4&sid=98a8af13-4a14-4f99-8382-2ae67f8a7562%40sessionmgr4009>

Yang, C., & Hsu, Y. (2010). A review of accelerometry-based wearable motion detectors for physical activity monitoring. *Sensors*, 10(8), 7772-7788. doi:[10.3390/s100807772](https://doi.org/10.3390/s100807772)

Yasaswi, V., Keerthi, S., Jainab Begum, S., Krishna Sravan, Y., & Sridhar, B. (2015). Infrared thermal image segmentation for fault detection in electrical circuits using watershed algorithm. *International Journal of Engineering Trends and Technology (IJETT)*, 21(9), 423-429. doi:10.14445/22315381/IJETT-V21P282

Yeoh, W., Pek, I., Yong, Y., Chen, X., & Waluyo, A. B. (2008). Ambulatory monitoring of human posture and walking speed using wearable accelerometer sensors. Paper presented at the *30th Annual International Conference of the IEEE Engineering in Medicine and Biology Society, 2008. EMBS 2008*. 5184-5187. doi:10.1109/IEMBS.2008.4650382

Zhang, B., Wang, X., You, J., & Zhang, D. (2013). Tongue color analysis for medical application. *Evidence-Based Complementary and Alternative Medicine, 2013* <https://doi.org/10.1155/2013/264742>.

Zhang, J., Su, Y., Shi, Q., & Qiu, A. (2015). Microelectromechanical resonant accelerometer designed with a high sensitivity. *Sensors, 15*(12), 30293-30310. doi:10.3390/s151229803

Appendix 1: Sheffield Hallam University ethical approval



HARRIET NWAIZU [REDACTED]@my.shu.ac.uk>

RE: Ethics application from Harriet Nwaizu.

Saatchi, Reza [REDACTED]@exchange.shu.ac.uk>
To: "Uchenna, Harriet" [REDACTED]@my.shu.ac.uk>

6 April 2017 at 12:09

[REDACTED]

[REDACTED]

[REDACTED]

[REDACTED]

[REDACTED]

[REDACTED]

[REDACTED]

From: Rodrigues, Marcos
Sent: 06 April 2017 11:26
To: Saatchi, Reza
Cc: Rodrigues, Marcos; ! ACES Research Ethics Committee (FREC)
Subject: Re: Ethics application from Harriet Nwaizu.

Hi Reza,

I have had the opportunity to review all documents submitted by Harriet. It is a well put together application (both accelerometer and thermal imaging) with all required information in place including required NHS ethical approvals. It is my view that all data protection and ethical issues have been properly addressed and thus, the application is approved under Chair's action.

Andrea, would you please archive the received documents. Thank you.

Kind regards,

Marcos Rodrigues
FREC Joint Chair

 winmail.dat
12K

Appendix 2: NHS ethical approval



Health Research Authority

Dr Daniel P Hawley
Consultant Paediatric Rheumatologist
Sheffield Children's NHS Foundation Trust
Dept Paediatric Rheumatology
Sheffield Children's Hospital
Western Bank
S10 2TH

Email: hra.approval@nhs.net

30 January 2017

Dear Dr Hawley

Letter of HRA Approval

Study title:	Proof-of-concept study of an accelerometer device in children with active knee arthritis to describe joint movement.
IRAS project ID:	201610
REC reference:	16/YH/0347
Sponsor	Sheffield Children's NHS Foundation Trust

I am pleased to confirm that HRA Approval has been given for the above referenced study, on the basis described in the application form, protocol, supporting documentation and any clarifications noted in this letter.

Participation of NHS Organisations in England

The sponsor should now provide a copy of this letter to all participating NHS organisations in England.

Appendix B provides important information for sponsors and participating NHS organisations in England for arranging and confirming capacity and capability. Please read *Appendix B* carefully, in particular the following sections:

- *Participating NHS organisations in England* – this clarifies the types of participating organisations in the study and whether or not all organisations will be undertaking the same activities
- *Confirmation of capacity and capability* - this confirms whether or not each type of participating NHS organisation in England is expected to give formal confirmation of capacity and capability. Where formal confirmation is not expected, the section also provides details on the time limit given to participating organisations to opt out of the study, or request additional time, before their participation is assumed.
- *Allocation of responsibilities and rights are agreed and documented (4.1 of HRA assessment criteria)* - this provides detail on the form of agreement to be used in the study to confirm capacity and capability, where applicable.

Further information on funding, HR processes, and compliance with HRA criteria and standards is also provided.

It is critical that you involve both the research management function (e.g. R&D office) supporting each organisation and the local research team (where there is one) in setting up your study. Contact details and further information about working with the research management function for each organisation can be accessed from www.hra.nhs.uk/hra-approval.

Appendices

The HRA Approval letter contains the following appendices:

- A – List of documents reviewed during HRA assessment
- B – Summary of HRA assessment

After HRA Approval

The document "*After Ethical Review – guidance for sponsors and investigators*", issued with your REC favourable opinion, gives detailed guidance on reporting expectations for studies, including:

- Registration of research
- Notifying amendments
- Notifying the end of the study

The HRA website also provides guidance on these topics, and is updated in the light of changes in reporting expectations or procedures.

In addition to the guidance in the above, please note the following:

- HRA Approval applies for the duration of your REC favourable opinion, unless otherwise notified in writing by the HRA.
- Substantial amendments should be submitted directly to the Research Ethics Committee, as detailed in the *After Ethical Review* document. Non-substantial amendments should be submitted for review by the HRA using the form provided on the [HRA website](http://www.hra.nhs.uk), and emailed to hra.amendments@nhs.net.
- The HRA will categorise amendments (substantial and non-substantial) and issue confirmation of continued HRA Approval. Further details can be found on the [HRA website](http://www.hra.nhs.uk).

Scope

HRA Approval provides an approval for research involving patients or staff in NHS organisations in England.

If your study involves NHS organisations in other countries in the UK, please contact the relevant national coordinating functions for support and advice. Further information can be found at <http://www.hra.nhs.uk/resources/applying-for-reviews/nhs-hsc-rd-review/>.

If there are participating non-NHS organisations, local agreement should be obtained in accordance with the procedures of the local participating non-NHS organisation.

User Feedback

IRAS project ID	201610
-----------------	--------

The Health Research Authority is continually striving to provide a high quality service to all applicants and sponsors. You are invited to give your view of the service you have received and the application procedure. If you wish to make your views known please email the HRA at hra.approval@nhs.net. Additionally, one of our staff would be happy to call and discuss your experience of HRA Approval.

HRA Training

We are pleased to welcome researchers and research management staff at our training days – see details at <http://www.hra.nhs.uk/hra-training/>

Your IRAS project ID is 201610. Please quote this on all correspondence.

Yours sincerely

Thomas Fairman
HRA Assessor

Email: hra.approval@nhs.net

*Copy to: Ms Wendy Swann , Sheffield Children's NHS Foundation Trust,
(Sponsor Contact and Lead NHS R&D Contact)*

Appendix 3: Research Passport



D Floor Stephenson Wing
Sheffield Children's NHS Foundation Trust
Western Bank, Sheffield S10 2TH

Tel: 0114 226 7846 Fax: 0114 226 7844

www.sheffieldchildrenscrf.nhs.uk

26th November 2015

Dear Harriet Uchenna Nwaizu

Letter of access for research

As an existing NHS employee you do not require an additional honorary research contract with this NHS organisation. We are satisfied that the research activities that you will undertake in this NHS organisation are commensurate with the activities you undertake for your employer. Your employer is fully responsible for ensuring such checks as are necessary have been carried out. Your employer has confirmed in writing to this NHS organisation that the necessary pre-engagement check are in place in accordance with the role you plan to carry out in this organisation. This letter confirms your right of access to conduct research through Sheffield Children's NHS Foundation Trust for the purpose and on the terms and conditions set out below. This right of access commences on 26th November 2015 and ends on 5th May 2018 unless terminated earlier in accordance with the clauses below.

You have a right of access to conduct such research as confirmed in writing in the letter of permission for research from this NHS organisation. Please note that you cannot start the research until the Principal Investigator for the research project has received a letter from us giving permission to conduct the project.

You are considered to be a legal visitor to Sheffield Children's NHS Foundation Trust premises. You are not entitled to any form of payment or access to other benefits provided by this organisation to employees and this letter does not give rise to any other relationship between you and this NHS organisation, in particular that of an employee.

While undertaking research through Sheffield Children's NHS Foundation Trust, you will remain accountable to your place of study Sheffield Hallam University but you are required to follow the reasonable instructions of your nominated manager Professor Derek Burke in this NHS organisation or those given on his behalf in relation to the terms of this right of access.

Where any third party claim is made, whether or not legal proceedings are issued, arising out of or in connection with your right of access, you are required to co-operate fully with any investigation by this NHS organisation in connection with any such claim and to give all such assistance as may reasonably be required regarding the conduct of any legal proceedings.

You must act in accordance with Sheffield Children's NHS Foundation Trust policies and procedures, which are available to you upon request, and the Research Governance Framework.

You are required to co-operate with Sheffield Children's NHS Foundation Trust in discharging its duties under the Health and Safety at Work etc Act 1974 and other health and safety legislation and to take reasonable care for the health and safety of yourself and others while on Sheffield Children's NHS Foundation Trust premises. Although you are not a contract holder, you must observe the same standards of care and propriety in

dealing with patients, staff, visitors, equipment and premises as is expected of a contract holder and you must act appropriately, responsibly and professionally at all times.

If you have a physical or mental health condition or disability which may affect your research role and which might require special adjustments to your role, if you have not already done so, you must notify your employer and the Trust (Dr. Gillian Gatenby-Research Directorate Manager) prior to commencing your research role at the Trust.

You are required to ensure that all information regarding patients or staff remains secure and *strictly confidential* at all times. You must ensure that you understand and comply with the requirements of the NHS Confidentiality Code of Practice (<http://www.dh.gov.uk/assetRoot/04/06/92/54/04069254.pdf>) and the Data Protection Act 1998. Furthermore you should be aware that under the Act, unauthorised disclosure of information is an offence and such disclosures may lead to prosecution.

Sheffield Children's NHS Foundation Trust will not indemnify you against any liability incurred as a result of any breach of confidentiality or breach of the Data Protection Act 1998. Any breach of the Data Protection Act 1998 may result in legal action against you and/or your substantive employer.

You should ensure that, where you are issued with an identity or security card, a bleep number, email or library account, keys or protective clothing, these are returned upon termination of this arrangement. Please also ensure that while on the premises you wear your ID badge at all times, or are able to prove your identity if challenged. Please note that this NHS organisation accepts no responsibility for damage to or loss of personal property.

We may terminate your right to attend at any time either by giving seven days' written notice to you or immediately without any notice if you are in breach of any of the terms or conditions described in this letter or if you commit any act that we reasonably consider to amount to serious misconduct or to be disruptive and/or prejudicial to the interests and/or business of this NHS organisation or if you are convicted of any criminal offence. You must not undertake regulated activity if you are barred from such work. If you are barred from working with adults or children this letter of access is immediately terminated. Your employer will immediately withdraw you from undertaking this or any other regulated activity and you MUST stop undertaking any regulated activity immediately. Your substantive employer is responsible for your conduct during this research project and may in the circumstances described above instigate disciplinary action against you.

If your circumstances change in relation to your health, criminal record, professional registration or suitability to work with adults or children, or any other aspect that may impact on your suitability to conduct research, or your role in research changes, you must inform the NHS organisation that employs you through its normal procedures. You must also inform your nominated manager in this NHS organisation.

Yours sincerely



Wendy Swann
R&D Manager, Sheffield Children's NHS Foundation Trust

cc: HR department at Sheffield Children's NHS Foundation Trust
HR department of the substantive employer (and provider of honorary clinical contract, where applicable)

Appendix 4: Introduction to Good Clinical Practice eLearning (Secondary Care)



CERTIFICATE of ACHIEVEMENT

This is to certify that

Harriet Nwaizu

has completed the course

Introduction to Good Clinical Practice eLearning (Secondary
Care)

March 16, 2017

Modules completed:

Introduction to Research in the NHS
Good Clinical Practice and Standards in Research
Study Set Up and Responsibilities
The Process of Informed Consent
Data Collection and Documentation
Safety Reporting

This course is worth 4 CPD credits



National Institute for
Health Research
Clinical Research Network

Appendix 5: Informed consent in paediatric research

CERTIFICATE of ACHIEVEMENT

This is to certify that

Harriet Nwaizu

has completed the course

Informed Consent in Paediatric Research

March 15, 2017

This course is worth 1 CPD credit



National Institute for
Health Research
Clinical Research Network

Appendix 6: Information sheet for children aged 4 to 11 years (Thermal Imaging)



PARTICIPANT INFORMATION SHEET FOR CHILDREN

To be shown and read by parent/carer if required

Study title:
ThermRheum

1. What is research?

Research is a careful experiment to find out the answer to an important question.

2. Why is this research being done?

We want to try and find out if our new test can determine whether your joints are inflamed or not so that in future we can diagnose arthritis earlier and use fewer scans and blood tests when this happens.



3. Why me?

You have been chosen because you may have arthritis. You can help us find some answers that will help us improve the way we identify if arthritis is active or not. We are asking between 20 children in total.



4. Do I have to take part?

No you do not! It is up to you. We would like you to read this information sheet. If you agree to take part, we would like you to write your name on two forms. We will also ask your parent or carer to write their name on the forms and give one back to us. You can still change your mind later. If you don't want to take part, just say no!



5. What will happen?

When you come into hospital for your joints to be examined the doctors will examine your joints as they normally do.

Then you will be asked if you want to take part in this study. If you are happy to, pictures of your knees and ankles will be taken by a camera that can see how warm they are. The camera will also take a short video of your joints to check skin colour as inflammation can make your skin go red. This takes a few minutes. You can see these pictures yourself if you want to.

Your parent or carer will be with you all the time and you will be asked to complete a short questionnaire after the study.

6. Will joining in help me?

No, but it may help us to know more about joint inflammation in the future.

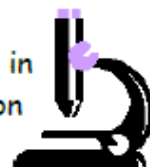


7. What else might happen?

The people doing the research may be in the room when taking the images of your joints. If you don't like this, we will not carry on.

8. What happens when the research study stops?

We will collect all the information and see if it is useful in telling us if the doctors can manage joint inflammation problems better in the future.



9. What if something goes wrong?

We do not think anything will go wrong, but if it does your parent or carer will be able to talk to someone who will be able to tell them what they need to do about it.

10. What if I don't want to do the research anymore?

Just tell your parent or carer, doctor or nurse at any time. They will not be cross with you. You will still have the same care whilst you are at hospital.

11. What if I want to complain about the study?

If you want to complain you or your parent or carer, can talk to Dr Dan Hawley at this hospital.



12. Will anyone else know I'm doing this?

The people in our research team will know you are taking part. The doctor looking after you while you are in hospital will also know. No one else will know because we will not use your name or address. You will get a special number that will be used instead.

13. What happens to what the researchers find out?

When we collect your information we will make sure it is kept in a safe place and only the people doing the research study can look at it.



We will use the information to help doctors learn how to find joint inflammation more easily, and we will publish our findings in magazines and on websites that doctors read.

A short summary will also be on the hospital's research website but your information will not be identified.

14. Did anyone else check the study is OK to do?

This study has been checked by several people, to make sure it is alright.

15. How can I find out more about this study?

Your parent or carer, or the doctors and nurses looking after you can also help you find out more about the study.



Thank you for taking the time to read this - please ask any questions if you need to.

Appendix 7: Information sheet for young persons aged 12 to 16 years (Thermal Imaging)



PARTICIPANT INFORMATION SHEET FOR YOUNG PEOPLE

Short title: ThermRheum

Part 1 – to give you first thoughts about the project

1. Invitation paragraph

We would like you to help us with our research study. Please read this information carefully and talk to your parent or carer about the study. Ask us if there is anything that is not clear or if you want to know more. Take time to decide if you want to take part. It is up to you if you want to do this. If you don't then that's fine, you'll be looked after at the hospital just the same.

2. Why are we doing this research?

We want to try and find out if Thermal Imaging is helpful in identifying if your joints are inflamed or not.



3. Why have I been asked to take part?

You have been chosen because you are already being examined for joint inflammation. We are asking 20 children and young people all together.

4. Do I have to take part?

No! It is entirely up to you. If you do decide to take part:

- You will be asked to sign a form to say that you agree to take part (an assent form)
- You will be given this information sheet and a copy of your signed assent form to keep.

You are free to stop taking part at any time during the research without giving a reason. If you decide to stop, this will not affect the care you receive whilst in hospital.



5. What will happen to me if I take part?

Your joints will be examined as usual by a doctor who will determine whether you have joint inflammation (arthritis) or not. They will record their findings for the study. You will be taken to a room where a Thermal Imaging camera attached to a computer will measure the temperature of your knee and ankle joints and also take a short video recording to record the colour of the skin over your joints. The equipment will not be in direct contact with you or cause harm. You will need to get used to the room temperature for 10 minutes and then the images will be taken (about 2 minutes). The images will be saved onto a laptop for our team to review. Therefore, this study is not part of your examination, but is to help doctors detect joint inflammation better in future.

Your treatment for joint inflammation (if found by your Doctor) will continue as normal. You will be asked to complete a questionnaire. You will go home as planned and have no further involvement in this research study.

Your parent or carer will be able to stay with you throughout the study.

6. What will I be asked to do?

You will be asked to:

- Change into shorts to allow us to see your knee and ankle joints
- Stand still facing the camera for about 1 minute while thermal images and video recordings are taken
- Stand still facing away from the camera for about 1 minute while thermal images and video recordings are taken.

You can see these images straight away after the recordings.

Research staff may be in your room for the duration of the recording. If this becomes a problem, then you can tell us and we can stop at any point.

You will not be asked to do anything else for the purposes of the research study.

7. Is there anything else to be worried about if I take part?

There is nothing else to worry about – the research tests will not be uncomfortable in any way.

8. Will the study help me?

No, but the information we get might help people with joint inflammation, including yourself in the future.

9. What happens when the research study stops?

We will collect all the images and process them to determine whether they can be used to show if joint inflammation.

10. Contact for further information

If you would like any further information about this study you could contact:

Name: Oliver Ward
Designation: Advanced Physiotherapist
Hospital/Department: Sheffield Children's Hospital
Tel: (0114) 2717227



Thank you for reading so far - if you are still interested in taking part then please go to Part 2 (overleaf).

Part 2 - more detail – information you need to know if you still want to take part.

11. What if I don't want to do the research anymore?

Just tell your parent or carer, doctor or nurse at any time. They will not be cross with you. You will still have the same care whilst you are at hospital.

12. What if there is a problem or something goes wrong?

We do not expect any problems or that anything will go wrong, but if does, tell us and we will try and sort it out for you straight away. You and your parent or carer can either contact the project co-ordinator:

Dr Dan Hawley
Consultant Rheumatologist
Sheffield Children's NHS Foundation Trust
Tel: (0114) 2717726



or you can use the normal hospital complaints procedure by contacting the following person:

Mrs Linda Towers
Patient Advice & Liaison Co-ordinator
Sheffield Children's NHS Foundation Trust
Tel: 0114 271 7594

13. Will anyone else know I'm doing this?

The people in our research team will know you are taking part. The doctor looking after you while you are in hospital will also know.

Your medical notes may also be looked at by staff working at the hospital to check that the study is being carried out correctly.

All information that is collected about you during the research will be kept strictly confidential. You will be given a unique number which will be used instead of your personal details.

ThermRheum
Participant Information Sheet Age 12-18
Version 5.0
Date 27/05/2016

Any information about you that leaves the hospital will have your name and address removed so that you cannot be recognised from it.

14. What will happen to the results of the research study?

When the study has finished we will present our findings to other doctors, and we will put the results in medical magazines and websites that doctors read.

We would also like to put a brief summary of the findings on the hospital research website so that you will be able to read about our results too. This could also go on the hospital research web site: www.sheffieldchildrens.nhs.uk/research and Sheffield Hallam University research sites. They will be anonymous, which means that you will not be identified from them.

15. Who is organising and funding the research?

The research is being organised jointly by Sheffield Hallam University and Sheffield Children's NHS Foundation Trust and funded for by the Sheffield Children's Hospital Charity.

16. Who has checked the study?

Before any research takes place it has to be checked by a Research Ethics Committee. This is a group of people who make sure that the research is safe to be carried out. This project has been approved by a Research Ethics Committee.

It has also will be checked by the Research Department at this hospital as well as the Research Ethic Committee of Sheffield Hallam University.

17. How can I find out more about research?

The Clinical Research Facility at this hospital has a section on its website <http://www.sheffieldchildrens.nhs.uk/research> or contact Dr Dan Hawley using the details above.

Thank you for taking the time to read this – please ask any questions if you need to.



Appendix 8: Information sheet for parent/guardian (Thermal Imaging)



PARENT/LEGAL GUARDIAN INFORMATION SHEET

Short title: ThermRheum

This information sheet has two parts:

Part 1: This part contains the main information, indicating the purpose of this study and what will happen to you and your child if you take part.

Part 2: This part contains additional information about the conduct of the study.

Part 1 – Introduction

1. Invitation paragraph

Your child is being invited to take part in a research study. Before you decide to participate it is important for you to understand why the research is being carried out and what it will involve. Please ask a member of the research team if there is anything that is not clear or if you would like more information. Please read the information carefully and take your time to decide whether or not you want your child to take part.

2. What is the purpose of the study?

When assessing a child for symptoms such as pain or stiffness of joints, doctors must decide whether or not there is inflammation (arthritis). Currently, the standard procedure to help doctors diagnose arthritis is to carry out an assessment (examination) of your child's musculoskeletal (bones, joints and muscles) system. Other investigations (blood tests, X-rays and scans) may help to determine if arthritis is present but have small risks and costs associated with them. Over the course of a child's journey with arthritis we are keen to minimise any risks children may be exposed to. As a technique which does not involve contact with the patient, Thermal Imaging holds promise as a tool which could aid the doctor's assessment, possibly reducing the need for further investigations, and allow the doctor to diagnose arthritis at an earlier stage.

The aim of the study is to investigate how effective Thermal Imaging is when used to look for joint inflammation of the knees and ankles. We would like to compare this new method with the examination findings of the doctor in 20 children with arthritis. Thermal Imaging does not involve any direct contact of the equipment with the child and does not involve any radiation.

3. Why has my child been chosen?

We are choosing children & young people who are attending the hospital for assessment or treatment of possible joint inflammation (arthritis) in the knees and ankles. This study will not in any way affect the quality of your child's routine treatment and the results of this study will not change their care decisions.

4. Does my child have to take part?

No. It is up to you and your child (wherever possible) to decide whether or not to take part. You are both free to withdraw from the research at any time and without giving a reason. Your decisions about this will not affect the standard of care your child will receive.

If you are happy to take part, and are satisfied with the explanations from the research team, you will be asked to sign a consent form. If your child is able to understand the research and is happy to take part and can write their name, they will be asked to sign an assent form as well. You will be given a copy of the information sheet and the signed consent/assent forms to keep for your records.

5. What will happen to my child if we agree take part?

The doctor will examine your child for signs of joint inflammation as they would do usually. The doctor will document their findings, which will form part of the research.

If you take part in the research study, you will be asked to go to a room where a Thermal Imaging camera connected to a computer will be available. Your child will need to get used to the room temperature with their knees and ankles uncovered for 10 minutes before the images are taken. Thermal images (recording the amount of heat emitted from the skin) and a short video recording (to document skin colour) will be taken of both knees and ankles. This should take about 2 minutes. The camera will not be in direct contact with your child, does not give off radiation and will not cause any harm. After this has been done, you will be asked to complete a short questionnaire seeking feedback on your experience of the procedure. This should take about 10 minutes to complete. After this, your child will have no further involvement in the research study.

You will be able to stay with your child throughout the study and the study will add approximately 30 minutes to your child's usual care procedure on this visit.

6. How the test is performed?

Your child will be asked to:

- Change into shorts (may be provided on the day if forgotten) to allow exposure of knee and ankle joints
- Stand still facing the camera with knees and ankles exposed for about 1 minute while thermal images and video recordings are taken
- Stand still facing away from the camera with knees and ankles exposed for about 1 minute while thermal images and video recordings are taken.

The images and video recordings taken will be stored anonymously on the computer. Later on, the research team will process the images to investigate whether the approach is useful to determine joint inflammation.

You will not be asked to do anything other than to reassure your child.

7. What are the possible disadvantages and risks of taking part?

Research staff may be in the room for the duration of the test. If this becomes a problem, then we will stop the test.

If at any time you or your child feels distressed or unable to continue, please don't hesitate to tell a member of the research team and the test will stop.

8. What are the possible benefits of taking part?

Your child will not benefit from taking part in this study and the results of the study will not affect his/her medical treatment. However the information we collect may help us to treat patients better in future.

9. What happens when the research study stops?

We will collect all the information together and we will decide if it is useful in the further development of this approach for detecting arthritis.

10. What if there is a problem?

Any complaint about the way you or your child has been dealt with during the study will be addressed. The detailed information on this is given in Part 2.

11. Will my child's taking part in the research project be kept confidential?

Yes. We will follow ethical and legal practice and all information about your child will be handled in confidence. The details are included in Part 2.

12. Contact for further information

If you would like any further information about this study you could contact:

*Oliver Ward
Advanced Physiotherapist
Sheffield Children's Hospital
Tel: 0114 271 7227*

This completes Part 1 of the Information Sheet.

If the information in Part 1 has interested you and you are considering participation, please continue to read the additional information in Part 2 before making any decision.

Part 2 - Additional Information

13. What will happen if we don't want to carry on with the research?

If you withdraw from the study, we will destroy all of your child's identifiable data relating to the study if you wish, but we will need to use the data collected up to their withdrawal.

14. What if there is a problem?

Complaints

If you have any reason to complain about any aspect of the way in which you or your child has been approached or treated during the course of this study, the normal National Health Service complaints mechanisms are available to you and are not compromised in any way because you have taken part in a research study. If you have any complaints or concerns please contact either the project co-ordinator:

*Dr Dan Hawley
Consultant Rheumatologist
Sheffield Children's NHS Foundation Trust
Tel: 0114 271 7726*

or you can use the normal hospital complaints procedure and contact the following person:

*Mrs Linda Towers
Patient Advice & Liaison Co-ordinator
Sheffield Children's NHS Foundation Trust
Tel: 0114 271 7594*

15. Harm

In the unlikely event that taking part in this research project harms your child there is no special compensation arrangement. If your child is harmed due to someone else's fault, then you may have grounds for legal action.

16. Will taking part in this study be kept confidential?

All information collected about your child during the course of the research will be kept strictly confidential. Any information about your child which leaves the hospital will have their name and address removed so that your child cannot be identified from it. Once the study is complete all information will be kept for 5 years in a secure location and then destroyed in accordance with standard operating procedures.

Our procedures for handling, processing, storage and destruction of data are compliant with the Data Protection Act 1998.

The Thermal Imaging videos will be stored on a computer. The data will be coded and only authorised people involved in the research study will have access.

Your child's medical notes may also be looked at by other staff within the hospital involved in the running and supervision of the study to check that it is being carried out correctly.

ThermRheum
Parent/Legal Guardian Information Sheet
Version 5.0
Date 27/05/2016

Page 4 of 5

17. What will happen to the results of the research study?

When the study has finished we hope to present our findings to other doctors and health professionals at professional events, and we may put the results in medical magazines and websites that doctors read. We would also like to put a brief summary on the hospital research website so that you will be able to read about our results too. This will be available at the end of the study, on www.sheffieldchildrens.nhs.uk/research. The results may also be included as part of a PhD student's and a BMedSci student's educational qualification. Although your child's identity will not be recognised from published results we will seek your separate consent to use images in any publications or presentations.

18. Who is organising and funding the research?

The research is being organised by Sheffield Children's NHS Foundation Trust and funded by the Sheffield Children's Hospital Charity.

19. Who has reviewed the study?

This study was given a favourable ethical opinion for conduct in the NHS by the Research Ethics Committee. It has also been approved by the Research Department at this hospital as well as by Sheffield Hallam University Ethics Committee.

20. How can we find out more about research?

The Clinical Research Facility at this hospital has a section on its website www.sheffieldchildrens.nhs.uk/research

If you and your child decide to take part in this study, you will be given this information sheet and signed consent and assent forms to keep.

Thank you for taking the time to read this information sheet.

Appendix 9: Information sheet for children below 10 years (Accelerometry)

Sheffield Children's 
NHS Foundation Trust



PARTICIPANT INFORMATION SHEET FOR CHILDREN AGE BELOW 10

To be read by the child or shown and read by parent/carer if the child is unable to read.

Simplified study title: Can a movement monitor help with arthritis detection?

1. What is research?

Research is trying to find out the answer to an important question.



2. What is arthritis?

Arthritis is when joints in the body (like the knee for example) become painful and swell up because of inflammation. Doctors watch joints moving to try and work out if a joint has arthritis or not.

3. Why is this study being done?

We are trying to find new ways to help Doctors know someone has arthritis or not. Movement monitors have been used to work out how much activity people do. This research will help Doctors know if movement monitors can show how leg movements change when someone has arthritis.



4. What happens during the tests?



Two soft elastic bands containing small movement detectors (shown in the picture) are gently placed above and below each knee. They should not hurt you. You will be asked to gently move your legs while either sitting on a chair or lying down. This takes about one minute but you can stop any time.

While the elastic bands are still attached, you will be asked walk in the examination room for about one minute. Again, you can stop anytime. After these two tests, the elastic bands are gently removed and you will be asked few questions about how comfortable the test was.

5. Who will be with me during the test?

The movement recording will be done by a member of research team. Your Mum, Dad or Carer who came with you today will be with you at all times.

6. Why me?

You have been chosen to take part in the study because you have arthritis and may be able to help us do this research.

7. Do I have to take part in the study?

No you do not! It is up to you. We would like you to read this information sheet or ask your Mum, Dad or Carer to read it to you. If you agree to take part, please write your name on the two forms called consent forms. You can still change your mind later. If you don't want to take part, just say no!



Children Participant Information Sheet Version 2, 6th September 2016
IRAS ID: 201610



8. Will joining in help me?

No, but by helping Doctors understand arthritis better it may help other children with arthritis in the future.

9. What happens when the research study stops?

We will carefully look at all information collected by this research to help know whether movement monitors might help Doctors understand arthritis better.



10. What if something goes wrong?

We do not think that anything will go wrong. If it does, please tell your Mum, Dad or Carer. They will be able to talk to the doctor that is looking after you at the hospital. His name is Dr Daniel Hawley.

11. What if I don't want to do the research anymore?

Just tell your Mum, Dad, Carer, doctor or nurse at any time. They will not be cross with you. You will still have the same care whilst you are at hospital.

12. Will anyone else know I'm doing this?

The people in our research team will know you are taking part. No one else will know because we will not use your name or address. You will get a number that will be used instead.



13. What happens to what the researchers find out?

We will use the information to find ways to help doctors examine body joints and put the results in magazines and on websites.

14. Did anyone else check the study is OK to do?

Several people have checked this study, and have said it is alright.



15. How can I find out more about this study?

Your Mum, Dad, Carer or other grownup you trust may be able to answer your questions. The doctors and nurses looking after you can also help you find out more about the study.



Thank you for taking the time to read this - please ask any questions if you need to.

Appendix 10: Information sheet for children aged 10 years and above (Accelerometry)



PARTICIPANT INFORMATION SHEET FOR CHILDREN: AGE 10 & ABOVE

To be read by the child or shown and read by parent/carer if child is unable to read.

Study title: Can a movement monitor device help with arthritis detection?

1. What is research?

Research is a careful study to find out the answer to an important question.

2. What is arthritis?

Arthritis is as a kind of joint inflammation. Recent work has shown its early detection improves its treatment. Currently its detection and monitoring are largely by visual examinations. The symptoms can sometimes be hard to detect and therefore better ways to aid detection of joint inflammations are very useful.

3. Why is this study being done?

We would like to develop new tools to improve detection and assessment arthritis. Once developed, the tools may be useful for doctors who examine patients with arthritis as they may improve the accuracy of the related examinations. The movement monitor we are using is called an accelerometer. It measures changes in speed when your legs are moving. This information can help us understand how arthritis changes the way joints (in this case the knee joint) move. Accelerometers have been used in the past to measure how much activity people do generally, but not exactly how particular joints move when they are affected by arthritis.

4. What happens during the tests?

Two soft elastic bands are gently placed around the upper and lower parts of each knee. They will not be too tight to cause discomfort. Each band contains a small movement monitor called an accelerometer that is connected to a computer. The units are fully contained in a purpose built casing so they will not make any contact with your body.

You will initially gently move your legs by sitting on a chair or lying down. This could take about 1 minute but you can stop any time if you felt further movement is causing discomfort or is tiring.

Then while the elastic bands are still attached, you will be asked to walk in the examination room for about 1 minute. Again, you can stop anytime if you felt further walking is causing discomfort or is tiring.

The movement information from these two tests is recorded by a computer and is processed later. After these two tests, the elastic bands are gently removed. There is a questionnaire to seek your view of the test, e.g. how comfortable the test was.

5. Who will be with me during the test?

The data recording will be done by a member of study team. Your Mum, Dad or carer who came with you today will be with you at all times. Taking part in this study does not include having any injections or blood tests. You can eat and drink anything you like as long as this is okay with your doctors and with your Mum, Dad or other carer.

6. Why me?

You have been referred to the hospital for a doctor to examine your joints. Your doctor has studied your medical records to ensure your joints' movement information will assist the study. We will be asking 10 children to take part in the study.

Accelerometry as a Method for Arthritis Assessment in Children 10 years & older
Children Participant Information Sheet Version 2, 8th September 2016
IRAS ID: 201610



7. Do I have to take part in the study?

No you do not! If you agree to take part, we would like you to write your name on two forms called consent forms. We will also ask your Mum, Dad or Carer to write their name on the forms and give a copy back to us. You can still change your mind later. If you don't want to take part, just say no!

8. Will joining in help me?

No, but it may help other children in the future, as it could give doctors a useful tool for examining joints for arthritis.



9. What else might happen?

Nothing else will happen.

10. What happens when the research study stops?

We will collect all the information and we will decide if it is useful in helping doctors better examine joints for detecting and monitoring arthritis.



11. What if something goes wrong?

We do not think that anything will go wrong. If it does, your Mum, Dad or Carer will be able to talk to the doctor named in section 12.

12. What if I don't want to do the research anymore?

Just tell your Mum, Dad, Carer, doctor or nurse at any time. They will not be cross with you. You will still have the same care whilst you are at hospital.

13. What if I wish to complain about the study?

If you want to complain, you or your Mum, Dad or Carer can talk to Dr Daniel Hawley at this hospital is leading this study.

14. Will anyone else know I'm doing this?

The people in our research team will know you are taking part. This includes the doctor looking after you while you are in the hospital. No one else will know because we will not use your name or address. You will get a number that will be used instead.

15. What happens to what the researchers find out?

When we collect your information we will make sure it is stored in a safe place and only the people doing the research study can look at it. We will use the information to find ways to help doctors examine body joints for arthritis, put the results in magazines and on websites.

A short summary will also be on the hospital's and Sheffield Hallam University websites. No-one will know you were in the study.

16. Did anyone else check the study is OK to do?

Several people have checked this study, and have said it is alright.



17. How can I find out more about this study?

Your mum, dad, carer or other grownup you trust may be able to answer your questions. The (doctors and nurses) looking after you can also help you find out more about the study.



Thank you for taking the time to read this information sheet.

Please ask any questions if you need to.

Appendix 11: Information sheet for parent/carer (Accelerometry)



PARTICIPANT INFORMATION SHEET FOR PARENT/CARER

Study title: Accelerometry as a Method for Arthritis Assessment in Children

Your child/young person is invited to take part in a research study. It is important for you to understand why the research is being done and what it will involve before deciding whether you will participate in the study. Please read this information sheet and talk to others about the study if you wish. Details of the contact persons are included in sections 1.10, 2.2 and 2.9. Please feel free to ask any questions you may have or if you would like more information. The information sheet has two parts.

- Part 1 explains the purpose of this study and its participation issues.
- Part 2 explains the conduct of the study.

Part 1 – Study's Purpose and Participation Issues

1.1 What is the purpose of the study?

The aim of this preliminary study is to explore whether computerised monitoring of leg movements using devices called accelerometers can assist in detection and monitoring of *Juvenile idiopathic arthritis (JIA)*.

Currently, diagnosis and monitoring of joint inflammation (arthritis) relies largely on examination by doctors. Examination findings may however be subtle in the early course of inflammation flares therefore further tools which can aid detection of joint inflammation are highly desirable.

An accelerometer is a very light-weight, small and safe device that already has well-established applications in industry. Once attached to a person, it measures movement information in three perpendicular directions. An accelerometer placed on a limb and connected to a computer enables limb movement information to be displayed as signals that are stored for later analysis. These resulting numeric data may assist clinicians to better detect and monitor JIA.

1.2 Why has my child/young person been chosen?

Your child/young person has been chosen to take part in the study because he/she has been referred to the hospital for a doctor to examine his/her joints. The doctor has already studied the related medical records to ensure your child/young person's joints' movement information will assist the study. We are asking 10 to 30 children to take part.

1.3 Does my child/young person have to take part?

No. It is up to you and your child/young person to decide whether or not to take part. You are free to withdraw from the research at any time and without giving a reason. Your decisions about this will not affect the standard of care your child/young person will receive.

If you are happy for your child/young person to participate, and are satisfied with the explanations from the research team, you will be asked to sign a consent form. You will be given a copy of the information sheet and the signed consent form to keep.

1.4 What will happen to my child/young person if we agree take part?

If you decide to take part, the tests will be performed and completed today. As soon as they have been performed, you will both be free to leave the hospital – as long as your child's/young person's doctor has discharged him/her. The tests will involve recording movement data from the leg joints using accelerometers. Accelerometers are small safe devices for measuring movements.

To perform the tests, a few (typically two) soft elastic bands are gently placed around the upper and lower parts of each knee. These will not be fastened too tight to cause any discomfort. Each band contains an accelerometer. The accelerometer is fully contained in a purpose built casing so it will not make any direct contact with your skin or cloths. The set-up is safe and does not pose any danger.

Your child/young person will initially sit on a chair or lay down and will be asked to gently move his/her legs. This data recording could take about 1 minute but the movements can be stopped any time if or when it is felt further movement is causing discomfort or is tiring for the child.

While the elastic bands are still attached, the child/young person will then be asked to walk in the examination room for about 1 minute. Again, this will be stopped anytime during the walking if it causes discomfort or is tiring for the child/young person.

The movement information from these two tests is recorded on a computer for later analysis and interpretation.

After these two tests, the elastic bands are gently removed.

There is a questionnaire to seek your view and your child/young person's view of the procedure (eg. How comfortable the procedure was).

1.5 What are the possible disadvantages and risks of taking part?

There are no known risks from taking part; you may however delay your stay in the hospital by up to 30 minutes.

1.6 What are the possible benefits of taking part?

There will be no benefits to you or to your child/young person, however in the future we may be able to use the developed tools to better detect and monitor JIA.

1.7 What happens when the research study stops?

Once we have collected all the data from all participants, it will be analysed and interpreted to determine whether accelerometers are useful in detecting and monitoring JIA. We are interested to explore whether JIA can be detected earlier with the developed tools.

1.8 What if there is a problem?

We do not anticipate any problems. However, any complaint about the way you have been dealt with during the study or any possible harm your child/young person might suffer will be addressed. The information on related processes is provided in Part 2.

1.9 Will my child's/young person's taking part in the research project be kept confidential?

Yes. We will follow ethical and legal practice and all information about your child/young person will be handled in confidence. The details are included in Part 2.

1.10 Contact for further information

If you would like any further information about this study you can contact:

Dr Daniel Hawley

Address – Rheumatology Department

Sheffield Children's Hospital, S10 2TH

Telephone – 0114 271 7726

Email - Daniel.Hawley@sch.nhs.uk

If the information in Part 1 has interested you and you are considering your child's/young person's participation, please continue to read the additional information in Part 2 before making any decision.

Part 2 - Study's Conduct

2.1 What will happen if we don't want to carry on with the study?

You can withdraw from the study any time during the data recording. Thereafter we will do our best to withdraw you if you so wish but please note study's results are intended to be published and once published their withdrawal may not be feasible.

2.2 What if there is a problem?

If you have a cause for complain about an aspect of the way in which you have been approached or treated during the course of this study, the normal National Health Service complaints mechanisms are available to you and are not compromised in any way because you have taken part in a research study. If you have any complaints or concerns please contact either the project lead:

Dr Daniel Hawley
Address – Rheumatology Department
Sheffield Children's Hospital, S10 2TH
Telephone – 0114 271 7726
Email - Daniel.Hawley@sch.nhs.uk

Or you can use the normal hospital complaints procedure and contact the following person:

Mrs Julie Mather
Patient Advice & Liaison Co-ordinator
Sheffield Children's NHS Foundation Trust
Telephone – 0114 271 7594

2.3 Will taking part in this study be kept confidential?

All information collected about your child/young person during the course of the research will be kept strictly confidential. Once the study is complete all information will be kept for five years and then destroyed.

Our procedures for handling, processing, storage and destruction of data are compliant with the Data Protection Act 1998.

Data collected during the study may be transferred for the purpose of (processing, analysis, etc.) to associated researchers within/outside the European Economic Area. Some countries outside Europe may not have laws to protect your privacy to the same extent as the Data Protection Act in the UK or European Law. Sheffield Children's NHS Foundation Trust will take all reasonable steps to protect your privacy.

Other people who work at the hospital may also look at your medical notes to check that the study is being carried out correctly.

2.4 What will happen to any samples my child/young person gives?

No samples will be collected.

2.5 Will any genetic tests be done?

No genetic tests will be performed.

2.6 What will happen to the results of the research study?

We will present our findings to other doctors and engineers, and we will put the results in magazines and websites that doctors and engineers read. We would also like to put a brief summary on the hospital and Sheffield Hallam University (partner in this study) research websites so that you and your child/young person will also be able to read about our results. The results will also be included as part of a PhD student's (Mrs Harriet Nwaizu) educational qualification; Mrs Harriet Nwaizu is currently registered with Sheffield Hallam University. Results will be anonymous, which means that your child/young person will not be able to be identified from them in any publication or report.

2.7 Who is organising and funding the research?

The research is being organised by Sheffield Children's NHS Foundation Trust. The PhD student involved is self-funded and is registered at Sheffield Hallam University. She is jointly supervised by staff from both the hospital and university.

2.8 Who has reviewed the study?

This study was given a favourable ethical opinion for conduct in the NHS Research Ethics Committee and Sheffield Hallam University Research Committee. It has also been approved by the Research Department at this hospital.

2.9 How can I find out more about research?

The Clinical Research Facility at this hospital has **Information for Families** section on its website www.sheffieldchildrens.nhs.uk/research-and-innovation.htm or you can contact the hospital Clinical Research Facility:

Mrs Wendy Swann
Research & Development Manager
Sheffield Children's NHS Foundation Trust
Tel: 0114 271 7417

If you decide to take part in this study, you will be given this information sheet and signed consent form to keep.

**Thank you for taking the time
to read this information sheet**

Please feel free to ask any question about the study.

Appendix 12: Assent form for children & young people (Thermal Imaging)



Participant identification number:

ASSENT FORM FOR CHILDREN & YOUNG PEOPLE (to be completed by the child/young person and their parent/carer)

Short title: ThermRheum

Child (or if unable, parent on their behalf)/young person to circle all they agree with:

Have you read (or had information read to you) about this project? Yes / No

Has somebody else explained this project to you? Yes / No

Do you understand what this project is about and that videos will be taken of your knees and ankles? Yes / No

Have you asked all the questions you want to ask? Yes / No

Have you had your questions answered in a way that you understand? Yes / No

Do you understand that it is OK to stop taking part at any time? Yes / No

Are you happy to take part? Yes / No

If any answers are 'No' or you don't want to take part, don't sign your name!

If you do want to take part, please write your name and today's date:

Your name _____ Date _____

Your parent or carer must write their name here too if they are happy for you to do the project

Name of Parent/Carer Date Signature

The medical staff and a member of the research team who explained this project to you needs to sign too:

Name of medical staff Date Signature

Authorised Researcher Date Signature

Thank you for your help.

1 copy for participant; 1 copy for researcher; 1 copy to be kept with hospital notes

Appendix 13: Consent form for parent/guardian (Thermal Imaging)



Patient identification number:

PARENT/LEGAL GUARDIAN CONSENT FORM

Title of project: ThermRheum

Names of researchers: Dr Shammi Ramlakhan (Principal Investigator), Dr Dan Hawley, Dr Reza Saatchi, Oliver Ward.

Please initial box

1. I confirm that I have read and understand the information sheet dated 27/05/2016 (version 5.0) for the above study and have had the opportunity to ask questions.
2. I understand that my child's participation is voluntary and that I am free to withdraw my child at any time, without giving any reason, without my child's medical care or legal rights being affected.
3. I understand that sections of any of my child's clinical record may be looked at by authorised researchers and those involved in the running and supervision of the study from Sheffield Children's NHS Foundation Trust where it is relevant to my child taking part in research. I give permission for Sheffield Children's NHS Foundation Trust staff to have access to my child's records.
4. I understand that as part of my child's involvement in the study, they will have short videos taken of their knee and ankle joints. The images/videos taken will be completely anonymised and a still image copy may be provided if required on the day that they are taken.
5. I understand that any images/videos taken of my child's joints may be anonymously reproduced at a later date in medical publications, presentations or press releases.
6. I agree to my child taking part in the above study.

Name of Parent/Guardian Date Signature

Name of medical staff taking consent Date Signature

Authorised Researcher Date Signature

1 copy for parent; 1 copy for researcher; 1 copy to be kept with hospital notes

Appendix 14: Assent form for children & young people (Accelerometry)



ASSENT FORM FOR CHILDREN

(To be completed by the child/young person and their parent/carer)

Simplified Project Title: Can a movement monitor help with arthritis detection?

Participant study number:

Names of researchers: Dr Daniel Hawley, Dr Reza Saatchi, Professor Derek Burke, Ms Harriet Nwaizu

Child (or if unable, parent on their behalf) / young person to circle all they agree with please:

- | | |
|---|----------|
| Have you read about this project? | Yes / No |
| Has somebody else explained this project to you? | Yes / No |
| Do you understand what this project is about? | Yes / No |
| Have you asked all the questions you want? | Yes / No |
| Have you had your questions answered in a way you understand? | Yes / No |
| Do you understand it is OK to stop taking part at any time? | Yes / No |
| Are you happy to take part? | Yes / No |

If any answers are 'No' or you don't want to take part, don't sign your name!

If you do want to take part, please write your name and today's date.

Your name _____ Date _____

Your parent or carer must write their name here too if they are happy for you to do the project

Name of Parent/Carer Date Signature

The person who explained this project to you needs to sign too:

Name of Researcher Date Signature

Thank you for your help.

1 copy for participant; 1 copy for researcher; 1 copy to be kept with hospital notes

Appendix 15: Consent form for parent/guardian (Accelerometry)



PARENT / LEGAL GUARDIAN CONSENT FORM

Title of project: *Accelerometry as a Method for Arthritis Assessment in Children*

Participant study number:

Names of researchers: Dr Daniel Hawley, Dr Reza Saatchi, Professor Derek Burke, Ms Harriet Nwaizu

Please initial box

1. I confirm that I have read and understand the information sheet for the above study and have had the opportunity to ask my questions.
2. I understand that my child's participation is voluntary and that I am free to withdraw my child at any time, without giving any reason, without my child's medical care or legal rights being affected.
3. I understand that relevant sections of any of my child's medical notes may be looked at by researchers and those involved in the running and supervision of the study from Sheffield Children's NHS Foundation Trust or from regulatory authorities, where it is relevant to my child taking part in research. I give permission for these individuals to have access to my child's records.
4. I agree to my child taking part in the above study.

Name of Parent/Guardian Date Signature

Name of Person taking consent
(if different from researcher) Date Signature

Researcher Date Signature

1 copy for parent; 1 copy for researcher; 1 copy to be kept with hospital notes

Appendix 16: Developments in denoising the accelerometer signal

Data fusion developments

Accelerometers can accurately estimate tilt angles in static conditions, however, in a dynamic condition, they are prone to high frequency noise. Some work to explore means to denoise the accelerometry signal by including a gyroscope device to make it more effective in estimating tilt angles was carried out. Data fusion algorithms, to combine and integrate the signals gotten from the accelerometer and gyroscope sensors in order to deal with and minimize the errors (Sasiadek, 2002) were investigated.

One of the well-known, widely used technique are the complementary filters, and this was evaluated in this study.

Complementary filter

The complementary filter (CF) is obtained by a simple analysis in the frequency domain (Higgins, 1975). The principle behind the complementary filter as shown in Figure 16-1 involves passing the accelerometer data which contains low frequency signals through a low pass filter and the gyroscope data which contains high frequency signals through a high pass filter to estimate angles. By doing this, the high frequency noise and low frequency drift associated with accelerometer and gyroscope measures respectively are eliminated. The idea is to combine outputs of the accelerometer and rate gyroscope to obtain good estimate of orientation, thus compensating for drift of the rate gyroscope and the slow dynamics of the accelerometer (Baerveldt & Klang, 1997). The filters share the same cut-off frequency as shown in the frequency response diagram in Figure 16-2.

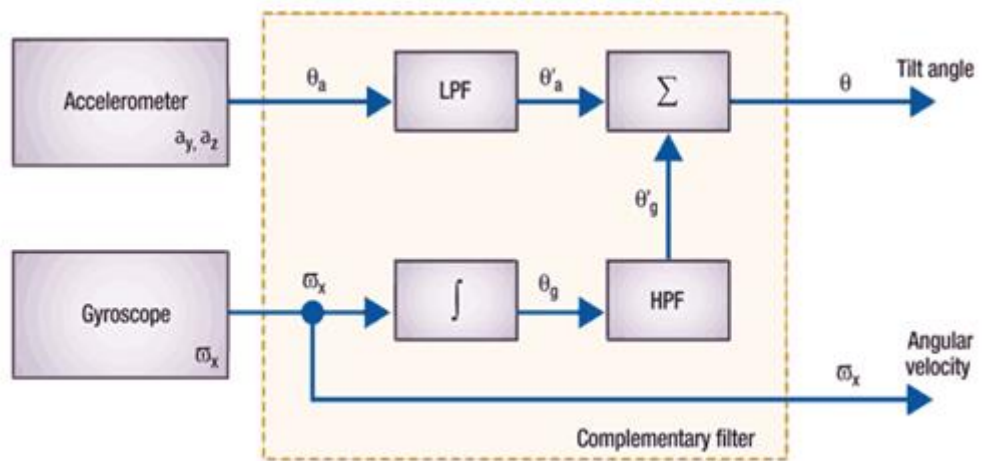


Figure 16-1: Block diagram of a typical complementary filter (Esfandyari et al., 2011)

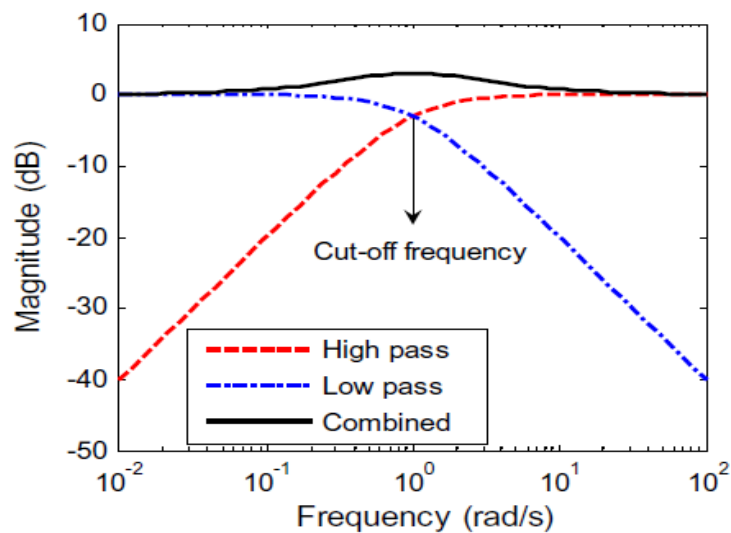


Figure 16-2: Frequency response of complementary filters (Shen, Yao, Jia, & Yuan, 2012)

The complementary filter is designed using Equation 16-1

$$angle = a(angle + gyro \times dt) + (1 - a) \theta_a \quad (16-1)$$

where a is the filter coefficient, $gyro$ is gyroscope values (in degrees per seconds-dps), dt is the sampling time interval (in seconds) and θ_a is tilt angle estimated by the accelerometer (in degrees).

The filter coefficient is related to the filter time constant- which is the relative duration of signal it will act on. The filter time constant should be chosen as low as possible in

order to minimize the influence of offsets of the rate gyroscope (Baerveldt & Klang, 1997). So, knowing the desired time constant and sampling frequency, one can find the filter coefficient. Alternatively, for best results, the cut-off frequency of the high/low pass filters must be carefully defined to keep the valid signals as well as suppress the unwanted noisy response of the sensors (Tseng, Wen-Lung, Chih-Yang, Jia-Wei, & Chin-Sheng, 2011).

The pros to this method include: fast estimates of angle and not very processor-intensive (Colton, 2007)

The major limitation is that the parameters of the CF such as filter coefficient, once selected are fixed and so to determine the best filter coefficients to use in every case will involve a careful study of the signal and continuous tweaking to select the coefficient that give the best results.

Experiments and Results

One of the challenges encountered with the accelerometry systems is that they suffer from high-frequency noise during movement's initiation or when there is a sudden change in the movements' direction (Nwaizu, Saatchi, & Burke, 2017). A suitably designed low pass filter (LPF) was used to denoise the signal in this study, to accurately estimate angular rotation, velocity, and acceleration.

Developments in denoising the accelerometry system, which in theory will improve the effectiveness of accelerometry systems at accurately measuring movement data, were considered.

Inclusion of a gyroscope

A gyroscope provides a rate of rotation, and integration is needed to obtain the rotational angle. An initial offset in the gyroscope's output signal produces an amplitude drift that increases with time. So, by combining outputs from accelerometer and gyroscope, using a suitable filter, these issues can be dealt with to an extent.

Experiments were performed to investigate the ability of the conventional complementary filter to accurately track the signal recorded from an IMU device (LSM9DS0) consisting of an accelerometer, gyroscope and magnetometer. However, only the accelerometer and gyroscope data were considered for processing as the

magnetometer measures are highly disturbed by the presence of ferromagnetic materials, and this was not put into consideration at this experiment.

The aim of the experiment was to investigate if the complementary filter could accurately remove the errors associated with the desired signal (i.e. the noise and drift).

The IMU was hooked up to the Arduino board (in this case, the Arduino Uno) connected to a computer and two recordings were obtained each with the IMU attached to the thigh and leg (the lower limb segment of the body) of an adult subject while walking in different patterns and speeds.

The complementary filter algorithm was designed using a filter coefficient a , of 0.98 as shown in Equation 16-2 making the design rely more on the data from the gyroscope (98% gyroscope data, $gyro$ and 2% accelerometer data, θ_a) such that they complemented each other. The sampling interval, dt , was 0.018 seconds.

$$angle = 0.98(angle + (gyro \times dt)) + 0.02 \theta_a \quad (16-2)$$

Figures 16-3 and 16-4 show a section of the results obtained. The accelerometer signal (black) as can be seen is noisy due to large accelerations, the gyroscope signal (blue) is drifting while the complementary filtered signal shown (in red) is able to estimate the angles as well as remove the noise and drift from the accelerometer and gyroscope respectively.

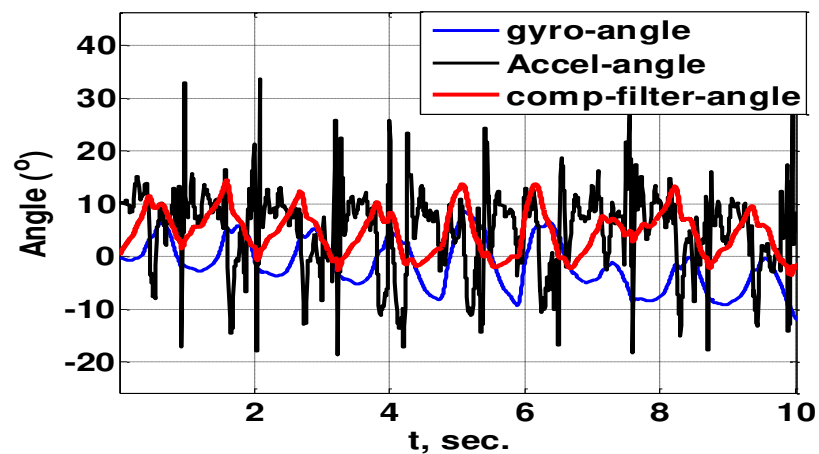


Figure 16-3 Angles estimated with IMU attached to the thigh

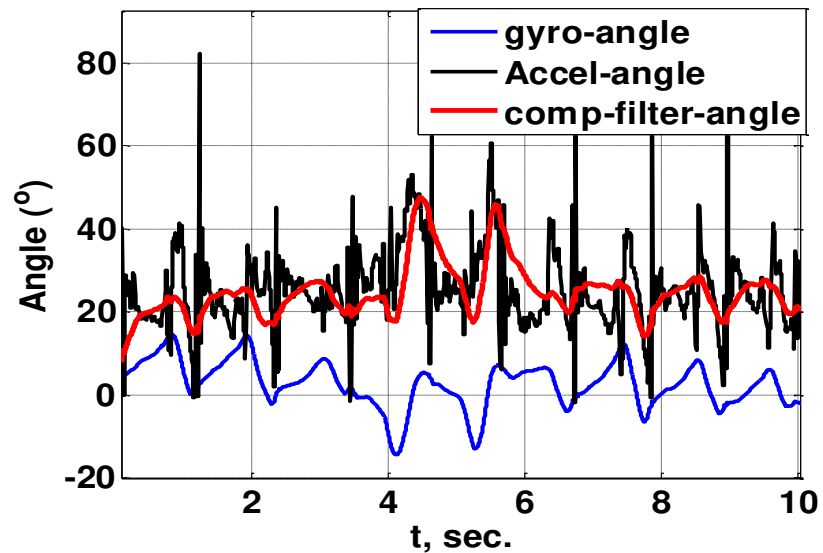


Figure 16-4 Angles estimated with IMU attached to the shank

Wavelet packet-based developments for denoising accelerometer signals

A wavelet packet decomposition-based technique to denoise a simulated accelerometer signal using a simulated gyroscope signal as a guide was developed and its effectiveness was compared with the conventional complementary filter method.

Experiments were carried out using simulated accelerometer and gyroscope signals (Figure 16-5) to assist with the evaluation of the effectiveness of the method. Simulated signals were used to demonstrate the concepts but in future studies these could be applied to signals obtained from real devices.

An accelerometer signal (shown in Figure 16-5, top) was generated to simulate a leg's movement in a simplified form. Gaussian noise was added to this signal to represent the effect of measurement noise (shown in Figure 16-5, middle). The simulated gyroscope signal (shown in Figure 16-5, bottom) was the guide signal. Simulations were done in MATLAB®.

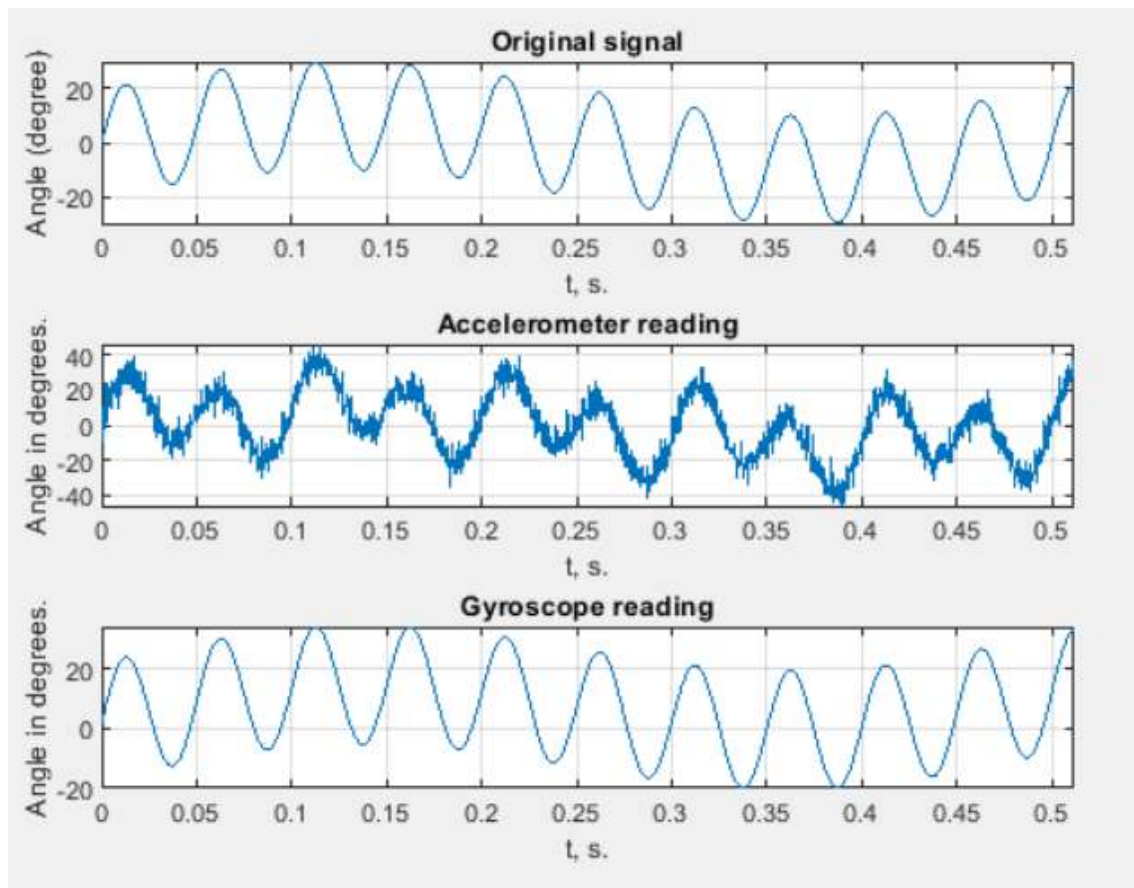


Figure 16-5 Simulated signals for reference, accelerometer and gyroscope readings

In the wavelet packet decomposition algorithm, a signal is successively decomposed to a specified level, by suitably chosen lowpass and high-pass filters, and the outputs from the filters down sampled by a factor of 2 to give the approximation and detail coefficients respectively.

The noisy accelerometer and drifting gyroscope signals were decomposed separately to 8 levels using the Daubechies 20 wavelet family. The coefficients of the terminal nodes are represented by nodes 255 to 510. These decomposed coefficients for both accelerometer and gyroscope signals were then compared for similarity by performing cross correlation. The two nodes with the highest correlation magnitudes (indicating closest to similarity) were selected to be used for reconstructing the accelerometer signal, while the values of coefficients not selected were set to zero.

The wavelet packet-based reconstructed accelerometer signal was compared with that obtained from the complementary filter. Complementary filter combines the accelerometer and gyroscope signals to generate a signal affected less by the noise

and drift. The movement angle from the complementary filter was obtained using Equation 16-3.

$$\theta_{current} = \alpha(\theta_{previous} + \Delta_t\theta_g) + (1 - \alpha)\theta_a \quad (16-3)$$

The complementary filter algorithm was designed using a filter coefficient $\alpha = 0.98$, making the design rely more on gyroscope's-based angle (θ_g) than that from the accelerometer, (θ_a). The sampling interval $\Delta_t = 0.018$ seconds (sample rate 55 samples per second).

The processing was performed in MATLAB[®]. The correlation between the decomposed coefficients show nodes 255 and 258 to have the highest similarities (Figure 16-6) and were selected for use in reconstructing the accelerometry signal (Figure 16-7).

The wavelet packet method was more effective in representing the original reference accelerometer signal than the complementary filter (Figure 16-8). This part of the study demonstrated the potential of wavelet transform in denoising accelerometry signals. For the work carried out on patients only accelerometers were used and thus in future inclusion of gyroscopes should be considered as they may improve the analysis.

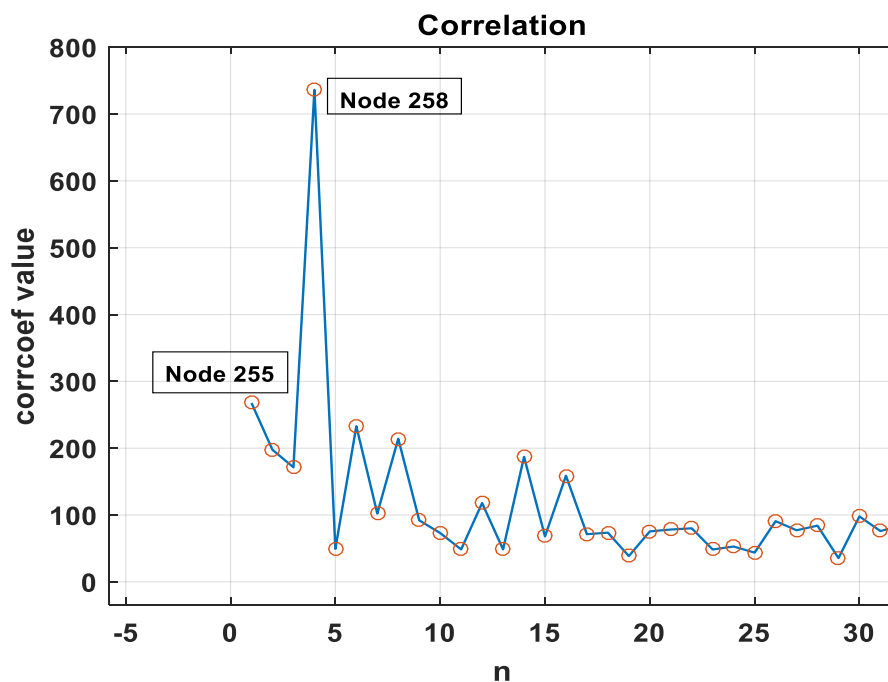


Figure 16-6 Wavelet packet coefficient correlation plot

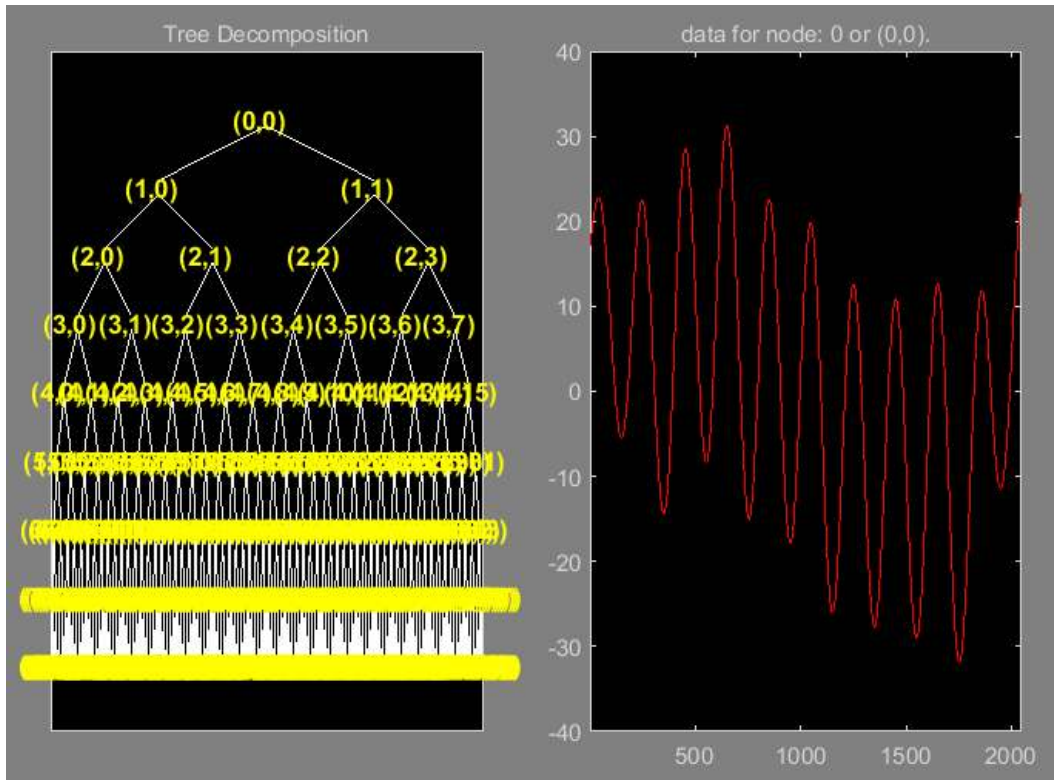


Figure 16-7 Decomposition tree showing 8 levels and the reconstructed accelerometer signal

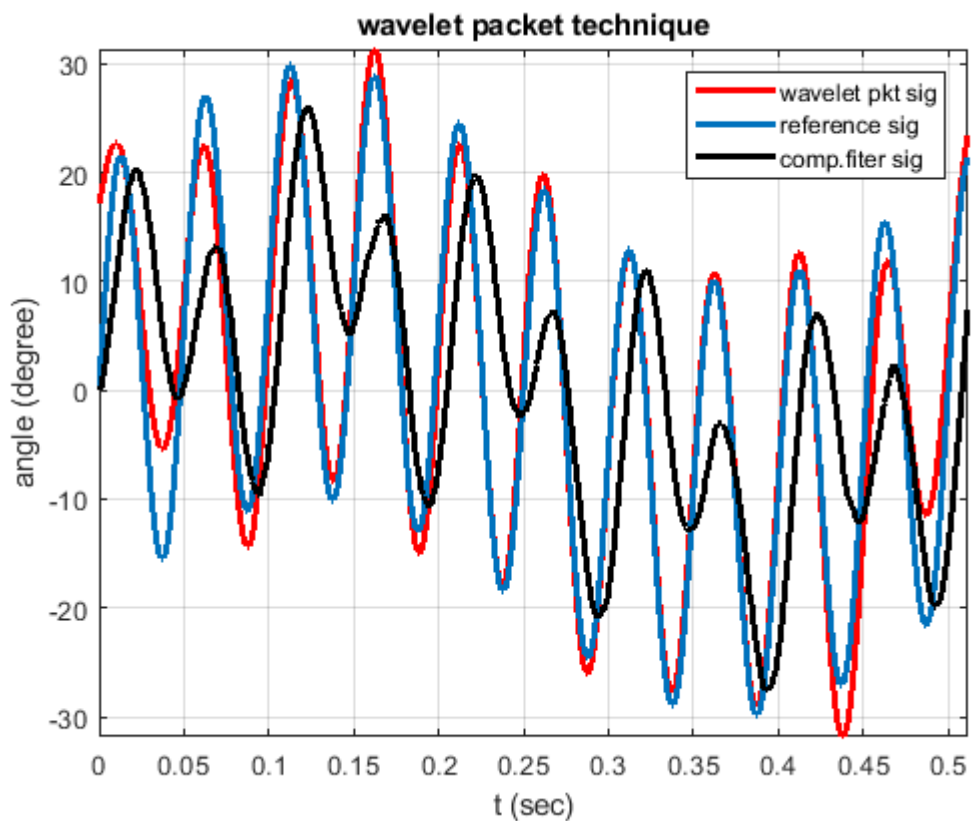


Figure 16-8 The signal obtained using the complementary filter and the accelerometer signal obtained from the wavelet packet.